

# STK33 kinase inhibitor BRD-8899 has no effect on KRAS-dependent cancer cell viability

Tuoping Luo<sup>a,b,1</sup>, Kristina Masson<sup>a,1</sup>, Jacob D. Jaffe<sup>a</sup>, Whitney Silkworth<sup>a</sup>, Nathan T. Ross<sup>a,2</sup>, Christina A. Scherer<sup>a</sup>, Claudia Scholl<sup>c</sup>, Stefan Fröhling<sup>c</sup>, Steven A. Carr<sup>a</sup>, Andrew M. Stern<sup>a</sup>, Stuart L. Schreiber<sup>a,b,d,3</sup>, and Todd R. Golub<sup>a,d,e,3</sup>

<sup>a</sup>Broad Institute of Harvard and MIT, 7 Cambridge Center, Cambridge, MA 02142; <sup>b</sup>Department of Chemistry and Chemical Biology, Harvard University, Cambridge, MA 02138; <sup>c</sup>Department of Internal Medicine III, University Hospital of Ulm, 89081 Ulm, Germany; <sup>d</sup>Howard Hughes Medical Institute, Bethesda, MD 20817; and <sup>e</sup>Department of Pediatric Oncology, Dana-Farber Cancer Institute, Harvard Medical School, Boston, MA 02215

Contributed by Stuart L. Schreiber, December 14, 2011 (sent for review September 23, 2011)

**Approximately 30% of human cancers harbor oncogenic gain-of-function mutations in KRAS.** Despite interest in KRAS as a therapeutic target, direct blockade of KRAS function with small molecules has yet to be demonstrated. Based on experiments that lower mRNA levels of protein kinases, KRAS-dependent cancer cells were proposed to have a unique requirement for the serine/threonine kinase STK33. Thus, it was suggested that small-molecule inhibitors of STK33 might have therapeutic benefit in these cancers. Here, we describe the development of selective, low nanomolar inhibitors of STK33's kinase activity. The most potent and selective of these, BRD8899, failed to kill KRAS-dependent cells. While several explanations for this result exist, our data are most consistent with the view that inhibition of STK33's kinase activity does not represent a promising anti-KRAS therapeutic strategy.

Oncogenic mutations in the RAS family member KRAS are among the most common mutations in human cancer (1). For example, KRAS-mutation frequencies in lung, colon, and pancreas adenocarcinoma are 30%, 50%, and 90% respectively (2). These observations, coupled with functional studies, suggest that KRAS is a highly attractive therapeutic target for many cancers. Unfortunately, small-molecule targeting of KRAS has not yet been achieved, and no effective KRAS inhibitors have been described. Blockade of prenylation of the KRAS C-terminal membrane anchoring domain with farnesyltransferase inhibitors has met with limited success, due at least in part to increased expression of geranylgeranyl transferase (3). Similarly, targeting other steps in the processing of the KRAS C-terminal region through the inhibition of Ras-converting enzyme or isoprenylcysteine-carboxymethyltransferase has yet to be clinically validated (2). Efforts to target the downstream effector pathways of KRAS with MEK inhibitors alone or in combination with PI3K inhibitors have shown promising preclinical results and are currently being evaluated in the clinic (4). Nevertheless, the therapeutic targeting of KRAS remains one of the grand challenges in cancer research.

Recently, an alternative approach to targeting KRAS has been proposed—namely, the RNA interference (RNAi)-based screening for synthetic lethal gene/RNA interactions that might then suggest protein targets more “druggable” than the targeted mRNA or the KRAS protein itself (5–9). A recently reported RNAi screen suggested the serine-threonine kinase STK33 as such a target (9). Knock down of STK33 was reported to induce apoptosis in KRAS-dependent AML cancer cell lines but spare KRAS wild-type cells. While the normal function of the STK33 protein is unknown, the results led the authors to propose that a small-molecule inhibitor of STK33's protein kinase activity would selectively kill KRAS-mutant cancer cells. As no such small-molecule inhibitors exist, we set out to discover them, and to characterize their activity as anti-KRAS agents.

## Results

**High Throughput Screening for STK33 Kinase Inhibitors.** We first established an assay suitable for screening for STK33 kinase

inhibitors. Using baculovirus-expressed full length human recombinant STK33 and the general kinase substrate myelin basic protein (MBP), a biochemical assay was optimized that quantified the STK33 kinase-dependent generation of ADP (see *Materials and Methods*). Radiometric analysis and mass spectroscopy (MS) (10, 11) were used to corroborate that the ADP generated was quantitatively coupled to phosphorylation of MBP (*SI Appendix*, Fig. S1). The reaction rate was linear with respect to time and enzyme concentration and Michaelis-Menten constants were determined (*SI Appendix*, Fig. S2). The relatively nonspecific kinase inhibitor dimethyl fasudil (BRD7446) was identified in a pilot screen as a low micromolar STK33 inhibitor; it therefore served as a positive control for subsequent screening (*SI Appendix*, Fig. S2E). A high throughput screen of 27,500 compounds from diverse chemical collections (*SI Appendix*, Table S1) was performed in duplicate at 100 μM ATP (threefold above the  $K_{M,ATP}$ ). Coefficients of variation (CVs) of 4–6% for the DMSO vehicle control and corresponding Z' factor values for the positive control between 0.64 and 0.76 were obtained (12). The hit rate was 0.4% at an inhibition threshold of 20% inhibition where Z' factor equaled zero (*SI Appendix*, Fig. S3). The IC<sub>50</sub> values of the 102 primary hits were measured at two ATP concentrations (100 and 25 μM) using both the ADP-Glo and HTRF assays.

The STK33-inhibitory activity of 95/102 compounds (93%) was verified in replicate experiments, and these compounds clustered into 37 discrete chemotypes (*SI Appendix*, Fig. S4). Four groups appeared to be ATP-noncompetitive inhibitors but were either very weak or contained chemically reactive moieties, and were therefore not prioritized. All other hits were ATP-competitive inhibitors with IC<sub>50</sub> values in the micromolar range, except the chemotype of staurosporine (a notoriously nonselective kinase inhibitor) that inhibited STK33 with low nanomolar potency. Fasudil (BRD7868) (Table 1), a known inhibitor of Rho-associated protein kinase (ROCK) (13) as well as seven of its analogs yielded a structure-activity relationship for inhibiting STK33. This series was therefore prioritized as the lead structure for chemical optimization due to its low micromolar potency, known selectivity for other kinases, physical properties, and synthetic feasibility.

Author contributions: T.L., K.M., J.D.J., W.S., N.T.R., S.A.C., A.M.S., S.L.S., and T.R.G. designed research; T.L., K.M., J.D.J., and W.S. performed research; C. Scholl and S.F. contributed new reagents/analytic tools; T.L., K.M., J.D.J., N.T.R., and C.A. Scherer analyzed data; and T.L., K.M., A.M.S., S.L.S., and T.R.G. wrote the paper.

The authors declare no conflict of interest.

Freely available online through the PNAS open access option.

<sup>1</sup>T.L. and K.M. contributed equally to this work.

<sup>2</sup>Present address: Novartis Institutes for BioMedical Research, 250 Massachusetts Avenue, Cambridge, MA 02142.

<sup>3</sup>To whom correspondence may be addressed. E-mail: stuart\_schreiber@harvard.edu or golub@broadinstitute.org.

This article contains supporting information online at [www.pnas.org/lookup/suppl/doi:10.1073/pnas.1120589109/DCSupplemental](http://www.pnas.org/lookup/suppl/doi:10.1073/pnas.1120589109/DCSupplemental).

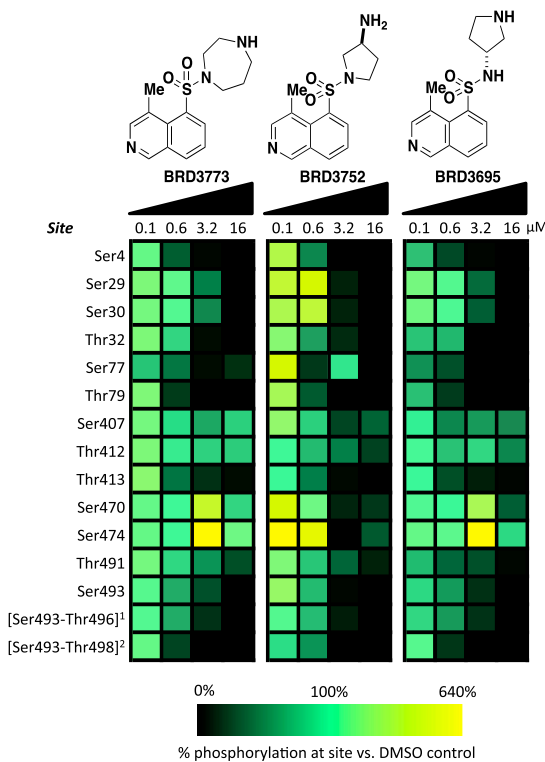


**Fig. 1.** Proteomic assessment of STK33 autophosphorylation. Sites on STK33 determined to be autophosphorylated are shown on the left. Increasing concentrations of the three fasudil analogs shown were added to an in vitro phosphorylation reaction in which the only substrate present was STK33 itself. The heatmap is colored according to how the level of phosphorylation at a given site changed in response to addition of compound at the specified concentration vs. DMSO control. Some compound concentrations were found to increase phosphorylations at given sites, leading to values >100%. <sup>1</sup>ambiguously localized phosphorylation within the span of bracketed amino acids. <sup>2</sup>ambiguously localized double phosphorylation within the span of bracketed amino acids.

**STK33 Can Autophosphorylate In Vitro and Is Inhibited by a Fasudil Analog.** During the optimization of STK33 inhibitors, we sought to confirm that the candidate inhibitors were truly functioning as STK33 inhibitors, and were not simply an artifact of a screening assay based on an artificial kinase substrate (MBP). To address this concern, we assessed whether STK33, like many kinases, is autophosphorylated, and if so, whether our candidate STK33-inhibitory compounds blocked such autophosphorylation (*SI Appendix*, Fig. S1A) (9, 14). Mass spectrometry revealed several sites of phosphorylation on STK33 (Fig. 1). Two sites (Thr440 and Ser441) were found to be phosphorylated in the preparation of recombinant STK33 itself and the remaining sites were due to bona fide in vitro kinase activity of the enzyme. Among the sites observed were the Thr491/Ser493/Thr496 cluster that had been previously reported to be regulated during the cell cycle in HeLa cells (15). We then verified that the lead scaffold that emerged from the biochemical screen (represented in BRD3773, BRD3752, and BRD3695, see structures in Table 1), indeed inhibited the autophosphorylation of STK33 at these sites in a concentration-dependent manner (Fig. 1). These results suggested that the scaffold was a suitable starting point for further optimization with respect to STK33 inhibition.

**Chemical Optimization of STK33 Inhibitors.** For chemical optimization, 250 fasudil analogs were synthesized and tested in the biochemical assay (*SI Appendix*, Schemes S1–S5, Table S13, and *SI Materials and Methods*). Structurally, fasudil comprises two fragments: an isoquinoline ring and a homopiperazine ring,

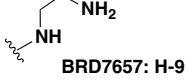
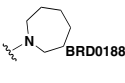
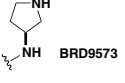
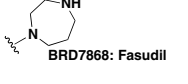
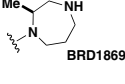
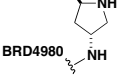
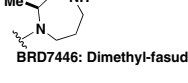
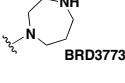
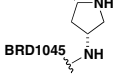
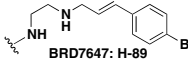
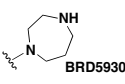
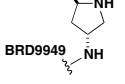
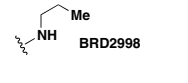
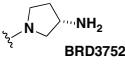
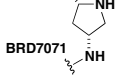
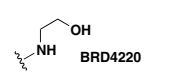
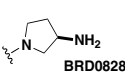
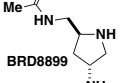
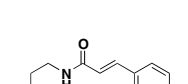
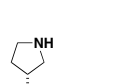
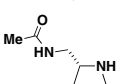
connected by the sulfonyl functionality on the 5-position of the isoquinoline. The sulfonamide functionality and nitrogen on the isoquinoline ring are critical for the potency against STK33 (*SI Appendix*, Table S2). Replacing the basic amine nitrogen with carbon or oxygen, or converting it to an amide, resulted in significantly reduced potency (BRD7657 vs. BRD2998 and BRD4220, BRD7868 vs. BRD0188, BRD7647 vs. BRD6818, Table 1, *SI Appendix*, Table S3). We observed that the two additional methyl groups in dimethyl fasudil lead to a sevenfold increase in potency compared to fasudil (BRD7446 vs. BRD7868). While one monomethyl fasudil isomer, namely BRD1869, was threefold less potent than fasudil (BRD7868), the other monomethyl fasudil isomer (BRD3773) was over 70-fold more potent against STK33 compared to fasudil (BRD7868). Therefore we explored the effect of monomethylation at several positions of the isoquinoline ring; only 4-methyl substitution significantly increased the potency (*SI Appendix*, Table S4). An SAR study performed on isoquinoline 4-substitution indicated that only a small alkyl group, such as ethyl (BRD5930), is tolerated, while polar or bulky groups resulted in decreased activity (*SI Appendix*, Table S5). Further optimization on the amine fragment led to two more nanomolar STK33 inhibitors (BRD3752 and BRD3695); their enantiomers were 60–100-fold less active (BRD0828 and BRD9573) (Table 1, *SI Appendix*, Table S6).

Further chemical optimization was guided by measures of STK33 selectivity. As measured by kinase activity profiling against 241 kinases (*SI Appendix*, Table S7), BRD3773 exhibited relative STK33 selectivity, inhibiting 36 kinases with estimated  $K_i$  values within 10-fold of that of STK33. Compound BRD3695 showed further selectivity with respect to those 36 kinases (*SI Appendix*, Fig. S5), with inhibition confined to the AGC subfamily of kinases, and therefore became the lead for further chemical optimization.

Modification of the pyrrolidine ring of BRD3695 (*SI Appendix*, Table S8) yielded more potent, low nanomolar analogs (BRD4980, BRD9949, and BRD8899). These compounds were more potent than their corresponding (2*R*, 4*S*) diastereomers (BRD1045, BRD7071, and BRD5749). The low nanomolar potency of BRD8899 against STK33 as well as other selected inhibitors was confirmed by competition binding assay (*SI Appendix*, Table S9) (16). Furthermore, the specificity of BRD8899 was retained, exhibiting significant off-target inhibition of a few other kinases, including RIOK1 (97% inhibition), MST4 (96%), RSK4 (89%), ATK1 (85%), KIT<sup>D816V</sup> (85%), ROCK1 (84%), and FLT3 (81%), while STK33 was inhibited by 89% (*SI Appendix*, Table S10). BRD8899 thus represents a 200-fold improvement in potency compared to the initial screening hit (BRD7446), with increased selectivity for STK33 (Fig. 2).

**Characterization of BRD8899 in Cell-Based Assays.** Having demonstrated that BRD8899 is a potent and selective inhibitor of STK33 kinase activity in biochemical assays, we next turned to its characterization in cells. It has been previously reported that STK33 knock down via RNAi results in the selective killing of mutant KRAS-dependent cancer cells (9), a result that we confirmed using the same shRNAs in *KRAS*-mutant AML cell lines (NOMO-1 and SKM-1 AML cells) compared to *KRAS*-wild-type lines (THP-1 and U937) (*SI Appendix*, Fig. S7). We next asked whether BRD8899 could recapitulate *KRAS*-associated pattern of cell killing. We therefore tested BRD8899 at a range of doses across 35 cancer cell lines, but observed no effect on cell viability in any of the lines at concentrations as high as 20 μM (Fig. 3A, *SI Appendix*, Fig. S6 and Table S12). (9) Because BRD8899 (our most potent STK33 inhibitor) failed to kill KRAS-mutant cell lines as predicted by the RNAi experiments, we tested additional analogs for their ability to kill cancer cells. While some of these compounds reduced cell viability, such cytotoxicity was uncorrelated with KRAS-mutation status across the panel of cell lines

Table 1. Biochemical activity of selected STK33 inhibitors

$R^1$	$R^2$	$IC_{50}$ ( $\mu M$ )	$R^1$	$R^2$	$IC_{50}$ ( $\mu M$ )	$R^1$	$R^2$	$IC_{50}$ ( $\mu M$ )
H		14	H		>186	Me		4.8
H		14	H		50	Me		0.037
Me		2.0	Me		0.19	Me		0.12
H		2.2	Et		0.28	Me		0.020
H		>186	Me		0.047	Me		0.42
H		110	Me		3.7	Me		0.011
H		>186	Me		0.063	Me		0.52

Representative fasudil analogs, tested for their inhibition of STK33 kinase activity in vitro. The side groups for  $R^1$  and  $R^2$  are presented for each analog (see the top structure for positions), along with the compound name and the  $IC_{50}$  at 25  $\mu M$  ATP.

(Fig. 3B, *SI Appendix*, Fig. S6). We therefore conclude that the observed cell death is most likely explained by off-target effects of these less potent compounds, rather than by STK33-inhibitory activity.

**Establishing Bioactivity of BRD8899 in Cells.** The experiments described above suggest that treatment of KRAS-mutant cancer cells with low nanomolar biochemical potency against STK33 does not result in cell death, arguing against the notion that the enzymatic function of STK33 represents an attractive therapeutic target in KRAS-mutant cancers. However, it is possible that while BRD8899 is highly potent in biochemical assays, it fails to inhibit STK33 in cells—even at 1,000-fold higher concentrations. To address this possibility, we sought a biomarker of BRD8899 activity in cells. We first looked for evidence of STK33 autophosphorylation in cells, given the observation that such autophosphorylation occurs with recombinant STK33, and is inhibited by BRD8899. However, looking across multiple cell lines, we found endogenous STK33 to be expressed at low levels, and phosphorylation was not detectable by mass spectrometry (for details, see *Materials and Methods*). We therefore turned to the kinase profiling data for BRD8899, where we observed similarly potent inhibition of the kinase MST4 in addition to STK33. Treatment of Nomo-1 cells with BRD8899 resulted in decreased phosphorylation of the MST4 substrate ezrin (Fig. 4A), but had no effect on ERK phosphorylation, as predicted from the kinase profiling data (Fig. 4B). This finding suggests that BRD8899

indeed gets into cells, inhibits the activity of a target (MST4) predicted by kinase profiling experiments, and yet does not kill KRAS-mutant cancer cells. These results are most consistent with BRD8899 likely inhibiting STK33 in cells, but STK33 kinase activity not serving as a compelling target for KRAS-mutant tumors. Of course in the absence of a direct biomarker of STK33 activity in cells, we cannot exclude that whereas BRD8899 inhibits MST4 (as an off-target effect), it does not effectively inhibit STK33 in cells.

## Discussion

Cancer genomes have served as powerful guides to the development of cancer therapeutics that target oncogene dependencies. Several examples point to the utility of targeting mutant, oncogenic kinases with small-molecule inhibitors, with dramatic clinical success being seen in chronic myeloid leukemia (17), gastrointestinal stromal tumors (18), lung cancer (19), and melanoma (20). However, the therapeutic path for nonkinase mutations in cancer is less established. In particular, recurrent mutations in KRAS have been known to exist for over a quarter century, and yet KRAS has been considered “undruggable.”

A general solution to approaching cancer targets, however, has recently been suggested. Borrowing from the concepts of synthetic lethality first explored in yeast, “nononcogene addiction” has been proposed (8, 21). One avenue to identify non-oncogene codependencies (proteins on which oncogenes are dependent yet not themselves mutated) relies on genetic screens

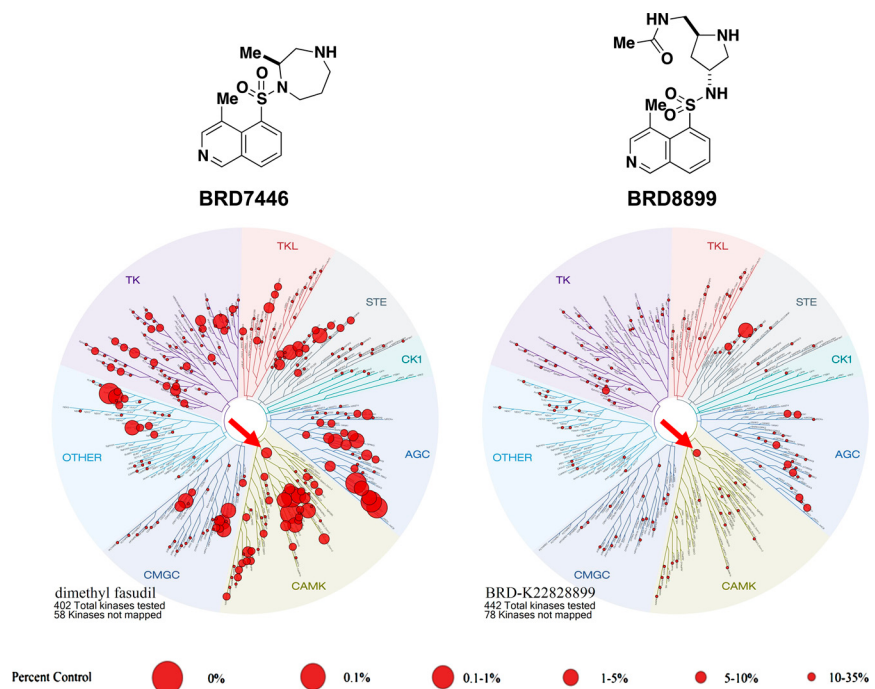


**Fig. 2.** Small molecule/kinase interaction maps for BRD7446 and BRD8899. The kinase profiling (16) was done at 5  $\mu$ M for BRD7446 and 1  $\mu$ M for BRD8899, resulting in equal inhibition of STK33 in a biochemical assay. Kinases found to bind are marked with red circles; larger circles indicate higher affinity binding. STK33 is indicated by the red arrow.

to infer potentially more readily druggable proteins whose inhibition is selectively lethal in the context of particular mutations. Such approaches are highly attractive because they do not require prior knowledge of the biological basis of the synthetic lethal interaction—rather, the relationship is revealed through an unbiased screen such as an RNAi screen. On the other hand, while this approach might establish a synthetic relationship between a genetic feature of a cancer and the lowering of a target mRNA, they do not establish such a relationship involving a function of the encoded protein. Assuming RNAi-induced changes in mRNA levels and small-molecule-modulated protein function are equivalent, the report of STK33 essentiality in mutant KRAS-dependent cancer cells (9) was encouraging because STK33, as a serine/threonine kinase, was in principle an accessible target of small molecules, and such compounds could form the basis of anti-KRAS therapeutics. We therefore developed a biochemical STK33 kinase assay to identify specific STK33 inhibitors that could be evaluated in cellular proof-of-principle studies. A high throughput screen identified a series of STK33 kinase-inhibitory compounds, which were subsequently optimized for potency (representing 200–1,000-fold increase in potency) while minimizing off-target effects (inhibiting only three other kinases more potently than STK33). Specifically, our lead compound, BRD8899, exhibited an  $IC_{50}$  of 11 nM in an STK33 biochemical assay. However, contrary to essentiality of STK33 predicted by initial genetic studies of STK33, BRD8899 failed to kill KRAS-mutant cells at concentrations as high as 20  $\mu$ M.

There are a number of explanations of the failure of a potent STK33 kinase inhibitor to kill KRAS-mutant cells, and several are offered here. It is conceivable that while BRD8899 (and its analogs) inhibit STK33 kinase activity in biochemical assays, it does not do so in living cells. For example, it is possible that BRD8899 does not penetrate cells. However, several pieces of evidence argue against this possibility. Ideally, one would have a direct measure of STK33 kinase activity in cells, but to date, no such biomarker has been developed for STK33. We attempted to identify such a direct biomarker, looking for evidence of the STK33 autophosphorylation we observed using recombinant STK33 protein. Unfortunately, owing to the low level of STK33 expression in the two cancer cell lines analyzed (NOMO-1 and SKM-1), we were unable to document such phosphorylation.

We therefore turned to indirect measures of BRD8899 bioactivity, using the predicted off-target effects of the compound suggested by kinase specificity profiling. Indeed, we found that BRD8899 inhibits the kinase MST4 in cells (resulting in subsequent decreased phosphorylation of an MST4 substrate, ezrin). These biomarker studies, while indirect, suggest that BRD8899 does in fact enter cells, and can inhibit the activity of its kinase targets. While it is conceivable that BRD8899 inhibits MST4 but not STK33, we consider that scenario less likely. Although other explanations exist, such as a cellular context dependency recently reported with small-molecule inhibitors of PKC and PDK1 (23, 24), overall we surmise that inhibiting STK33 kinase activity is not likely to be an effective therapeutic strategy for KRAS-mutant cancer.

While inhibition of STK33 kinase activity may not result in KRAS-related cell killing, it is possible that nonkinase activities of STK33 may be responsible for its observed essentiality in RNAi-based studies. For example, STK33 could have a distinct function other than its kinase activity. It is conceivable that STK33 has a more structural, scaffolding function that is required for the proper function of a multiprotein complex. Whereas RNAi-mediated knock down of STK33 might disrupt such putative scaffolding activity, a small-molecule kinase inhibition may not. Such nonkinase activities of STK33 cannot be excluded by our present studies. A similar conclusion was reached in a recent independent study (22).

An alternative explanation for the failure of STK33 inhibitors to recapitulate STK33 the knock-down phenotype is that the shRNA reagents have off-target (non-STK33) effects. Arguing against this alternative explanation is the observation that a dominant-negative STK33 construct was shown to result in selective lethality to KRAS-dependent cell lines (9). Nevertheless, until clear rescue experiments using non-RNAi-inhibitable STK33 expression constructs demonstrate rescue of shRNA-mediated killing, an off-target mechanism must remain a formal possibility. We note that a recent study using STK33 siRNA oligonucleotides transiently transfected into AML cell lines failed to show a KRAS-specific killing effect (22). However, the transfection efficiency was not reported and only partial STK33 knock down was achieved in those experiments, making it difficult to interpret the results.

It has been recently suggested that while gain of function mutations within oncogenes lead to increases in rate-determining

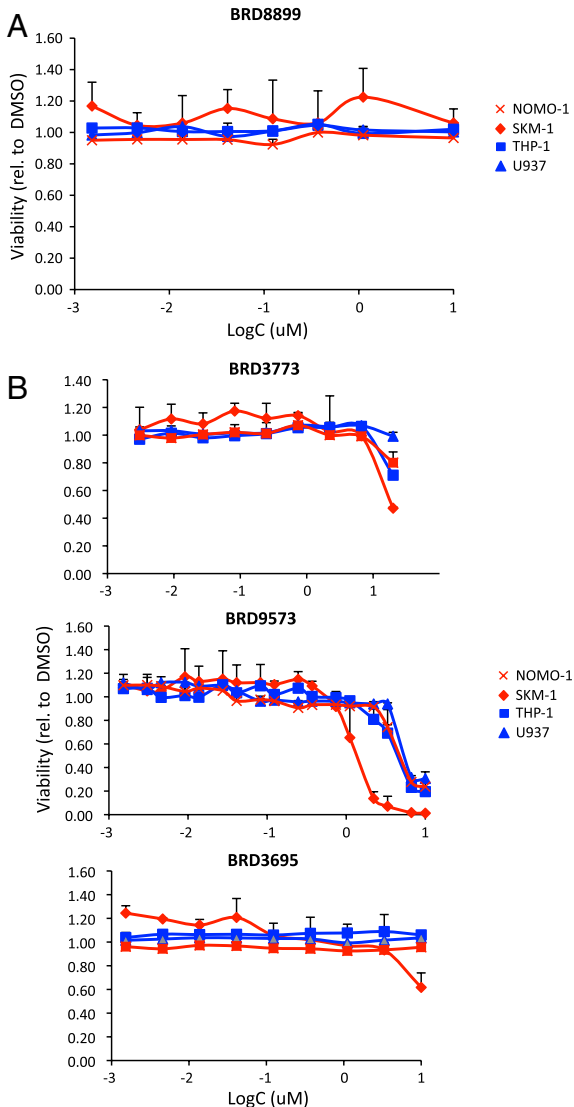


**Fig. 3.** Cell viability assay for fasudil analogs BRD8899, BRD3773, BRD9573, and BRD3695. (A and B). Dose-response curves of KRAS and STK33 dependent Nomo-1 and SKM-1 cells and KRAS and STK33 independent THP-1 and U937 cells (as previously confirmed by RNAi), using CellTiter Glo as a measurement for viability. Cells were plated in 384-well plates and treated with compounds for 72 h. The luminescence values of each compound treatment divided by the median of all DMSO values for each individual cell line was taken as a measurement of relative viability. Error bars represent the standard deviation of three replicates. KRAS mutant and KRAS wild-type cell lines are depicted in red or blue, respectively. For 31 additional cell lines screened, see *SI Appendix, Fig. S6*.

steps in signaling, their synthetic lethal partners may operate through relatively rapid signaling steps (8). Although these fast steps might be modulated by “irreversible” maneuvers such as RNAi knock down and dominant negative expression, achieving this same level of target modulation with reversible small molecule competitive inhibitors may be more difficult. The extent to which this phenomenon explains our STK33 results remains to be determined.

The experiments described here used cell viability as the readout of STK33 modulation. As such, these studies do not preclude the possibility of an important role of STK33 in other cancer phenotypes (e.g., migration, adhesion). However, our study indicates that the pharmaceutical targeting of STK33 kinase activity may not result in an effective strategy for patients with KRAS-mutant cancers. Nevertheless, the potential of synthetic-lethal RNAi screens should not be underestimated; they

represent a powerful strategy for identifying promising new anticancer targets.

## Materials and Methods

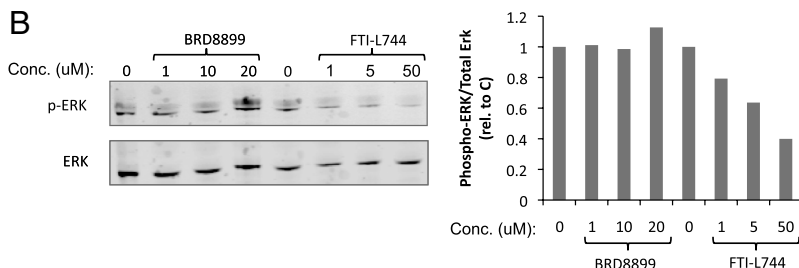
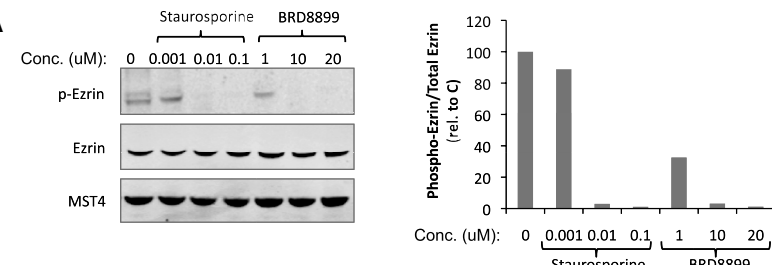
**STK33 and Kinase Assays.** Human full length STK33 containing an amino terminal histidine tag expressed by baculovirus in Sf21 cells was purchased from Millipore Corporation (catalog # 14-671-K, purity >93% by SDS-PAGE and Coomassie blue staining). Myelin basic protein (bovine) was purchased from Millipore Corporation (catalog # 13-104). ATP, ADP, 4-Morpholinepropanesulfonic acid (MOPS), MgCl<sub>2</sub>, Brij-35, glycerol, 2-mercaptoethanol, and BSA were purchased from Sigma-Aldrich. The 384-well general plates were purchased from VWR (Corning 3570); 384-well low volume plates were purchased from Greiner Bio-One (384W SV, HiBase, PS, LUMITRAC 200, Medium Binding, 30 μL/well, catalog # 784075). CyBi®-Well vario was purchased from CyBio AG. CyBi tips were purchased from CyBio AG (CyBi-Tip Trays 384 standard; catalog # OL 3800-25-513-N). HTRF Transcreener ADP assay was purchased from Cis-bio US (catalog # 62ADPPC); ADP-Glo assays were purchased from Promega Corporation (catalog # V9103). The Envision 2012 multilabel reader was purchased from PerkinElmer, Inc. Multi-drip Combi reagent dispenser and cassettes were purchased from Thermo Fisher Scientific, Inc.

Kinase reactions were performed under 10 mM MOPS-NaOH (pH 7.0), 10 mM MgCl<sub>2</sub>, 0.3 mM EDTA, 0.001% Brij-35, 0.5% glycerol, 0.01% 2-mercaptoethanol, and 0.1 mg/mL BSA. The enzyme concentration (STK33) and substrate concentration (MBP and ATP) were varied depending on the experiment. Reactions were initiated by the addition of ATP (final concentration 25 ~ 500 μM depending on experiments) and incubated at 30 °C or room temperature for the indicated time. For additional details, see *SI Appendix, SI Materials and Methods*.

**Mass Spectrometric Assessment of Phosphorylation State of MBP and STK33 for In Vitro Assays.** For MBP, assay conditions were as described in “STK33 and Kinase Assays” and *SI Appendix, Fig. S1*. For STK33, 1 μg of total STK33 was incubated with 100 μM ATP, in the absence or presence of the concentration of fasudil analog indicated in Fig. 1. The reaction was terminated by the addition of SDS-PAGE loading buffer containing 1% SDS containing 10 mM DTT and heating to 95 °C for 5 min. Samples were reduced at room temperature for 30 min and cysteines were subsequently alkylated with 30 mM iodoacetamide for 30 min. SDS-PAGE separation and gel band sample preparation was done as described (10). Liquid Chromatography—Mass spectrometry (LC/MS) was performed on an Orbitrap mass spectrometer (ThermoFisher Scientific) coupled to a nano-flow chromatography system (Agilent 1100), as described (11). For each survey scan, the top 10 most abundant peptidic ions were selected for collision-induced dissociation (MS/MS sequencing), using intelligent sampling dynamic exclusion principles (21). The data were analyzed using SpectrumMill Proteomics Workbench (Agilent) as described (21). Extracted ion chromatograms corresponding to the phosphopeptides from either MBP or STK33 were generated using XCalibur (ThermoFisher Scientific) ( $\pm 7.5$  ppm window width). Area under these curves was used as the basis for quantification of the effect of the fasudil analogs on site-specific phosphorylation. All peak areas were normalized to total protein amount for each condition, as determined by the peak area under a peptide that could not be phosphorylated in the assay.

**Analysis of STK33 Expression in Cells.** Nomo-1 and SKM-1 cells were grown in SILAC (stable isotope labeling with amino acids in culture) heavy medium. Recombinant STK33 was added at known concentrations in SILAC light medium and proteins within lysates were separated on gel electrophoresis and then analyzed by MS. Based on the light standard, the levels of endogenous STK33 were estimated to approximately 10 ng/1.5 × 10<sup>8</sup> cells. Similar experiments were done using Nomo-1 cells stably expressing Flag-STK33 in a pLenti6.2 vector, and the levels of overexpressed protein were estimated to be approximately 10-fold higher. For the phosphorylation studies by MS, synthetic phospho-peptides for STK33 (based on known phosphorylation sites from the in vitro kinase assay) were added into the digest of Flag-STK33 expressed in Nomo-1 cells to estimate the detectable amounts of phospho-STK33 in cells.

**Cell Lines and Culture Conditions.** Nomo-1, SKM-1, NB4, THP-1, U937, OCI-AML3, MM1S, and RPMI-8226, were kindly provided by Gary Gilliland (Brigham and Women's Hospital, Boston). TF-1, P31/FUJ, MOLM-16, PL-21, EOL-1, GDM-1, Colo-205, HeyA8, OvCar-3, CaOV3, OvCar-8, and KYSE-405 cells were provided by the Broad-Novartis Cancer Cell Line Encyclopedia. The remaining cell lines were obtained from the American Type Culture Collection and the German Collection of Microorganism and Cell Cultures.



All cell lines were maintained under the manufacturer's recommended standard conditions.

**STK33 and KRAS Knock Down.** Generation of virus, transduction, and selection of cells was done as previously described (9). In brief, cells were transduced with pLKO.1puromycin lentiviral shRNA vectors from the TRC shRNA library, and selected with 4 µg/mL puromycin for 48 h. Cell viability was measured at timepoints 0 and 72 h after selection. Hairpins targeting the following sequences in *STK33* were used: GCAGTTCAAGTTTACATCTA (2,078) GAACACATCATACATGGAA (2,079) and CTTGCCATTAACTTGCTGCTA (2,081). Hairpins targeting the following sequences in *KRAS* were used: GCAGACGTATATTGTATCATT (33,259) GAGGGCTTCTTTGTATT (33,260) and CCTATGGTCTAGTAGGAAAT (33,262).

**Cell Viability Assays.** Cells were plated in 384-well plates at optimized densities and incubated overnight prior to treatment. Compounds were added to cells using a CyBio Well Vario after which cells were cultured under standard condition for 72 h (unless stated otherwise). Cell viability was measured using CellTiter Glo luminescence (Promega) and readout using an LJL Biosystems Analyst microplate reader. Raw numbers were the normalized to the median of the DMSO treated wells for each plate.

1. Friday BB, Adjei AA (2005) K-ras as a target for cancer therapy. *Biochim Biophys Acta* 1756:127–144.
2. Karnoub AE, Weinberg RA (2008) Ras oncogenes: split personalities. *Nat Rev Mol Cell Biol* 9:517–531.
3. Downward J (2003) Targeting RAS signalling pathways in cancer therapy. *Nat Rev Cancer* 3:11–22.
4. Engelman JA, et al. (2008) Effective use of PI3K and MEK inhibitors to treat mutant Kras G12D and PIK3CA H1047R murine lung cancers. *Nat Med* 14:1351–1356.
5. Hartwell LH, Szankasi P, Roberts CJ, Murray AW, Friend SH (1997) Integrating genetic approaches into the discovery of anticancer drugs. *Science* 278:1064–1068.
6. Barbie DA, et al. (2009) Systematic RNA interference reveals that oncogenic KRAS-driven cancers require TBK1. *Nature* 462:108–112.
7. Luo J, et al. (2009) A genome-wide RNAi screen identifies multiple synthetic lethal interactions with the Ras oncogene. *Cell* 137:835–848.
8. Luo J, Solimini NL, Elledge SJ (2009) Principles of cancer therapy: oncogene and non-oncogene addiction. *Cell* 136:823–837.
9. Scholl C, et al. (2009) Synthetic lethal interaction between oncogenic KRAS dependency and STK33 suppression in human cancer cells. *Cell* 137:821–834.
10. Kinter M, Sherman NE (2000) *Protein Sequencing and Identification Using Tandem Mass Spectrometry* (Wiley-Interscience, New York).
11. Jaffe JD, et al. (2008) Accurate inclusion mass screening: a bridge from unbiased discovery to targeted assay development for biomarker verification. *Mol Cell Proteomics* 7:1952–1962.
12. Zhang JH, Chung TD, Oldenburg KR (1999) A simple statistical parameter for use in evaluation and validation of high throughput screening assays. *J Biomol Screen* 4:67–73.
13. Breitenlechner C, et al. (2003) Protein kinase A in complex with Rho-kinase inhibitors Y-27632, Fasudil, and H-1152P: structural basis of selectivity. *Structure* 11:1595–1607.
14. Brauksiepe B, et al. (2008) The Serine / threonine kinase STK33 exhibits autophosphorylation and phosphorylates the intermediate filament protein Vimentin. *BMC Biochem* 23:9–25.
15. Daub H, et al. (2008) Kinase-selective enrichment enables quantitative phosphoproteomics of the kinase across the cell cycle. *Mol Cell* 31:438–448.
16. Karaman MW, et al. (2008) A quantitative analysis of kinase inhibitor selectivity. *Nat Biotechnol* 26:127–132.
17. Capdeville R, Buchdunger E, Zimmermann J, Matter A (2002) Glivec (ST1571, imatinib), a rationally developed, targeted anticancer drug. *Nat Rev Drug Discov* 1:493–502.
18. Reichardt P, Reichardt A, Pink D (2011) Molecular targeted therapy of gastrointestinal stromal tumors. *Curr Cancer Drug Tar* 11:688–697.
19. Okamoto I, Mitsudomi T, Nakagawa K, Fukuoka M (2010) The emerging role of epidermal growth factor receptor (EGFR) inhibitors in first-line treatment for patients with advanced non-small cell lung cancer positive for EGFR mutations. *Therapeutic Advances in Medical Oncology* 2:301–307.
20. Flaherty KT, et al. (2010) Inhibition of mutated, activated BRAF in metastatic melanoma. *N Engl J Med* 363:809–819.
21. Sharma SV, Settleman J (2007) Oncogene addiction: setting the stage for molecularly targeted cancer therapy. *Genes Dev* 21:3214–3231.
22. Babij C, et al. (2011) STK33 kinase activity is non-essential in KRAS-dependent cancer cells. *Cancer Res* 71:5818–5826.
23. Prince JT, Ahn NG (2010) The case of the disappearing drug target. *Mol Cell* 37:455–456.
24. Hoshi N, et al. (2010) Interaction with AKAP79 modifies the cellular pharmacology of PKC. *Mol Cell* 37:541–550.

**Fig. 4.** MST4 and ERK kinase activity was used as surrogate biomarker and negative control for BRD8899, respectively. (A and B.) Nomo-1 cells were treated with the indicated concentrations of staurosporine, the farnesyl transferase inhibitor L744 (as positive controls) or the fasudil analog BRD8899 for 24 h. Samples were lysed and subjected to immunoblotting for phosphorylated and total levels of Ezrin (T576) and total MST4 (A) or phosphorylated and total levels of ERK (B). Quantifications for each lane were generated using ImageJ software. The normalized values to total protein levels are presented next to the blots.

**Protein Assays and Western Blotting.** Whole-cell lysates were prepared using a lysis buffer from Cell Signaling Technology (# 9803) and subjected to Western blotting according to standard procedures. The membranes were developed using a LI-COR Odyssey Infrared Imaging system, and the images were analyzed by Adobe Photoshop and ImageJ softwares. The following antibodies were used: anti-MST4 (Cell Signaling, #3822), anti-ezrin (Cell Signaling, #3245), anti-phospho-ezrin (Cell Signaling, #3141), anti-phospho-ERK (Cell Signaling, #437) and anti-ERK (Santa Cruz, #135900).

**ACKNOWLEDGMENTS.** We thank members of the Broad Institute Chemical Biology Platform for high throughput screening assistance. We also thank D. Gary Gilliland at Merck Research Laboratories and Robert J. Gould at Epizyme for helpful advice. This study was supported by a Starr Cancer Consortium grant. In addition, T.L. was supported by a grant from the National Institute of General Medical Sciences (GM38627 awarded to S.L.S.), K.M. was supported by the Swedish Research Council (Vetenskapsrådet), and C.S. was supported by an Emmy Noether Fellowship from the German Research Foundation. Support for these studies was also provided by the National Institutes of Health (NIH) Genomics Based Drug Discovery-Driving Medical Projects Grant RL1-GM084437 and RL1-CA133834, administratively linked to NIH grants RL1-HG004671 and UL1-DE019585.

## **Supporting Information**

### **STK33 kinase inhibitor BRD-8899 has no effect on KRAS-dependent cancer cell viability**

Tuoping Luo<sup>a,b,1</sup>, Kristina Masson<sup>a,1</sup>, Jacob D. Jaffe<sup>a</sup>, Whitney Silkworth<sup>a</sup>, Nathan T. Ross<sup>a,c</sup>, Christina A. Scherer<sup>a</sup>, Claudia Scholl<sup>d</sup>, Stefan Fröhling<sup>d</sup>, Steven A. Carr<sup>a</sup>, Andrew M. Stern<sup>a</sup>, Stuart L. Schreiber<sup>a,b,e,2</sup> and Todd R. Golub<sup>a,e,f,2</sup>

<sup>a</sup> Broad Institute of Harvard and MIT, 7 Cambridge Center, Cambridge, MA 02142 USA.

<sup>b</sup> Department of Chemistry and Chemical Biology, Harvard University, Cambridge, MA 02138 USA

<sup>c</sup> Current address: Novartis Institutes for BioMedical Research, 250 Massachusetts Avenue, Cambridge, MA 02142 USA.

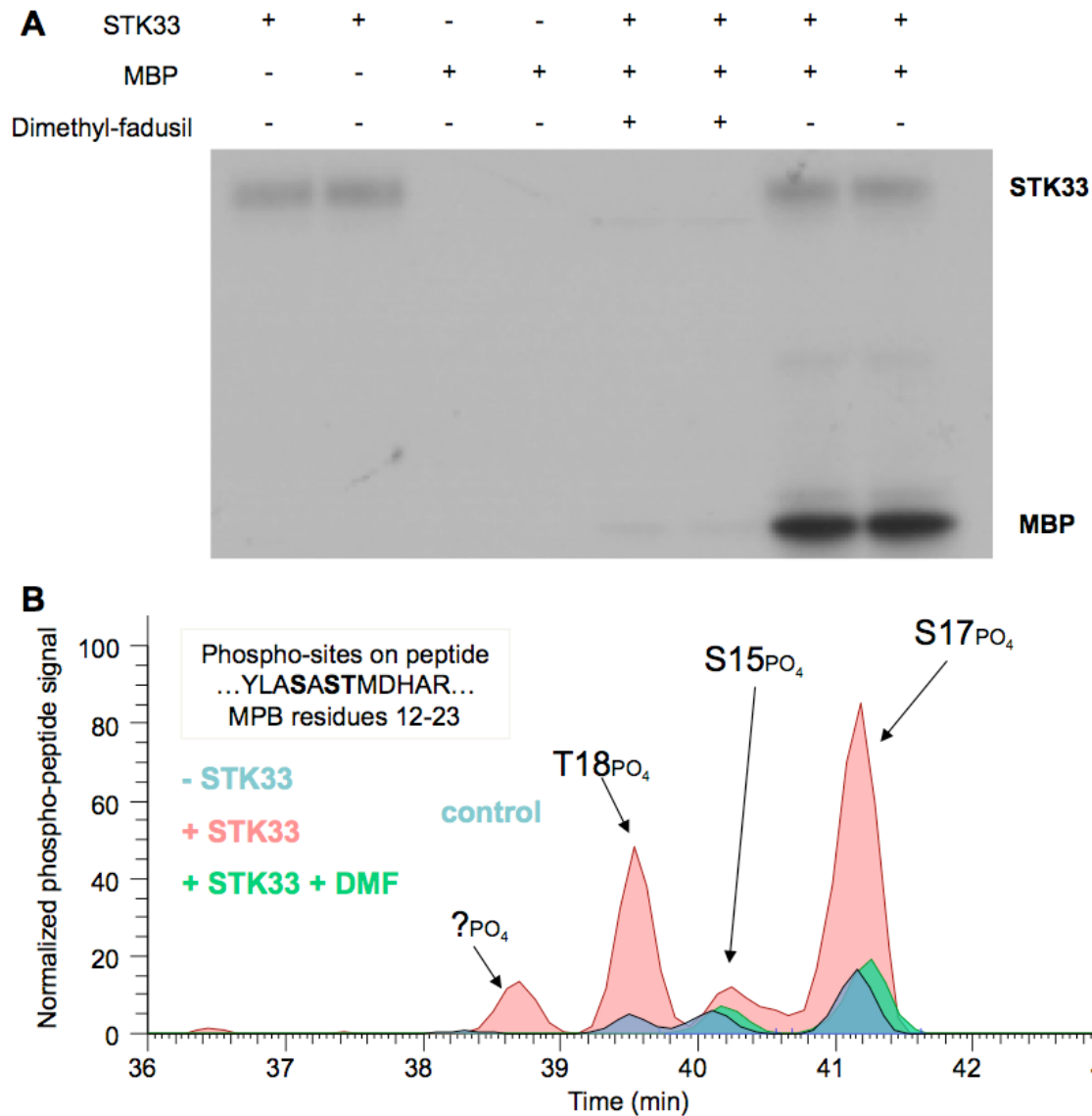
<sup>d</sup> Department of Internal Medicine III, University Hospital of Ulm, 89081 Ulm, Germany.

<sup>e</sup> Howard Hughes Medical Institute, Bethesda, MD 20881 USA.

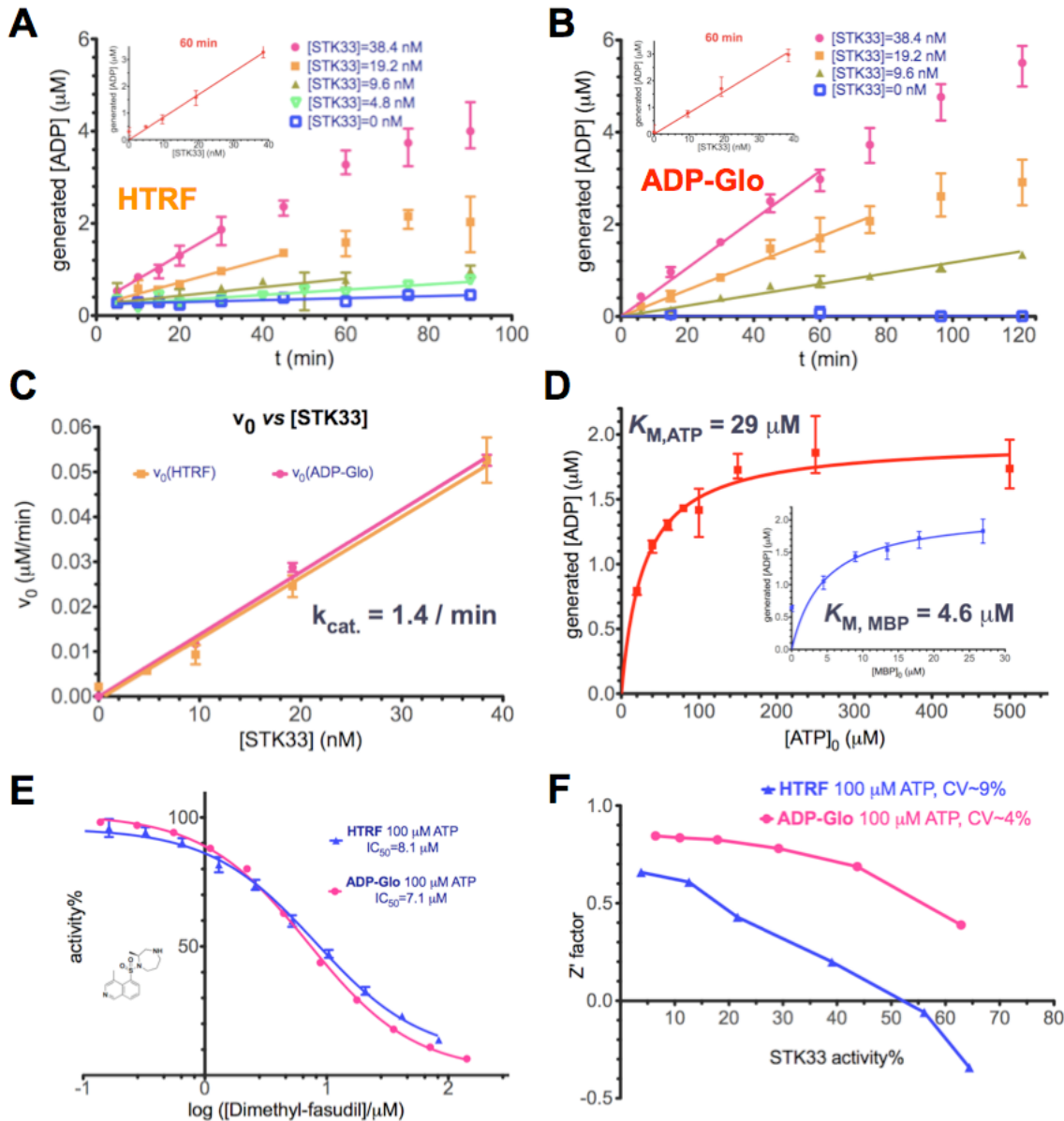
<sup>f</sup> Department of Pediatric Oncology, Dana-Farber Cancer Institute, Harvard Medical School, Boston, MA 02215 USA.

<sup>1</sup> These authors contributed equally to this work.

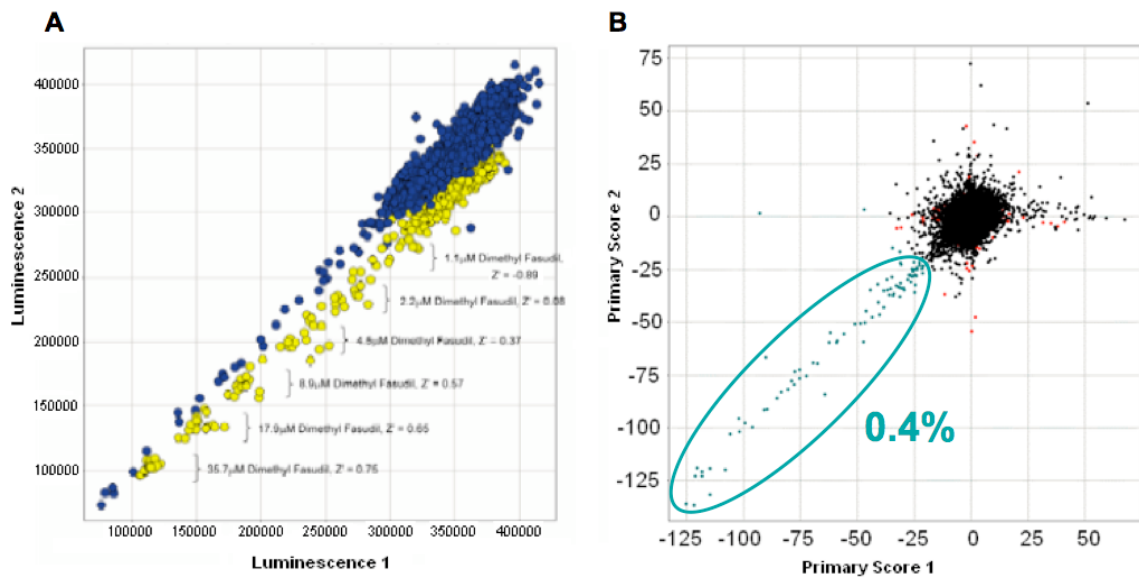
<sup>2</sup> To whom correspondence should be addressed. Stuart L. Schreiber tel: (617) 714-7080, fax: (617) 714-8969, [stuart\\_schreiber@harvard.edu](mailto:stuart_schreiber@harvard.edu), Todd R. Golub, tel: (617) 714-7050, fax: (617) 714-7059, [golub@broadinstitute.org](mailto:golub@broadinstitute.org)



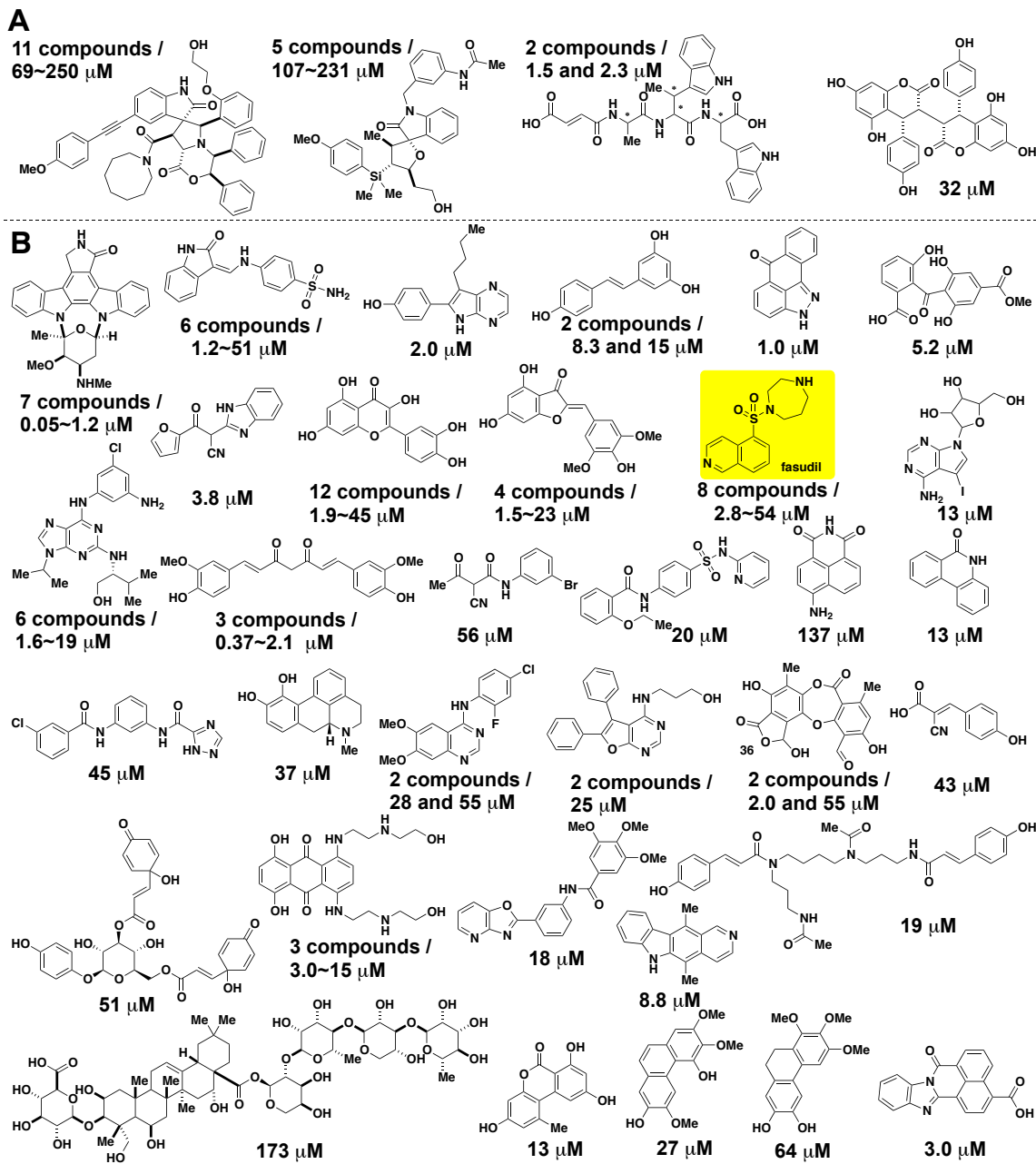
**Figure S1.** (A) Radiolabeled experiment confirming MBP phosphorylation and STK33 autophosphorylation. Kinase reactions were performed with 38.4 nM STK33, 24.5  $\mu$ M MBP, and 100  $\mu$ M ATP (28.6  $\mu$ Ci/mL [ $\gamma$ - $^{32}$ P]-ATP). Reactions were initiated by the addition of ATP and incubated at 24 °C for 60 minutes. (B) Mass spectrometry data confirming phosphorylation of MBP by STK33. Kinase reactions were performed with 38.4 nM STK33, 24.5  $\mu$ M MBP, and 100  $\mu$ M ATP, in the absence and presence of 20  $\mu$ M dimethylfasudil (DMF, **BRD7446**).



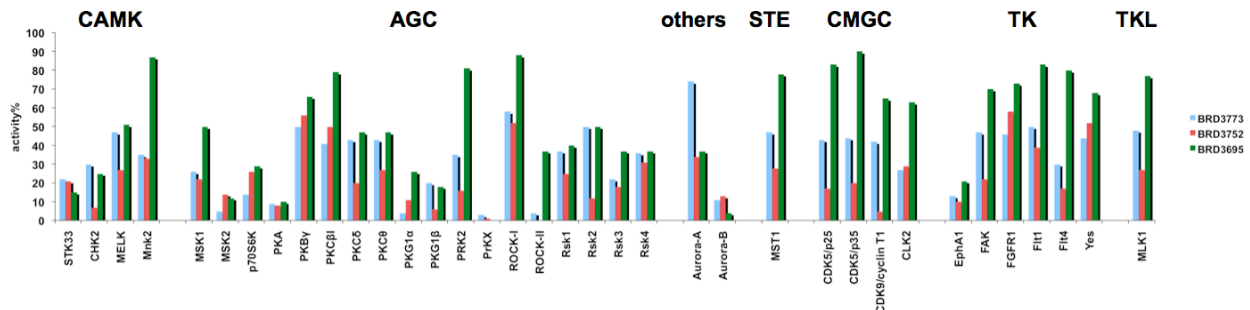
**Figure S2.** (A) The generation of ADP as a function of time and STK33 concentration (HTRF); (B) the generation of ADP as a function of time and STK33 concentration (ADP-Glo); (C) the initial velocity as a function of STK33 concentration; (D) determination of  $K_M$ ; (E) dose-response curves of dimethyl fasudil; (F) Z' factors. Kinase reactions were performed with 38.4 nM STK33, 24.5  $\mu\text{M}$  MBP, and 100  $\mu\text{M}$  or 500  $\mu\text{M}$  ATP. Reactions were initiated by the addition of ATP and incubated at 24 °C for 60~70 minutes. The error bars represent the range of 12 replicate values.



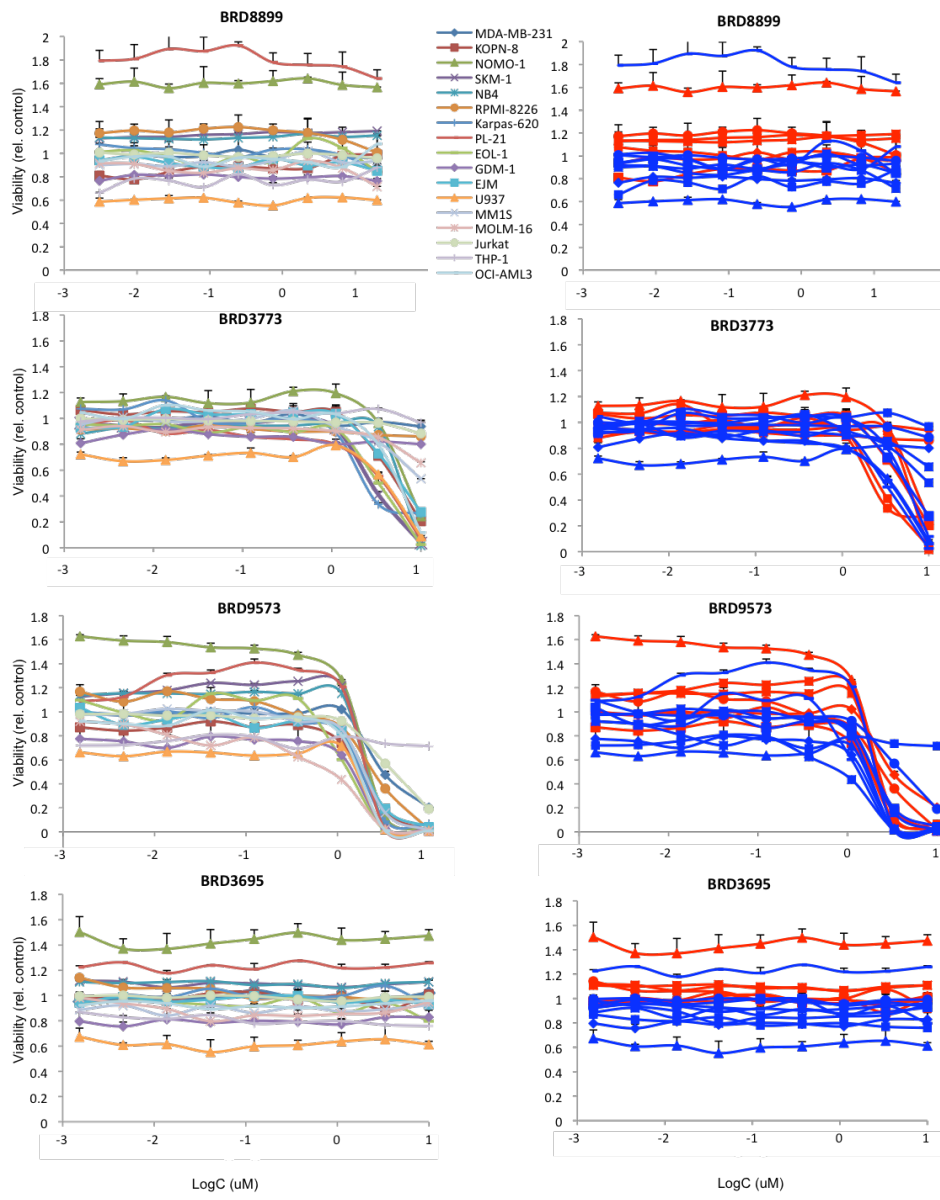
**Figure S3.** Results of plate replicates from the high throughput *in vitro* kinase screen. (A) Screen of 2,240 compounds under 100  $\mu$ M ATP as a validation set, dimethyl fasudil is shown in yellow; (B) HTS screen of 27,500 compounds under 100  $\mu$ M ATP, negative control DMSO is shown in red, and primary hits are shown in green. The hit rate is 0.4%. Negative control (DMSO) is scaled to 0, whereas positive control (89  $\mu$ M dimethyl fasudil, 90% inhibition) is scaled to -100.



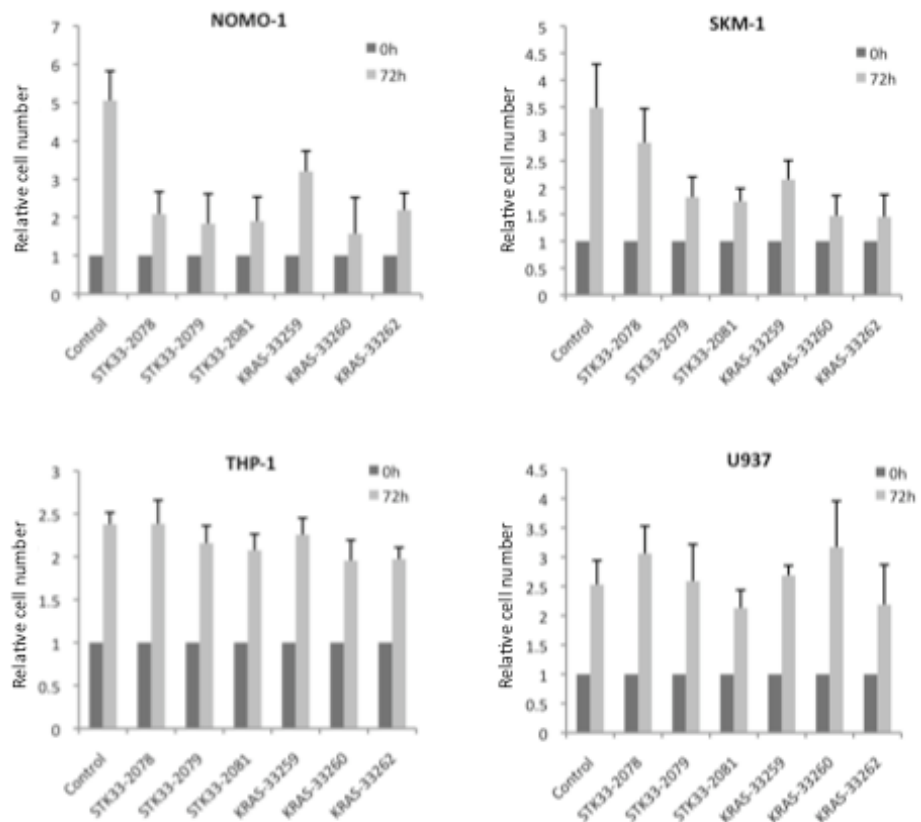
**Figure S4.** Clustering of primary hits and IC<sub>50</sub> under 25  $\mu\text{M}$  ATP. (A) ATP-noncompetitive inhibitors; (B) representative ATP-competitive inhibitors.



**Figure S5.** Biochemical kinase profiling of compounds **BRD3773**, **BRD3752** and **BRD3695** (2.5  $\mu$ M) against 36 kinases under [ATP]= $K_{M,ATP}$ . Y axial: the percent of kinase activity remained in the presence of the inhibitor.



**Figure S6. Cell viability assay for fasudil analogs BRD8899, BRD3773, BRD9573 and BRD3695.** Dose-response curves of the indicated cell lines using CellTiter Glo as a measurement for viability. The luminescence values of each compound treatment divided by the median of all DMSO values for each individual cell line was taken as a measurement of relative viability. Error bars represent the standard deviation of three replicates. Curves to the left are color coded based on cell line and the right ones are the same plots, but showing KRAS mutant and KRAS wild-type cell lines depicted in red or blue, respectively.

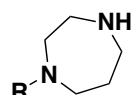
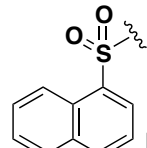
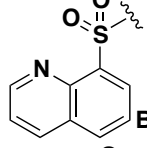
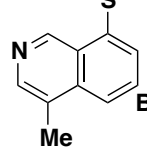
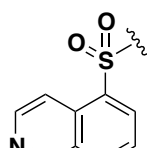
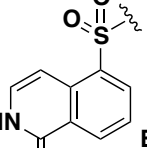
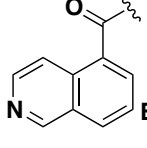


**Figure S7. Effects of different *STK33* and *KRAS* shRNAs on cell viability.** NOMO-1, SKM-1 (KRAS mutant), THP-1 and U937 (KRAS wild type) cells were transduced with shRNAs constructs targeting different regions of the *STK33* or *KRAS* transcripts, as well as with a nontargeting control shRNA. Cell number was measured using CellTiter Glo on days 4 (0 h) and 8 (72 h) post transduction. Experiments were performed in triplicate. All samples are normalized to time point 0h and are represented as mean  $\pm$  SEM.

**Table S1.** Compound sources

Library Name	Compound Number	Hit Number
Commercial collection	1280	1
Natural products	1920	41
Bioactives	2560	61
Structural diversity (DOS)	960	0
Chemical biology library initiative (DOS)	9600	0
Kinase-biased	11520	8

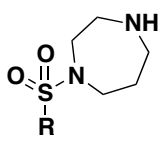
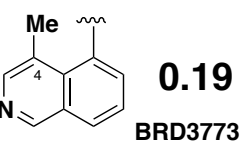
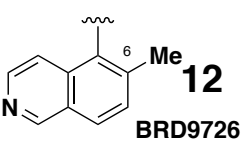
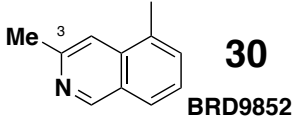
**Table S2.**

		
R	IC <sub>50</sub> (μM) @ 25 μM ATP	IC <sub>50</sub> (μM) @ 100 μM ATP
 BRD5288	>186	>186
 BRD1651	>186	>186
 BRD4469	>186	>186
R	IC <sub>50</sub> (μM) @ 25 μM ATP	IC <sub>50</sub> (μM) @ 100 μM ATP
 fasudil BRD7868	14	29
 BRD6825	5.3	11
 BRD0811	>186	>186

**Table S3.**

R	IC <sub>50</sub> (μM) @ 25 μM ATP	IC <sub>50</sub> (μM) @ 100 μM ATP	R	IC <sub>50</sub> (μM) @ 25 μM ATP	IC <sub>50</sub> (μM) @ 100 μM ATP
	<b>BRD2998</b> <b>&gt;186</b>	<b>&gt;186</b>		<b>BRD2751</b> <b>29</b>	<b>64</b>
	<b>BRD4220</b> <b>110</b>	<b>&gt;186</b>		<b>BRD7527</b> <b>&gt;186</b>	<b>&gt;186</b>
	<b>BRD7390</b> <b>&gt;186</b>	<b>&gt;186</b>		<b>BRD9836</b> <b>&gt;186</b>	<b>&gt;186</b>
	<b>BRD6818</b> <b>&gt;186</b>	<b>&gt;186</b>		<b>BRD3518</b> <b>26</b>	<b>60</b>
	<b>BRD0188</b> <b>&gt;186</b>	<b>&gt;186</b>		<b>BRD9802</b> <b>36</b>	<b>175</b>

**Table S4.**

					
R	IC <sub>50</sub> (μM) @ 25 μM ATP	IC <sub>50</sub> (μM) @ 100 μM ATP	R	IC <sub>50</sub> (μM) @ 25 μM ATP	IC <sub>50</sub> (μM) @ 100 μM ATP
	<b>0.19</b> BRD3773	<b>0.56</b>		<b>26</b> BRD9726	
	<b>&gt;186</b> BRD6042	<b>&gt;186</b>		<b>9.1</b> BRD5087	<b>20</b>
	<b>30</b> BRD9852	<b>51</b>		<b>176</b> BRD5257	<b>205</b>

**Table S5.**

R	IC <sub>50</sub> (μM) @ 25 μM ATP	IC <sub>50</sub> (μM) @ 100 μM ATP	R	IC <sub>50</sub> (μM) @ 25 μM ATP	IC <sub>50</sub> (μM) @ 100 μM ATP
H fasudil BRD7868	<b>14</b>	<b>29</b>	Br BRD8880	<b>24</b>	<b>49</b>
Me BRD3773	<b>0.19</b>	<b>0.56</b>	NH <sub>2</sub> BRD2749	<b>21</b>	<b>39</b>
Me BRD5930	<b>0.28</b>	<b>0.81</b>	HO BRD7648	<b>21</b>	<b>71</b>
Cyclopropyl BRD5796	<b>0.24</b>	<b>0.68</b>	OH BRD5505	<b>95</b>	<b>203</b>
Fluoromethyl BRD8757	<b>0.48</b>	<b>1.1</b>	O=CH BRD4734	<b>6.9</b>	<b>18</b>
Allyl BRD7032	<b>0.94</b>	<b>2.9</b>	Me C(=O)NH BRD0859	<b>26</b>	<b>74</b>
Propyl BRD7132	<b>1.6</b>	<b>3.2</b>	CO <sub>2</sub> Me BRD7198	<b>13</b>	<b>44</b>
Isobutyl BRD9078	<b>4.0</b>	<b>8.6</b>			

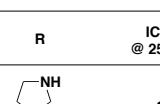
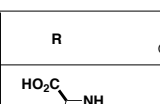
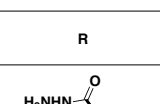
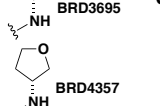
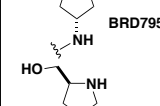
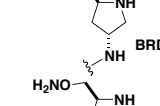
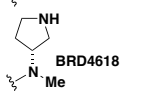
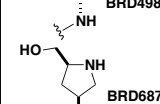
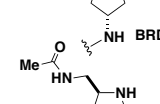
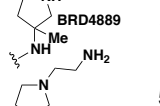
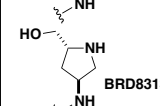
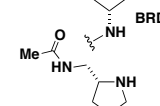
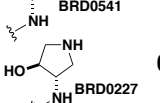
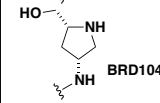
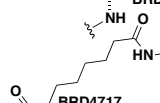
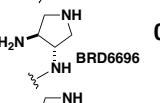
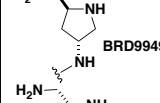
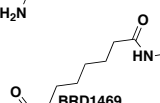
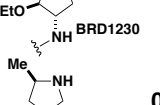
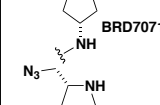
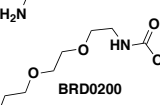
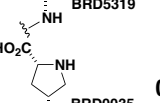
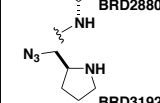
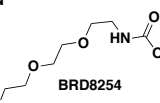
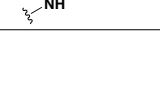
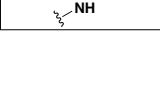
**Table S6.**

A	Compound	IC <sub>50</sub> (μM) @ 25 μM ATP	IC <sub>50</sub> (μM) @ 100 μM ATP	A	Compound	IC <sub>50</sub> (μM) @ 25 μM ATP	IC <sub>50</sub> (μM) @ 100 μM ATP	A	Compound	IC <sub>50</sub> (μM) @ 25 μM ATP	IC <sub>50</sub> (μM) @ 100 μM ATP
	BRD7657 (R = H)	14	29		BRD7868 (R = H)	14	29		BRD2246 (R = H)	201	>714
	BRD5549 (R = Me)	1.6	3.2		BRD3773 (R = Me)	0.19	0.56		BRD7471 (R = Me)	4.2	11
	BRD4220 (R = H)	110	>186		BRD7364 (R = H)	71	>186		BRD2751 (R = H)	29	64
	BRD3610 (R = Me)	11	25		BRD9027 (R = Me)	1.7	4.1		BRD9575 (R = Me)	0.79	1.9
	BRD4153 (R = H)	>186	>186		BRD0322 (R = H)	23	30		BRD2297 (R = H)	16	31
	BRD9391 (R = Me)	52	>186		BRD5419 (R = Me)	1.2	2.1		BRD4942 (R = Me)	1.4	4.2
	BRD7647 (R = H)	2.2	6.6		BRD0112 (R = H)	15	46		BRD0841 (R = H)	6.1	16
	BRD9330 (R = Me)	2.1	4.6		BRD9740 (R = Me)	2.0	3.6		BRD3376 (R = Me)	1.6	2.6
	BRD4009 (R = H)	1.0	2.1		BRD1742 (R = Me)	2.7	5.3		BRD1199 (R = H)	62	>186
	BRD3407 (R = Me)	3.7	6.4		BRD3590 (R = H)	9.3	24		BRD3436 (R = Me)	1.2	2.8
	BRD8531 (R = H)	46	98		BRD3752 (R = Me)	0.047	0.13		BRD3033 (R = H)	13	31
	BRD6995 (R = Me)	1.8	4.7		BRD3490 (R = H)	16	41		BRD2668 (R = Me)	2.6	5.6
	BRD9091 (R = H)	>186	>186		BRD0828 (R = Me)	3.7	13		BRD0561 (R = H)	36	78
	BRD7177 (R = Me)	35	89		BRD3501 (R = H)	7.1	16		BRD4209 (R = Me)	0.99	1.5
	BRD5149 (R = H)	8.6	16		BRD3695 (R = Me)	0.063	0.17		BRD3518 (R = H)	26	60
	BRD8198 (R = Me)	2.8	6.6		BRD8943 (R = H)	10	39		BRD2986 (R = Me)	1.2	2.8
	BRD4958 (R = H)	7.4	19		BRD9573 (R = Me)	4.8	10		BRD5717 (R = H)	38	96
	BRD3966 (R = Me)	0.29	0.57		BRD7481 (R = H)	397	>714		BRD7682 (R = Me)	7.9	16
	(R = H)	--	--		(R = Me)	--	--		BRD2594 (R = H)	16	47
	BRD9325 (R = Me)	0.65	1.2		BRD7425 (R = H)	>714	>714		BRD5731 (R = Me)	2.3	5.1
	BRD5991 (R = H)	19	42		(R = Me)	--	--		BRD4209 (R = Me)	0.99	1.5
	BRD5337 (R = Me)	0.84	1.3								

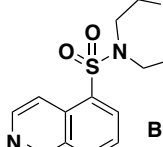
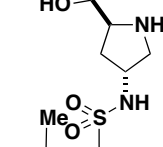
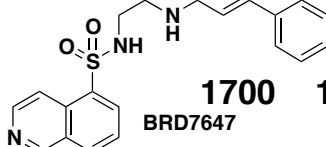
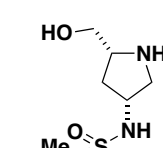
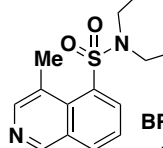
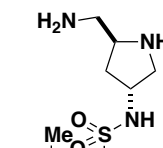
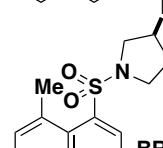
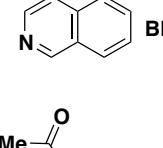
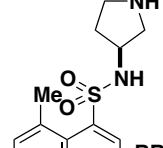
**Table S7.**

Kinase	activity%	Kinase	activity%	Kinase	activity%	Kinase	activity%
PrKX(h)	3	ALK4(h)	70	ASK1(h)	95	PDGFR $\beta$ (h)	105
PKG1 $\alpha$ (h)	4	SGK2(h)	70	MAPKAP-K2(h)	95	HIPK2(h)	106
ROCK-II(h)	4	Fyn(h)	71	NEK11(h)	95	HIPK3(h)	106
MSK2(h)	5	CaMKII $\beta$ (h)	72	TrkB(h)	95	IKK $\alpha$ (h)	106
PKA(h)	9	FGFR2(h)	72	IGF-1R(h)	96	MAPK1(h)	106
Aurora-B(h)	11	PhK $\gamma$ 2(h)	72	IKK $\beta$ (h)	96	PKC $\gamma$ (h)	106
EphA1(h)	13	CaMKII $\delta$ (h)	73	PKB $\alpha$ (h)	96	Src(T341M)(h)	106
p70S6K(h)	14	EphA2(h)	73	WNK3(h)	96	Ab1(h)	107
PKG1 $\beta$ (h)	20	Plk3(h)	73	EphA8(h)	97	EGFR(h)	107
Rsk3(h)	22	Aurora-A(h)	74	JAK3(h)	97	HIPK1(h)	107
STK33(h)	22	GRK5(h)	74	Rse(h)	97	MAPK2(h)	107
MSK1(h)	26	ARK5(h)	76	SRPK1(h)	97	NEK7(h)	107
CLK2(h)	27	Lyn(h)	77	WNK2(h)	97	PAK2(h)	107
CHK2(h)	30	GRK6(h)	79	CDK6/cyclinD3(h)	98	PIP4K2 $\alpha$ (h)	107
Flt4(h)	30	TAO3(h)	81	IRR(h)	98	PRAK(h)	107
Mnk2(h)	35	CLK3(h)	82	PIP5K1 $\alpha$ (h)	98	ALK(h)	108
PRK2(h)	35	FGFR4(h)	82	Ron(h)	98	IR(h), activated	108
Rsk4(h)	36	BrSK1(h)	84	CaMKII $\gamma$ (h)	99	MSSK1(h)	108
Rsk1(h)	37	CDK2/cyclinE(h)	84	DYRK2(h)	99	PAK4(h)	108
PKC $\beta$ II(h)	41	JNK3(h)	84	Fer(h)	99	PDGFR $\alpha$ (h)	108
CDK9/cyclin T1(h)	42	Lck(h)	84	PI3 Kinase (p110 $\beta$ /p85 $\alpha$ )(h)	99	PI3 Kinase (p110 $\gamma$ )(b)	108
CDK5/p25(h)	43	PI3KC2 $\alpha$ (h)	84	PIP5K1 $\gamma$ (h)	99	CK1 $\gamma$ 2(h)	109
PKC $\delta$ (h)	43	CaMKIV(h)	85	PKB $\beta$ (h)	99	DAPK2(h)	109
PKC $\theta$ (h)	43	MST2(h)	85	TAO2(h)	99	mTOR/FKBP12(h)	109
CDK5/p35(h)	44	Axl(h)	86	TBK1(h)	99	ACK1(h)	110
Yes(h)	44	BRK(h)	86	Tec(h) activated	99	CSK(h)	110
FGFR1(h)	46	cSRC(h)	87	TLK2(h)	99	MEK1(h)	110
FAK(h)	47	PAK3(h)	87	Arg(h)	100	NEK6(h)	110
MELK(h)	47	Snk(h)	87	SAPK2b(h)	100	PAK6(h)	110
MST1(h)	47	CDK1/cyclinB(h)	88	BTK(h)	101	CK1 $\gamma$ 3(h)	111
MLK1(h)	48	MARK1(h)	88	DMPK(h)	101	CK2 $\alpha$ 2(h)	111
Flt1(h)	50	MST3(h)	88	EphA4(h)	101	DAPK1(h)	111
PKB $\gamma$ (h)	50	PDK1(h)	88	Flt3(h)	101	ZAP-70(h)	111
Rsk2(h)	50	ULK2(h)	88	Hck(h) activated	101	CaMKI(h)	112
AMPK $\alpha$ 2(h)	51	VRK2(h)	88	MAPKAP-K3(h)	101	SAPK2a(h)	112
BrSK2(h)	51	Lck(h) activated	89	MKK4(m)	101	cKit(h)	113
TAO1(h)	52	MKK6(h)	89	MLCK(h)	101	ErbB4(h)	113
LOK(h)	54	NLK(h)	90	Syk(h)	101	GSK3 $\alpha$ (h)	113
Mer(h)	54	Pyk2(h)	90	ZIPK(h)	101	Itk(h)	113
Fes(h)	56	SAPK4(h)	90	MINK(h)	102	JNK1 $\alpha$ 1(h)	113
PKC $\eta$ (h)	56	IRAK1(h)	91	NEK2(h)	102	MuSK(h)	113
Fgr(h)	57	PASK(h)	91	Pim-1(h)	102	Pim-3(h)	113
KDR(h)	57	DCAMKL2(h)	92	PKC $\epsilon$ (h)	102	Ros(h)	114
PTK5(h)	57	EphA5(h)	92	RIPK2(h)	102	SRPK2(h)	114
GRK7(h)	58	PKC $\alpha$ (h)	92	Txk(h)	102	mTOR(h)	115
ROCK-I(h)	58	SGK3(h)	92	CK1 $\gamma$ 1(h)	103	GSK(h)	115
Src(1-530)(h)	58	Bmx(h)	93	c-RAF(h)	103	CHK1(h)	116
PKC $\beta$ II(h)	59	CDK3/cyclinE(h)	93	PAK5(h)	103	CK2(h)	116
CDK7/cyclinH/MAT1(h)	60	EphA7(h)	93	PI3 Kinase (p110 $\beta$ /p85 $\alpha$ )(h)	103	IR(h)	116
SIK(h)	60	EphB2(h)	93	Tie2(h)	103	CaMKI $\delta$ (h)	117
TrkA(h)	60	EphB4(h)	93	CK1 $\delta$ (h)	104	JNK2 $\alpha$ 2(h)	118
GCK(h)	61	GSK3 $\beta$ (h)	93	eEF-2K(h)	104	TSSK2(h)	119
LIMK1(h)	62	LKB1(h)	93	EphB3(h)	104	Pim-2(h)	120
AMPK $\alpha$ 1(h)	63	PKC $\zeta$ (h)	93	IGF-1R(b), activated	104	MKK7 $\beta$ (b)	122
Hck(h)	64	TAK1(h)	93	IRAK4(h)	104	DDR2(h)	123
Ret(h)	64	ULK3(h)	93	MRCK $\beta$ (h)	104	JAK2(h)	136
PKC $\mu$ (h)	66	CDK2/cyclinA(h)	94	PAR-1Ba(h)	104	Fms(h)	149
FGFR3(h)	67	DRAK1(h)	94	SAPK3(h)	104	TSSK1(h)	195
EphB1(h)	68	Met(h)	94	EphA3(h)	105		
Haspin(h)	69	PKD2(h)	94	MRCK $\alpha$ (h)	105		
PKC $\epsilon$ (h)	69	Plk1(h)	94	NEK3(h)	105		

**Table S8.**

								
R	IC <sub>50</sub> (μM) @ 25 μM ATP	IC <sub>50</sub> (μM) @ 100 μM ATP	R	IC <sub>50</sub> (μM) @ 25 μM ATP	IC <sub>50</sub> (μM) @ 100 μM ATP	R	IC <sub>50</sub> (μM) @ 25 μM ATP	IC <sub>50</sub> (μM) @ 100 μM ATP
	<b>0.063</b>	0.17		<b>1.8</b>	3.7		2.0	4.6
	<b>32</b>	56		<b>0.037</b>	0.090		<b>0.067</b>	0.15
	<b>1.2</b>	3.2		<b>2.8</b>	9.2		<b>0.011</b>	0.025
	<b>2.7</b>	9.2		<b>0.81</b>	3.2		<b>0.52</b>	1.2
	<b>5.9</b>	10		<b>0.12</b>	0.25		<b>0.073</b>	0.14
	<b>0.54</b>	1.6		<b>0.020</b>	0.032		<b>0.061</b>	0.13
	<b>0.42</b>	1.7		<b>0.42</b>	0.87		<b>0.084</b>	0.21
	<b>4.2</b>	12		<b>0.24</b>	0.53		<b>0.037</b>	0.11
	<b>0.065</b>	0.14		<b>0.78</b>	2.2		<b>0.26</b>	1.0

**Table S9.** Comparison of the biochemical  $K_i$  with  $K_d$  in the Ambit binding assay

Compound	Biochemical $K_i$ (nM)	Ambit $K_d$ (nM)	Compound	Biochemical $K_i$ (nM)	Ambit $K_d$ (nM)
 <b>BRD7868</b>	<b>6800</b>	<b>4600</b>	 <b>BRD4980</b>	<b>25</b>	<b>14</b>
 <b>BRD7647</b>	<b>1700</b>	<b>1300</b>	 <b>BRD1045</b>	<b>74</b>	<b>43</b>
 <b>BRD3773</b>	<b>89</b>	<b>130</b>	 <b>BRD9949</b>	<b>14</b>	<b>29</b>
 <b>BRD3752</b>	<b>35</b>	<b>120</b>	 <b>BRD8899</b>	<b>2.6</b>	<b>11</b>
 <b>BRD3695</b>	<b>20</b>	<b>32</b>			
 <b>BRD9573</b>	<b>3700</b>	<b>3200</b>			

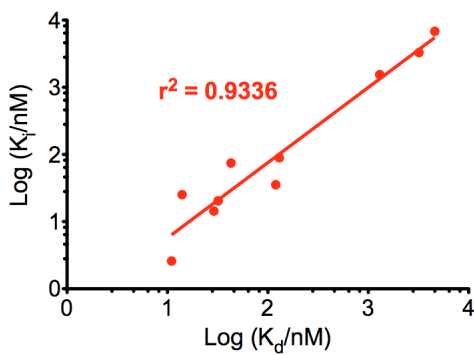


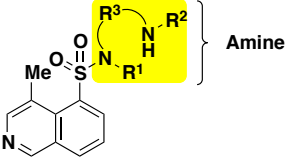
**Table S10.**

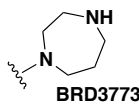
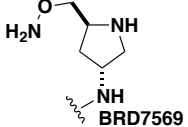
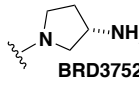
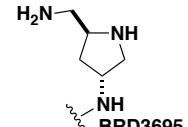
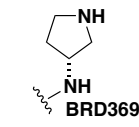
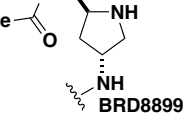
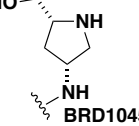
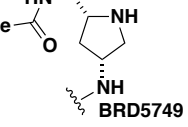
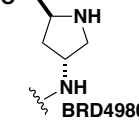
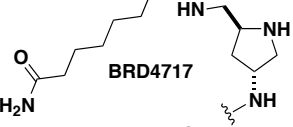
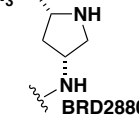
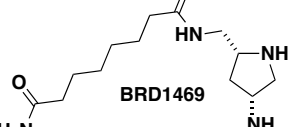
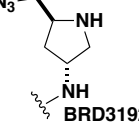
KINOMEscan Gene Symbol	Control%	KINOMEscan Gene Symbol	Control%	KINOMEscan Gene Symbol	Control%
RIOK1	2.6	DCAMKL1	74	JNK2	90
MST4	4	PKN2	74	p38-gamma	90
STK33	11	RSK1(Kin Dom 2-C-terminal)	74	PKAC-beta	90
RSK4(Kin Dom 1-N-terminal)	11	TESK1	74	SIK2	90
AKT1	15	BRSK1	75	SNARK	90
KIT(D816V)	15	EPHA2	75	TIE1	90
ROCK1	16	ABL1(E255K)-phosphorylated	76	ULK1	90
FLT3(TID)	19	EPHB1	76	ULK3	90
EPHA1	20	FAK	76	CAMK2G	91
FLT3(D835Y)	20	PRKCO	76	DYRK1B	91
PRKCE	21	RAF1	76	EPHAS	91
PRKCD	22	CSNK1A1	77	MYLK2	91
ROCK2	23	FRK	77	BMX	92
PRKX	25	MEK3	77	CDEKL2	92
ABL1(H396P)-monophosphorylated	27	EGFR(L861Q)	78	CDEKL3	92
PIP3K1A	32	FGFR1	78	FLT3(D835H)	92
MST2	35	INSR	78	MAPMK4	92
NEK5	36	IRAK4	78	MARK1	92
GRK7	38	TYK2(JH1domain-catalytic)	78	MKK7	92
ULK1	38	CDK11	79	MLK2	92
ABL1(T313I)-phosphorylated	40	ZAK	79	MRCKA	92
LZK	40	ABL1-nonphosphorylated	80	PIK3CA(1800L)	92
ABL1-phosphorylated	41	KIT(D816H)	80	PRP4	92
S6K1	41	PRKD3	80	STK36	92
MST3	42	SRPK3	80	TRKA	92
PHKG2	43	DCAMKL1	81	AKT2	93
RIOK3	43	MARK4	81	EGFR(E746-A750del)	93
ABL1(F317L)-phosphorylated	44	PIP3K1C	81	EGFR(L747-S752del_P753S)	93
JAK3(JH1 domain-catalytic)	45	FES	82	PLK2	93
PLK4	47	KIT(V59D)	82	ABL1(F317I)-monophosphorylated	94
FLT3	48	MARK2	82	ABL1(Q252H)-monophosphorylated	94
MERTK	48	MST1R	82	ADCK4	94
MET(M1250T)	48	PAK7	82	EPHA5	94
DLK	50	CLK1	83	EPHA7	94
PRAC-alpha	52	CSEFR	83	GRK4	94
B1KE	55	PIK3B(M.tuberculosis)	83	IRAK1	94
CAMKK2	56	JNK1	84	MARK3	94
FLT3(N841I)	56	LYN	84	p38-beta	94
TBK1	56	PDPK1	84	RIOK2	94
AURKB	57	PRKG1	84	LRRK2(G2019S)	95
RSK2(Kin Dom 1-N-terminal)	57	EPHA6	85	PFTAIRE2	95
ABL1(F317L)-nonphosphorylated	58	GRK1	85	PIK3CB	95
EPHA3	58	PIK3CG	85	SRMS	95
AURKC	59	PYK2	85	EGFR(L747-T751del_Sims)	96
HIPK1	59	CDK3	86	EPHB3	96
MAP4K3	59	EGFR(T790M)	86	ERBB4	96
IRAK3	60	ERK3	86	GAK	96
SRC	61	HIPK4	86	PCTK1	96
ABL1(H396P)-phosphorylated	62	JAK1(JH1 domain-catalytic)	86	RIPK4	96
PHKG1	63	PIP3K2B	86	TAK1	96
AKT3	65	SLK	86	OSR1	97
CDEK7	65	TAOK1	86	RIPK1	97
YSK1	66	TGFBR1	86	BMPR2	98
ABL1(M351T)-phosphorylated	67	TLK1	86	EGFR(L838R)	98
ABL1(Q252H)-phosphorylated	67	TNNI3K	86	LATS1	98
ABL1(Y253F)-phosphorylated	67	CSNK1A1	87	MYO3B	98
RSK3(Kin Dom 2-C-terminal)	67	HPK1	87	YANK3	98
MELK	68	LDMK2	87	CDK8	99
TRPM6	68	MAP3K4	87	DMPK2	99
RET(M518T)	69	RSK1(Kin Dom 1-N-terminal)	87	EPHB3	99
KIT(V59D,I670I)	70	ANKK1	88	EPHB6	99
PDGFRB	70	EGFR(G719C)	88	LATS2	99
RSK4(Kin Dom 2-C-terminal)	70	MAP4K5	88	ROS1	99
STK35	70	PRKCH	88	ABL1(F317I)-phosphorylated	100
KIT	71	DAPK1	89	ABL1(T313I)-nonphosphorylated	100
TRKB	71	KIT(L716P)	89	ABL2	100
ERN1	72	MAP3K3	89	ACVR1	100
FGR	72	MAP4K2	89	ACVR1B	100
CDR2	73	PIK3CA(E542K)	89	ACVR1L	100
WEE2	73	PRKG2	89	ADCK3	100
AAK1	74	ACVR1A	90	ALK	100
ACVR1B	74	CAMK1G	90	AMPK-alpha1	100
AXL	74	FGFR2	90	AMPK-alpha2	100
CDKL1	74	FGFR4	90	ARK3	100

**Table S10 (continued).**

KINOMEscan Gene Symbol	Control%	KINOMEscan Gene Symbol	Control%	KINOMEscan Gene Symbol	Control%
ASK1	100	FYN	100	PDGFRα	100
ASK2	100	GCN2(Kin Dom.2,SB08G)	100	PFCDPK1(Pfalciparum)	100
AURKA	100	GSK3A	100	PFPK1(Pfalciparum)	100
BLK	100	GSK3B	100	PFTK1	100
BMPR1A	100	HCK	100	PIK3C2B	100
BMPR1B	100	HIPK2	100	PIK3C2G	100
BRAF	100	HIPK3	100	PIK3CA	100
BRAF(V600E)	100	HUNK	100	PIK3CA(C420R)	100
BRK	100	ICK	100	PIK3CA(E545A)	100
BRSK2	100	IGF1R	100	PIK3CA(E545K)	100
BTK	100	IKK-alpha	100	PIK3CA(H1047L)	100
CAMK1	100	IKK-beta	100	PIK3CA(H1047Y)	100
CAMK1D	100	IKK-gamma	100	PIK3CA(M104S)	100
CAMK1A	100	INSR	100	PIK3CA(Q546K)	100
CAMK1B	100	ITR	100	PIK3CD	100
CAMK1D	100	JAK1(JH1 domain-catalytic)	100	PIK4CB	100
CAMK4	100	JAK1(JH2 domain-pseudokinase)	100	PIM1	100
CAMKK1	100	JNK3	100	PIM2	100
CASK	100	KIT(A829P)	100	PIM3	100
CDC2L1	100	KIT(V559D-V654A)	100	PIP5K1C	100
CDC2L2	100	LCK	100	PKM1T1	100
CDC2L5	100	LIMK1	100	PKN1	100
CDK4-cyclinD1	100	LKB1	100	PLK1	100
CDK4-cyclinD3	100	LOK	100	PLK3	100
CDK5	100	LRRK2	100	PRKCI	100
CDK9	100	LTK	100	PRKD1	100
CDKL5	100	MAK	100	PRKD2	100
CHEK1	100	MAP3K1	100	PRKR	100
CHEK2	100	MAP3K15	100	QSK	100
CIT	100	MAP3K2	100	RET	100
CLK2	100	MAPKAPK2	100	RET(V804L)	100
CLK3	100	MAPKAPK5	100	RET(V804M)	100
CLK4	100	MAST1	100	RIPK2	100
CSK	100	MEK1	100	RIPK5	100
CSNK1A1L	100	MEK2	100	RP56KA4(Kin Dom. 1-N-terminal)	100
CSNK1D	100	MEK4	100	RP56KA4(Kin Dom. 2-C-terminal)	100
CSNK1E	100	MEK5	100	RP56KA5(Kin Dom. 1-N-terminal)	100
CSNK1G1	100	MET	100	RP56KA5(Kin Dom. 2-C-terminal)	100
CSNK1G2	100	MET(Y1235D)	100	RSK3(Kin Dom. 1-N-terminal)	100
CSNK1G3	100	MINK	100	SBK1	100
CSNK1A2	100	MKNK1	100	S6k110	100
CTK	100	MKNK2	100	SGK3	100
DAPK2	100	MLCK	100	SIK	100
DAPK3	100	MLK1	100	SNRK	100
DCAMKL3	100	MLK3	100	SRPK1	100
DDR1	100	MRCKB	100	SRPK2	100
DDR2	100	MST1	100	STK16	100
DMPK	100	MTOR	100	STK39	100
DRAK1	100	MUSK	100	SYK	100
DRAK2	100	MYLK	100	TAOK2	100
DYRK1A	100	MYLK4	100	TAOK3	100
DYRK2	100	MYO3A	100	TEC	100
EGFR	100	NDR1	100	TGFBR2	100
EGFR(G719S)	100	NDR2	100	TIE2	100
EGFR(L747-E749del, A750P)	100	NEK1	100	TLK2	100
EGFR(L858R, T790M)	100	NEK11	100	TNK1	100
EGFR(S732-T739del)	100	NEK2	100	TNK2	100
EIF2AK1	100	NEK3	100	TRKC	100
EPHA4	100	NEK4	100	TSSK1B	100
EPHB4	100	NEK6	100	TTK	100
ERBB2	100	NEK7	100	TXK	100
ERBB3	100	NEK9	100	TYK2(JH1 domain-pseudokinase)	100
ERK1	100	NTM1	100	TYRO3	100
ERK2	100	NLK	100	VEGFR2	100
ERK4	100	p38-alpha	100	VRK2	100
ERK5	100	p38-delta	100	WEE1	100
ERK8	100	PAK1	100	YANK1	100
FER	100	PAK2	100	YANK2	100
FGFR3	100	PAK3	100	YES	100
FGFR3(G697C)	100	PAK4	100	YSK4	100
FLT1	100	PAK6	100	ZAP70	100
FLT3(K663Q)	100	PCTK2	100		
FLT3(R834Q)	100	PCTK3	100		
FLT4	100				

**Table S11.**



Amine	STK33	AurB	Amine	STK33	AurB
	<b>0.19</b>	<b>0.31</b>		<b>0.067</b>	<b>0.19</b>
	<b>0.047</b>	<b>0.22</b>		<b>0.020</b>	<b>0.24</b>
	<b>0.063</b>	<b>0.17</b>		<b>0.011</b>	<b>0.17</b>
	<b>0.12</b>	<b>0.55</b>		<b>0.52</b>	<b>1.0</b>
	<b>0.037</b>	<b>0.40</b>		<b>0.073</b>	<b>0.074</b>
	<b>0.24</b>	<b>0.68</b>		<b>0.061</b>	<b>0.70</b>
	<b>0.037</b>	<b>0.11</b>			

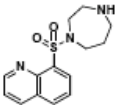
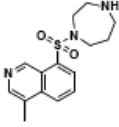
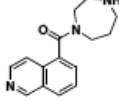
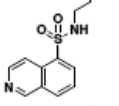
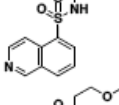
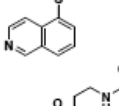
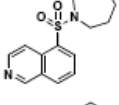
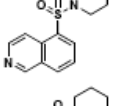
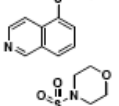
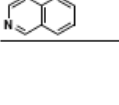
**Table S12. Cell lines used for the cell-based screens.**

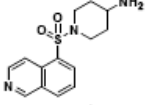
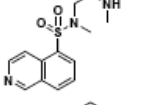
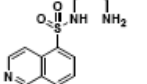
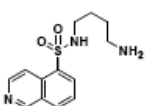
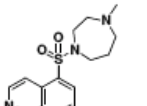
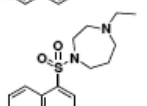
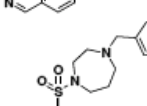
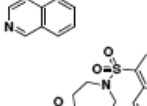
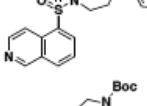
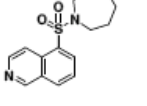
Name	Origin	KRAS status <sup>i</sup>
NOMO-1	AML	G13D
SKM-1	AML	K117N
NB4	AML	A18D
THP-1	AML	WT
U937	AML	WT
OCI-AML3	AML	WT
MOLM-16	AML	WT
PL-21	AML	WT
EOL-1	AML	WT
GDM-1	AML	WT
KOPN-8	ALL	G13D
JURKAT	ALL	WT
Karpas-620	Multiple myeloma	G13D
RPMI-8226	Multiple myeloma	G12A
EJM	Multiple myeloma	WT
MM.1S	Multiple myeloma	WT
DLD-1	Colon cancer	G13D
HCT-15	Colon cancer	G13D
COLO205	Colon cancer	WT
HeyA8	Ovarian cancer	G13D
OVCAR-3	Ovarian cancer	WT
CaOV3	Ovarian cancer	WT
OVCAR-8	Ovarian cancer	WT
KYSE-450	Esophageal cancer	WT
MDA-MB-231	Breast cancer	G13D

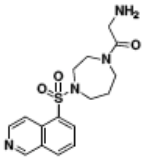
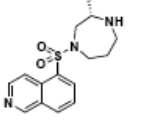
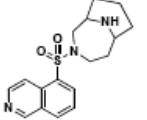
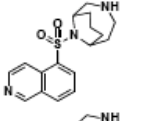
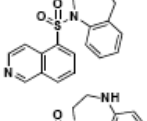
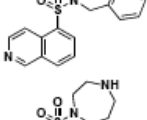
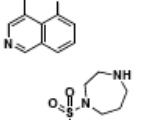
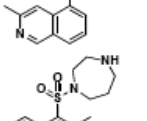
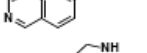
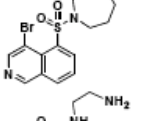
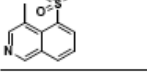
A549	NSCLC	G12S
H2009	NSCLC	G12A
H1792	NSCLC	G12C
H23	NSCLC	G12C
H1975	NSCLC	WT
H1568	NSCLC	WT
H1437	NSCLC	WT
H522	NSCLC	WT

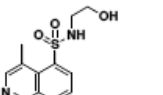
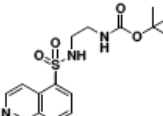
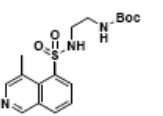
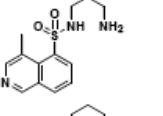
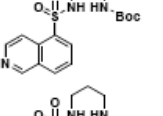
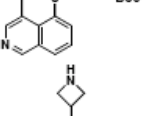
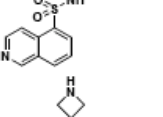
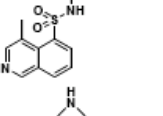
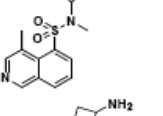
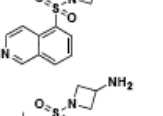
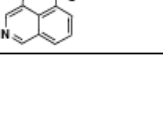
<sup>1</sup> According to the Catalogues of Somatic Mutations in Cancer (COSMIC).

**Table S13. Biochemical IC<sub>50</sub> values for inhibition of STK33, synthesis yield and QC data**

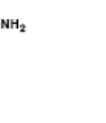
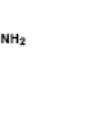
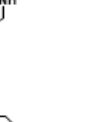
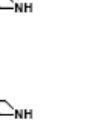
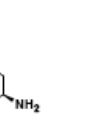
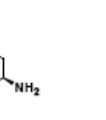
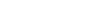
Structure	Compound	IC <sub>50</sub> ( $\mu$ M) @ 100 $\mu$ M ATP	IC <sub>50</sub> ( $\mu$ M) @ 25 $\mu$ M ATP	yield (%)	Mass ([M+H])	observed Mass	Rt (min) (LC MS)	Rt (min) (prepHPLC)
	BRD1651	>186	>186	99	292.16	292.23	0.72	
	BRD4469	>186	>186	21	306.13	306.23	0.88	3.72
	BRD0811	>186	>186	55	256.15	256.25	0.3	2.27
	BRD2998	>186	>186	59	251.09	251.11		2.49
	BRD4220	>186	100	57	253.07	253.16	0.79	1.5
	BRD7390	>186	>186	67	267.08	267.16	0.9	1.43
	BRD6818	>186	>186	45	462.03	462.06	1.29	3.55
	BRD0188	>186	>186	53	291.12	291.26	1.36	2.84
	BRD2751	64.00	29.00	99	279.09	278.15	0.94	
	BRD7527	>186	>186	31	277.1	277.18	1.24	3.72
	BRD9836	>186	>186	38	279.08	279.16	0.99	2.67

Structure	Compound	IC <sub>50</sub> ( $\mu$ M) @ 100 $\mu$ M ATP	IC <sub>50</sub> ( $\mu$ M) @ 25 $\mu$ M ATP	yield (%)	Mass ([M+H])	observed Mass	Rt (min) (LC MS)	Rt (min) (prepHPLC)
	BRD3518	<b>60</b>	<b>26</b>	54	292.11	292.18	0.83	4.24
	BRD9802	<b>174</b>	<b>36</b>	48	280.11	280.27	0.79	2.54
	BRD8531	<b>98</b>	<b>46</b>	74	266.1	266.12		1.03
	BRD1688	> <b>714</b>	<b>259</b>	25	280.11	280.15	0.79	1.8
	BRD0322	<b>30</b>	<b>23</b>	12	306.13	306.25	0.63	2.05
	BRD5039	<b>48</b>	<b>42</b>	10	320.15	320.2	0.73	2.02
	BRD5076	<b>177</b>	<b>40</b>	19	382.16	382.12	1.43	3.5
	BRD2660	<b>165</b>	<b>98</b>	10	483.12	483.2	1.21	
	BRD0272	> <b>186</b>	> <b>186</b>	47	382.17			
	BRD8033	> <b>186</b>	> <b>186</b>	42	334.12	334.3	0.91	1.67

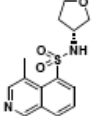
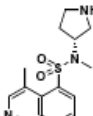
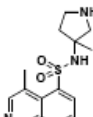
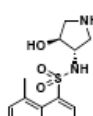
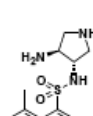
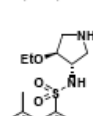
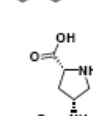
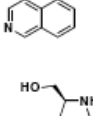
Structure	Compound	IC <sub>50</sub> ( $\mu$ M) @ 100 $\mu$ M ATP	IC <sub>50</sub> ( $\mu$ M) @ 25 $\mu$ M ATP	yield (%)	Mass ([M+H])	observed Mass	Rt (min) LC MS	Rt (min) prepHPLC
	BRD5624	>186	>186	50	349.14	349.17	0.84	3.33
	BRD4719	70	24	53	306.13	306.26	0.89	3.28
	BRD3954	127	64	25	332.15	332.15	0.83	4.27
	BRD2533	>714	107	42	332.15	332.2	0.96	3.3
	BRD1104	219	123	77	340.11	340.26	0.86	1.17
	BRD0114	>186	>186	4	340.11	340.21	1.23	3.88
	BRD3773	0.56	0.19	78	306.13	306.19	0.8	4.08
	BRD9852	51	30	55	306.13	306.21	0.87	2.51
	BRD9726	26	12	2	306.13	306.25	0.86	2.9
	BRD8880	49	24	51	372.02	372.13	1.5	1.5
	BRD5549	3.2	1.6	25	266.1	266.26	0.66	1.55

Structure	Compound	IC <sub>50</sub> ( $\mu$ M) @ 100 $\mu$ M ATP	IC <sub>50</sub> ( $\mu$ M) @ 25 $\mu$ M ATP	yield (%)	Mass ([M+H])	observed Mass	Rt (min) (LC MS)	Rt (min) (prepHPLC)
	BRD3610	<b>25</b>	<b>11</b>	40	267.08	267.21	0.86	1.6
	BRD4153	>186	>186	39	352.14			
	BRD9391	>186	<b>52</b>	95	366.15	366.4	1.13	
	BRD6995	<b>4.7</b>	<b>1.8</b>	21	280.11	280.2	0.7	1.75
	BRD9091	>186	>186	62	366.15			
	BRD7177	<b>89</b>	<b>35</b>	48	380.17	380.5	1.25	
	BRD4958	<b>19</b>	<b>7.4</b>	33	264.08	264.19	0.7	0.69
	BRD3966	<b>0.57</b>	<b>0.29</b>	45	278.1	278.2	0.81	1.88
	BRD9325	<b>1.2</b>	<b>0.65</b>	47	282.11	282.27	0.87	3.15
	BRD5991	<b>42</b>	<b>19</b>	55	264.08	264.2	0.84	3.38
	BRD5337	<b>1.3</b>	<b>0.84</b>	72	278.1	278.23	0.84	2.93

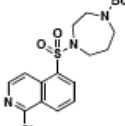
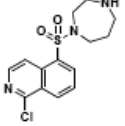
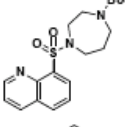
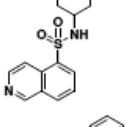
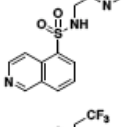
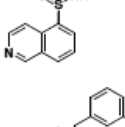
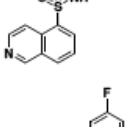
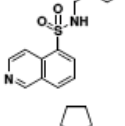
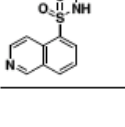
Structure	Compound	$IC_{50}$ ( $\mu M$ ) @ 100 $\mu M$ ATP	$IC_{50}$ ( $\mu M$ ) @ 25 $\mu M$ ATP	yield (%)	Mass ([M+H])	observed Mass	Rt (min) MS	Rt (min) (LC prepHPLC)
	BRD7364	>186	71.43	70	320.11	320.2	0.9	1.52
	BRD9027	4.1	1.7	85	334.12	334.47	1.05	2.57
	BRD5419	2.1	1.2	78	320.15	320.29	0.84	4.02
	BRD1742	5.3	2.7	59	318.13	318.25	0.88	3.48
	BRD3590	24	9.3	67	278.1	278.17	0.8	2.67
	BRD3752	0.13	0.047	75	292.11	292.21	0.8	3.63
	BRD3490	41	16	60	278.1	278.2	0.79	3.32
	BRD0828	13	3.7	75	292.11	292.21	0.84	3.67
	BRD3501	16	7.1	91	278.1	278.24	0.83	1.92
	BRD3695	0.17	0.063	60	292.11	292.24	0.73	2.47

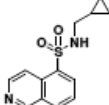
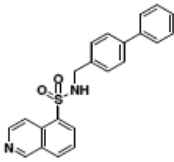
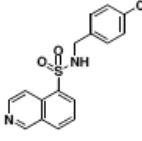
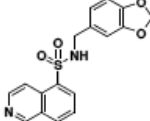
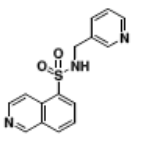
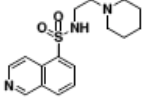
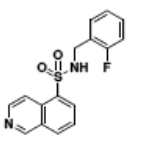
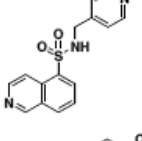
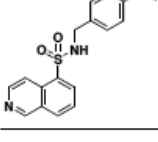
Structure	Compound	IC <sub>50</sub> (μM) @ 100 μM ATP	IC <sub>50</sub> (μM) @ 25 μM ATP	yield (%)	Mass ([M+H] <sup>+</sup> )	observed Mass	Rt (min) (LC MS)	Rt (min) (prepHPLC)
	BRD8943	<b>39</b>	<b>10</b>	42	278.1	278.24	0.78	2.44
	BRD9573	<b>10</b>	<b>4.8</b>	61	292.11	292.17	0.73	2.25
	BRD7481	>714	<b>397.00</b>	64	306.13	306.19	0.77	4.23
	BRD7425	>714	>714	64	306.13	306.19	0.78	4.24
	BRD2246	>714	<b>201.00</b>	53	292.11	292.23	0.82	2.07
	BRD7471	<b>11</b>	<b>4.2</b>	60	306.13	306.22	0.85	2.64
	BRD9575	<b>1.9</b>	<b>0.79</b>	87	292.11	292.21	0.83	4.24
	BRD2297	<b>31</b>	<b>16</b>	66	290.1	290.25	0.77	3.99
	BRD4942	<b>4.2</b>	<b>1.4</b>	69	304.11	304.22	0.82	4.2
	BRD0841	<b>16</b>	<b>6.1</b>	63	292.11	292.21	0.75	4.24
	BRD3376	<b>2.6</b>	<b>1.6</b>	92	306.13	306.21	0.84	4.27

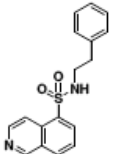
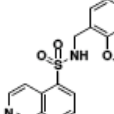
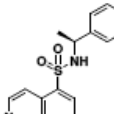
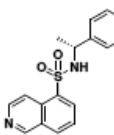
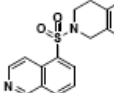
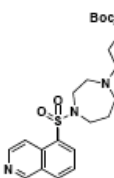
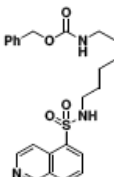
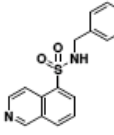
Structure	Compound	IC <sub>50</sub> ( $\mu$ M) @ 100 $\mu$ M ATP	IC <sub>50</sub> ( $\mu$ M) @ 25 $\mu$ M ATP	yield (%)	Mass ([M+H])	observed Mass	Rt (min) (LC MS)	Rt (min) (prepHPLC)
	BRD1199	>186	62	66	292.11	292.21	0.81	3.4
	BRD3436	2.8	1.2	77	306.13	306.22	0.88	2.67
	BRD3033	31	13	49	292.11	292.28	0.75	2.88
	BRD2668	5.6	2.6	31	306.13	306.28	0.8	3.95
	BRD0561	78	36	39	292.11	292.24	0.77	2.78
	BRD4209	1.5	0.99	38	306.13	306.21	0.8	3.95
	BRD2986	2.8	1.2	88	306.13	306.25	0.88	4.25
	BRD5717	96	38	26	292.11	292.18	0.72	3.98
	BRD7682	16	7.9	69	306.13	306.25	0.78	4.22
	BRD2594	47	16	67	290.1	290.21	0.84	2.09
	BRD5731	5.1	2.3	60	304.11	304.22	0.86	2.62

Structure	Compound	$\text{IC}_{50}$ ( $\mu\text{M}$ ) @ 100 $\mu\text{M}$ ATP	$\text{IC}_{50}$ ( $\mu\text{M}$ ) @ 25 $\mu\text{M}$ ATP	yield (%)	Mass ([M+H])	observed Mass	Rt (min) (LC MS)	Rt (min) (prepHPLC)
	BRD4357	<b>56</b>	<b>32</b>	92	283.1	282.07	0.97	1.82
	BRD4618	<b>3.2</b>	<b>1.2</b>	21	306.13	306.36	0.8	2.85
	BRD4889	<b>9.2</b>	<b>2.7</b>	5	306.13	306.3	0.74	3.87
	BRD0227	<b>1.6</b>	<b>0.54</b>	40	308.11	308.2	0.77	1.48
	BRD6696	<b>1.7</b>	<b>0.42</b>	54	307.13	307.26	0.9(acid)	0.75
	BRD1230	<b>12</b>	<b>4.2</b>	23	336.14	336.23	0.91(acid)	3.25
	BRD0035	<b>2.2</b>	<b>0.78</b>	2	336.1	336.21	0.84	0.86
	BRD4980	<b>0.09</b>	<b>0.037</b>	44	321.12	322.24	0.79	1.86

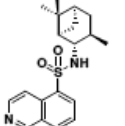
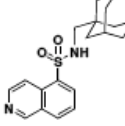
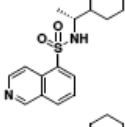
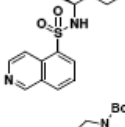
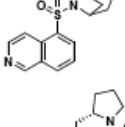
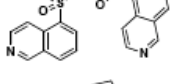
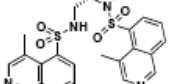
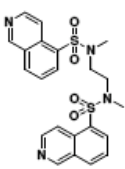
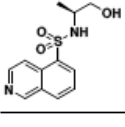
Structure	Compound	IC <sub>50</sub> ( $\mu$ M) @ 100 $\mu$ M ATP	IC <sub>50</sub> ( $\mu$ M) @ 25 $\mu$ M ATP	yield (%)	Mass ([M+H] <sup>+</sup> )	observed Mass	Rt (min) MS	Rt (min) (LC prepHPLC)
	BRD6875	<b>9.2</b>	<b>2.8</b>	77	322.12	322.21	0.63	1.98
	BRD8313	<b>3.2</b>	<b>0.81</b>	16	322.12	322.16	0.87	3.97
	BRD1045	<b>0.25</b>	<b>0.12</b>	45	321.12	322.21	0.7	1.83
	BRD7777	<b>4.6</b>	<b>2.0</b>	3	350.13	360.29	0.72	1.16
	BRD0119	<b>&gt;186</b>	<b>&gt;186</b>	40	440.17	439.95	1.52	3.87
	BRD5281	<b>&gt;186</b>	<b>&gt;186</b>	43	426.15	426.23	1.34	2.87
	BRD0649	<b>&gt;186</b>	<b>&gt;186</b>	65	378.15	378.26	1.31	3.97
	BRD9435	<b>&gt;186</b>	<b>&gt;186</b>	35	391.17	391.23	1.61	2.67

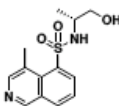
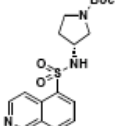
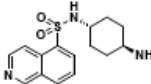
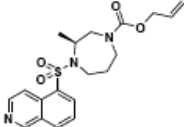
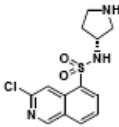
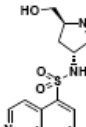
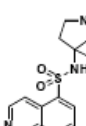
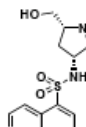
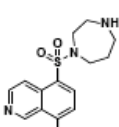
Structure	Compound	IC <sub>50</sub> ( $\mu$ M) @ 100 $\mu$ M ATP	IC <sub>50</sub> ( $\mu$ M) @ 25 $\mu$ M ATP	yield (%)	Mass ([M+H])	observed Mass	Rt (min) (LC MS)	Rt (min) (prepHPLC)
	BRD2109	>186	>186	85	426.13	426.25	1.57	2.25
	BRD0197	27.14	10.71		326.13	326.14	0.9	
	BRD9508	>186	>186	42	382.16	382.14	1.43	3.4
	BRD1968	>186	>186	51	291.12	291.21	1.3	3.98
	BRD2155	>186	>186	39	300.08	300.17	0.9	2.08
	BRD6736	>186	>186	12	291.04	291.14	1.11	0.82
	BRD8071	>186	>186	46	317.08	317.14	1.24	3.53
	BRD4041	>186	>186	49	335.07	335.13	1.28	3.62
	BRD3373	>186	>186	70	277.1	277.17	1.2	3.42

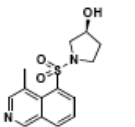
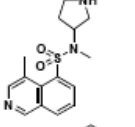
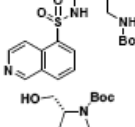
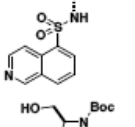
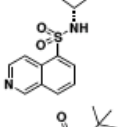
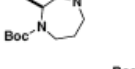
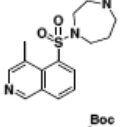
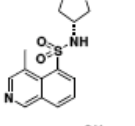
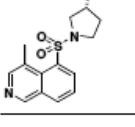
Structure	Compound	IC <sub>50</sub> ( $\mu$ M) @ 100 $\mu$ M ATP	IC <sub>50</sub> ( $\mu$ M) @ 25 $\mu$ M ATP	yield (%)	Mass ([M+H] <sup>+</sup> )	observed Mass	Rt (min) (LC MS)	Rt (min) (prepHPLC)
	BRD0572	>186	>186	53	263.09	263.13	1.12	2.67
	BRD8188	>186	>186	58	375.12	375.14	1.47	3.98
	BRD5670	>186	>186	50	333.05	333.1	1.33	4
	BRD1731	>186	>186	61	343.08	343.15	1.18	3.22
	BRD4553	>186	>186	39	300.08	300.18	0.83	1.87
	BRD9215	75.71	46.43	60	320.15	320.22	0.85	3.63
	BRD8584	>186	>186	61	317.08	317.14	1.21	3.37
	BRD9483	>186	>186	42	300.08	300.17	0.83	3.43
	BRD7266	>186	>186	6	329.1	329.18	1.2	3.4

Structure	Compound	IC <sub>50</sub> ( $\mu$ M) @ 100 $\mu$ M ATP	IC <sub>50</sub> ( $\mu$ M) @ 25 $\mu$ M ATP	yield (%)	Mass ([M+H] <sup>+</sup> )	observed Mass	Rt (min) (LC MS)	Rt (min) (prepHPLC)
	BRD0698	>186	>186	90	313.1	313.19	1.26	3.98
	BRD7209	>186	>186	74	329.1	329.15	1.23	3.82
	BRD7538	>186	>186	64	313.1	313.19	1.27	3.88
	BRD7505	>186	>186	77	313.1	313.19	1.27	3.88
	BRD4836	>186	>186	30	325.1	325.19	1.4	3.37
	BRD9370	36	46	68	449.19	449.29	1.18	
	BRD0413	>186	>186	43	442.18	442.22	1.4	3.43
	BRD2850	>186	>186	61	299.09	299.13	1.17	3.13

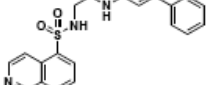
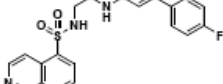
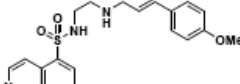
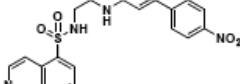
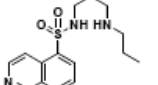
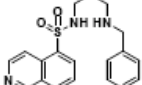
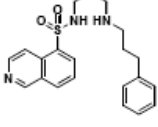
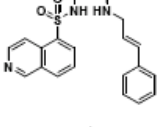
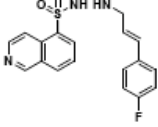
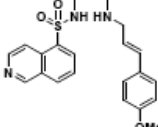
Structure	Compound	IC <sub>50</sub> ( $\mu$ M) @ 100 $\mu$ M ATP	IC <sub>50</sub> ( $\mu$ M) @ 25 $\mu$ M ATP	yield (%)	Mass ([M+H])	observed Mass	Rt (min) (LC MS)	Rt (min) (prepHPLC)
	BRD0886	>186	>186	54	400.14	400.16	1.21	
	BRD4857	351	104	83	292.11	292.19	0.87	0.39
	BRD4962	>714	>714	81	384.14	384.15	1.46	0.63
	BRD3419	>186	>186	37	314.1	314.17	0.87	0.39
	BRD3734	>186	>186	19	392.08	392.09	1.02	2.74
	BRD8652	>186	>186	32	382.12	382.15	1.21	3.28
	BRD1343	>186	>186	53	303.12	303.22	1.37	2.87
	BRD9796	33	16	17	346.16	346.2	0.96	3.03
	BRD9178	>186	>186	17	386.12	386.35	1.24	3.08
	BRD6382	>186	>186	28	414.15	413.97	1.32	3.09

Structure	Compound	IC <sub>50</sub> ( $\mu$ M) @ 100 $\mu$ M ATP	IC <sub>50</sub> ( $\mu$ M) @ 25 $\mu$ M ATP	yield (%)	Mass ([M+H])	observed Mass	Rt (min) (LC MS)	Rt (min) (prepHPLC)
	BRD7394	>186	>186	64	345.17	345.22	1.58 (acid)	2.09
	BRD2520	>186	>186	49	357.17	357.24	1.80(acid)	2.58
	BRD7178	>186	>186	51	319.15	319.24	1.42(acid)	1.75
	BRD2867	>186	>186	58	319.15	319.31	1.43(acid)	1.77
	BRD4468	>186	>186	60	432.2	432.24	1.54	3.97
	BRD3078	>714	166	5	483.12	483.2	0.82	3.25
	BRD2024	12	6.1	5	511.15	511.23	1.29	4.07
	BRD5499	>186	>186	4	471.12	471.3	1.27	4.04
	BRD7388	>186	>186	62	267.08	267.13	0.86	1.4

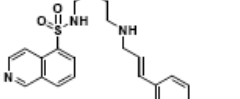
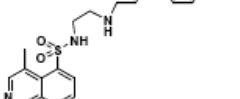
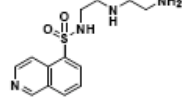
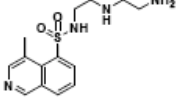
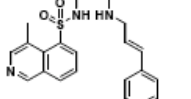
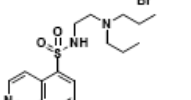
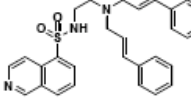
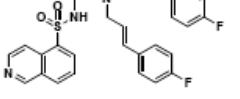
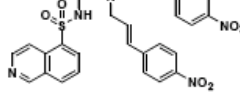
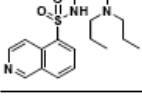
Structure	Compound	IC <sub>50</sub> ( $\mu$ M) @ 100 $\mu$ M ATP	IC <sub>50</sub> ( $\mu$ M) @ 25 $\mu$ M ATP	yield (%)	Mass ([M+H])	observed Mass	Rt (min) (LC MS)	Rt (min) (prepHPLC)
	BRD8939	<b>33</b>	<b>13</b>	61	281.1	281.25	0.92	2.1
	BRD9592	> <b>186</b>	> <b>186</b>	26	378.15	378.3	1.32	2.82
	BRD6645	> <b>357</b>	<b>102</b>	52	306.13	306.18	0.67(acid)	3.65
	BRD9304	> <b>186</b>	> <b>186</b>	88	390.15	390.57	1.29	
	BRD9082	<b>151</b>	<b>56</b>	58	312.06	312.16	0.91	1.43
	BRD1303	<b>7.9</b>	<b>2.6</b>	82	308.11	308.21	0.75	2.22
	BRD5165	<b>39</b>	<b>20</b>	7	282.11	282.28	0.8	2.6
	BRD7787	<b>16</b>	<b>6.2</b>	69	308.11	308.24	0.77	2.19
	BRD9509	<b>296</b>	<b>257</b>	38	372.02	372.19	0.91	3.82

Structure	Compound	$IC_{50}$ ( $\mu$ M) @ 100 $\mu$ M ATP	$IC_{50}$ ( $\mu$ M) @ 25 $\mu$ M ATP	yield (%)	Mass ([M+H] <sup>+</sup> )	observed Mass	Rt (min) MS	Rt (min) (LC prepHPLC)
	BRD2334	<b>29</b>	<b>13</b>	73	283.1	283.22	0.97	2.3
	BRD4275	<b>7.2</b>	<b>3.8</b>	49	306.13	306.31	0.92	3.06
	BRD9773	<b>&gt;186</b>	<b>&gt;186</b>	75	380.17			
	26			41	408.16	408.27	1.2	3.02
	27			45	408.16	408.27	1.11	3.48
	28			27	215.18	215.2	2.72	3.05
	29			90	299.2	299.33	1.47	
	9			61	406.18	406.27	1.46	
	10			88	392.17	392.23	1.3	
	25			85	283.1	283.18	0.96	

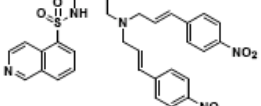
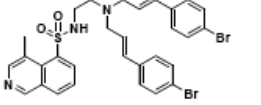
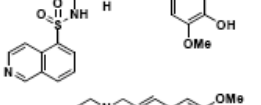
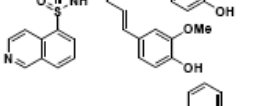
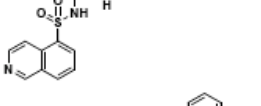
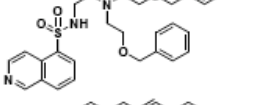
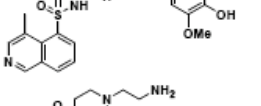
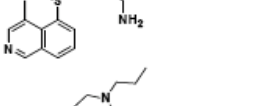
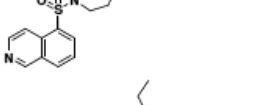
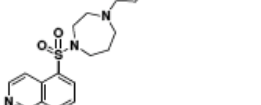
Structure	Compound	$IC_{50}$ ( $\mu$ M) @ 100 $\mu$ M ATP	$IC_{50}$ ( $\mu$ M) @ 25 $\mu$ M ATP	yield (%)	Mass ([M+H])	observed Mass	Rt (min) (LC MS)	Rt (min) (prepHPLC)
	22			45	422.18	422.32	1.14	2.57
	30			16	436.16	436.36	1.13	3.18
	31			72	345.22	345.29	0.92	2.76
	3			84	222.09	223.08	1.07	
	4			48	472.08	472.18	1.45	
	6			57	472.08	472.24	1.64	
	32			80	422.18	422.24	1.22	3.33
	BRD5145	<b>56.43</b>	<b>27.14</b>	24	294.13	294.28	0.92	2
	BRD3055	<b>138</b>	<b>71</b>	32	342.13	342.14	1.07	2.44
	BRD5294	<b>78</b>	<b>31</b>	5	370.16	370.18	1.26	2.2

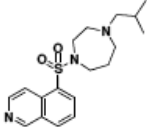
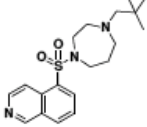
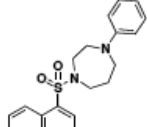
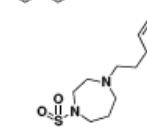
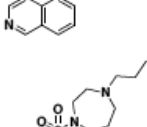
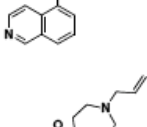
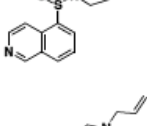
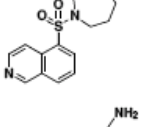
Structure	Compound	$IC_{50}$ ( $\mu M$ ) @ 100 $\mu M$ ATP	$IC_{50}$ ( $\mu M$ ) @ 25 $\mu M$ ATP	yield (%)	Mass ([M+H])	observed Mass	Rt (min) (LC MS)	Rt (min) (prepHPLC)
	BRD8469	<b>35</b>	<b>16</b>	28	368.15	368.15	1.12	3.18
	BRD3849	<b>32</b>	<b>16</b>	9	368.14	368.18	1.27	2.29
	BRD4701	<b>55</b>	<b>25</b>	18	398.16	398.25	1.15	2.2
	BRD3844	<b>18</b>	<b>7.9</b>	9	413.13	413.16	1.15	2.15
	BRD0073	<b>166</b>	<b>64</b>	2	308.15	308.22	0.8	3.31
	BRD2048	<b>224</b>	<b>98</b>	43	368.15	368.18	1.05	3.87
	BRD0124	<b>246</b>	<b>111</b>	15	384.18	384.22	1.27	2.59
	BRD5432	<b>246</b>	<b>66</b>	14	382.16	382.19	1.25	2.5
	BRD0277	<b>41</b>	<b>21</b>	12	400.15	400.21	1.25	2.57
	BRD7488	<b>116</b>	<b>39</b>	25	412.17	412.22	1.23	2.49

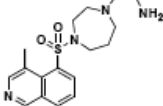
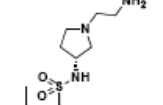
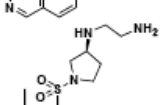
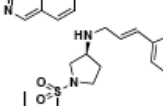
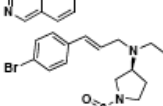
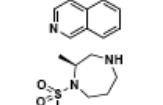
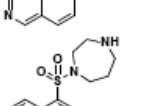
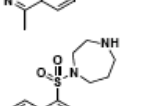
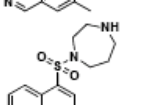
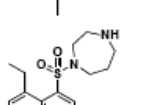
Structure	Compound	IC <sub>50</sub> ( $\mu$ M) @ 100 $\mu$ M ATP	IC <sub>50</sub> ( $\mu$ M) @ 25 $\mu$ M ATP	yield (%)	Mass ([M+H] <sup>+</sup> )	observed Mass	Rt (min) (LC MS)	Rt (min) (prepHPLC)
	BRD5149	<b>18</b>	<b>8.6</b>	16	460.07	460.13	1.42	3.51
	BRD9581	<b>31</b>	<b>14</b>	18	427.15	427.13	1.24	2.46
	BRD1524	>714	>714	17	322.16	322.22	0.94	3.6
	BRD6240	>714	<b>181</b>	22	370.16	370.18	1.12	3.28
	BRD0919	>186	>186	26	396.19	1.26	396.36	3.23
	BRD2874	<b>359</b>	<b>104</b>	23	396.18	396.26	1.14	4.07
	BRD1703	<b>207</b>	<b>93</b>	15	414.17	414.21	1.21	2.77
	BRD0939	<b>189</b>	<b>88</b>	13	426.19	426.25	1.33	2.83
	BRD6081	<b>49</b>	<b>30</b>	8	474.09	474.17	1.82	1.82

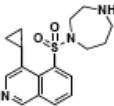
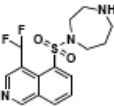
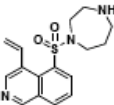
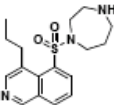
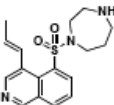
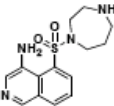
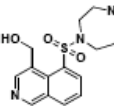
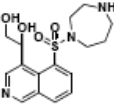
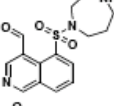
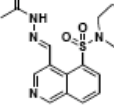
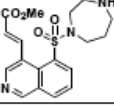
Structure	Compound	IC <sub>50</sub> ( $\mu$ M) @ 100 $\mu$ M ATP	IC <sub>50</sub> ( $\mu$ M) @ 25 $\mu$ M ATP	yield (%)	Mass ([M+H] <sup>+</sup> )	observed Mass	Rt (min) (LC MS)	Rt (min) (prepHPLC)
	BRD4397	<b>64</b>	<b>26</b>	5	441.16	441.16	1.33	1.75
	BRD9330	<b>4.6</b>	<b>2.1</b>	9	462.07	462.2	1.41	3.9
	BRD4009	<b>2.1</b>	<b>1.0</b>	34	295.13	295.15	0.47	3.07
	BRD3407	<b>6.4</b>	<b>3.7</b>	13	309.14	309.24	0.83	1.98
	BRD8198	<b>6.6</b>	<b>2.8</b>	6	474.09	474.2	1.35	4.09
	BRD6632	<b>&gt;186</b>	<b>46.43</b>	25	336.18	336.22	0.98	4.02
	BRD3747	<b>361</b>	<b>133</b>	24	484.21	484.25	1.53	4.25
	BRD0756	<b>172</b>	<b>136</b>	8	520.19	520.3	1.88	3.05
	BRD2424	<b>19</b>	<b>5.4</b>	7	574.18	574.19	1.59	3.73
	BRD0330	<b>&gt;186</b>	<b>&gt;186</b>	11	350.19	350.23	0.96	4.18

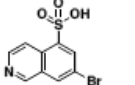
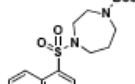
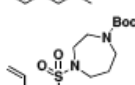
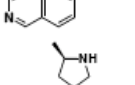
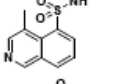
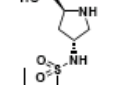
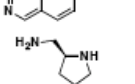
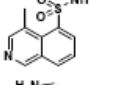
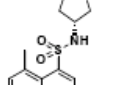
Structure	Compound	$IC_{50}$ ( $\mu M$ ) @ 100 $\mu M$ ATP	$IC_{50}$ ( $\mu M$ ) @ 25 $\mu M$ ATP	yield (%)	Mass ([M+H])	observed Mass	Rt (min) (LC MS)	Rt (min) (prepHPLC)
	BRD7012	>186	>186	6	460.21	460.31	1.47	4.27
	BRD8564	>186	>186	9	502.25	502.3	2.08	3.87
	BRD4835	213	114	13	498.22	498.28	1.82	4
	BRD3291	129	14	14	534.2	534.26	1.77	4
	BRD7419	77	46	18	568.24	568.3	1.76	3.88
	BRD8747	96	43	21	588.19	588.19	1.66	3.83
	BRD2686	216	161	24	512.24	512.32	2.48	4.34
	BRD5822	290	137	32	548.22	548.29	1.61	3.9
	BRD3146	238	126	16	572.26	572.27	1.92	4.05

Structure	Compound	$IC_{50}$ ( $\mu M$ ) @ 100 $\mu M$ ATP	$IC_{50}$ ( $\mu M$ ) @ 25 $\mu M$ ATP	yield (%)	Mass ([M+H])	observed Mass	Rt (min) MS	Rt (min) (LC prepHPLC)
	BRD7402	<b>63</b>	<b>53</b>	19	602.21	602.22	1.76	3.28
	BRD3116	<b>130</b>	<b>56</b>	6	656.04	656.22	1.94	4.52
	BRD8902	<b>16</b>	<b>5.9</b>	11	414.15	414.22	1	1.8
	BRD3758	<b>94</b>	<b>66</b>	29	576.22	576.25	1.21	3.3
	BRD1600	<b>35</b>	<b>16</b>	19	386.16	386.22	1.15	2.74
	BRD5967	<b>95</b>	<b>58</b>	11	520.23	520.35	1.84	4.2
	BRD9159	<b>7.9</b>	<b>3.1</b>	12	428.17	428.28	1.01	2.39
	BRD3394	<b>9.8</b>	<b>5.2</b>	24	352.18	352.27	0.88	3.95
	BRD5363	<b>24</b>	<b>56</b>	40	334.16	334.19	0.91	4.02
	BRD1943	<b>86</b>	<b>34</b>	33	362.19	362.22	1.03	4.22

Structure	Compound	$IC_{50}$ ( $\mu M$ ) @ 100 $\mu M$ ATP	$IC_{50}$ ( $\mu M$ ) @ 25 $\mu M$ ATP	yield (%)	Mass ([M+H])	observed Mass	Rt (min) MS	Rt (min) LC (prepHPLC)
	BRD3295	>186	<b>56</b>	33	348.18	348.22	1	4.22
	BRD5665	>186	<b>61</b>	52	362.19	326.22	0.83	0.02
	BRD5656	<b>212</b>	<b>88</b>	27	368.15	368.15	1.46	3.78
	BRD6148	<b>51</b>	<b>26</b>	35	396.18	396.2	1.13	4.12
	BRD5445	<b>34</b>	<b>27</b>	34	410.2	410.2	1.16	4.22
	BRD8218	<b>35</b>	<b>30</b>	29	408.21	408.21	1.15	4.15
	BRD9569	<b>39</b>	<b>29</b>	50	488.09	488.13	1.52	4.15
	BRD0112	<b>46</b>	<b>15</b>	29	335.16	335.22	0.96	3.43

Structure	Compound	IC <sub>50</sub> ( $\mu$ M) @ 100 $\mu$ M ATP	IC <sub>50</sub> ( $\mu$ M) @ 25 $\mu$ M ATP	yield (%)	Mass ([M+H])	observed Mass	Rt (min) (LC MS)	Rt (min) (prepHPLC)
	BRD9740	<b>3.6</b>	<b>2.0</b>	50	349.17	349.24	0.89	3.11
	BRD0541	<b>10</b>	<b>5.9</b>	25	336.16	335.27	0.8	3.3
	BRD1596	<b>2.6</b>	<b>1.7</b>	28	335.16	335.28	0.83	3.4
	BRD8155	<b>3.2</b>	<b>1.7</b>	67	488.09	488.05	1.19	2.86
	BRD3615	<b>9.8</b>	<b>3.9</b>	11	682.06	682.13	2	4.1
	BRD1869	<b>59</b>	<b>50</b>	89	306.13	306.29	0.88	2.29
	BRD6042	> <b>186</b>	> <b>186</b>	47	306.13	306.32	0.83	2.94
	BRD5087	<b>20</b>	<b>9.1</b>	80	306.13	306.25	0.96	3.88
	BRD5257	<b>205</b>	<b>176</b>	21	306.13	306.3	0.88	2.19
	BRD5930	<b>0.81</b>	<b>0.28</b>	20	320.15	320.3	0.82	2.93

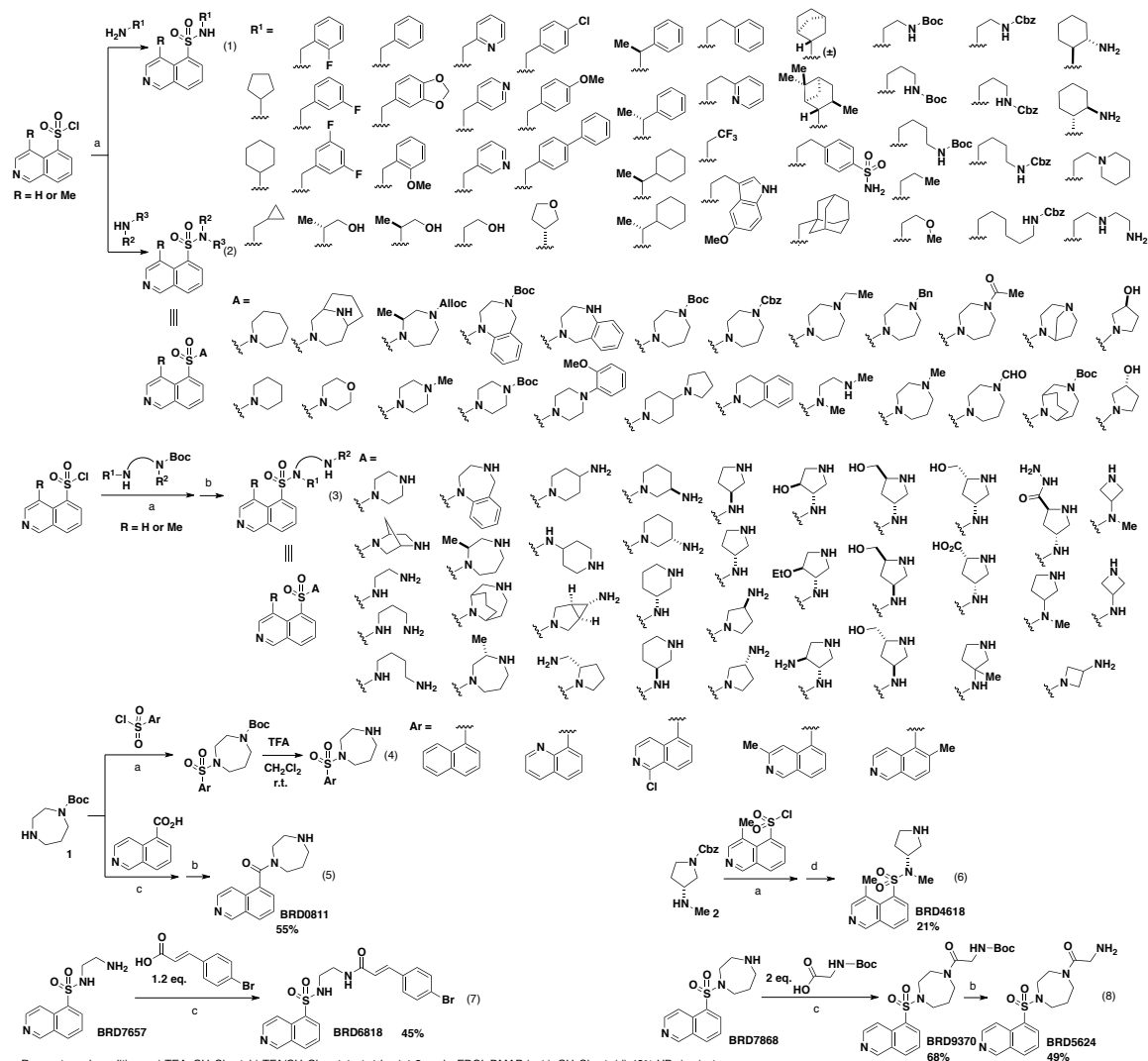
Structure	Compound	IC <sub>50</sub> ( $\mu$ M) @ 100 $\mu$ M ATP	IC <sub>50</sub> ( $\mu$ M) @ 25 $\mu$ M ATP	yield (%)	Mass ([M+H] <sup>+</sup> )	observed Mass	Rt (min) (LC MS)	Rt (min) (prepHPLC)
	BRD5796	<b>0.68</b>	<b>0.24</b>	57	332.15	332.27	0.96(acid)	3.08
	BRD8757	<b>1.1</b>	<b>0.48</b>	22	342.11	342.21	0.9	3.62
	BRD7032	<b>2.9</b>	<b>0.94</b>	71	318.13	318.31	0.8	3.4
	BRD7132	<b>3.2</b>	<b>1.6</b>	54	334.16	334.32	1.04	3.82
	BRD9078	<b>8.6</b>	<b>4.0</b>	84	332.15	332.29	0.99	3.21
	BRD2749	<b>39</b>	<b>21</b>	26	307.13	307.21	0.74	2.93
	BRD7648	<b>71</b>	<b>21</b>	17	322.12	322.26	0.59	2.73
	BRD5505	<b>203</b>	<b>95</b>	26	352.14	352.29	0.42	2.3
	BRD4734	<b>18</b>	<b>6.9</b>	20	320.11	320.16	0.77	1.82
	BRD0859	<b>74</b>	<b>26</b>	25	376.15	376.23	0.73	2.95
	BRD7198	<b>44</b>	<b>13</b>	75	376.14	376.23	0.98	2.74

Structure	Compound	IC <sub>50</sub> ( $\mu$ M) @ 100 $\mu$ M ATP	IC <sub>50</sub> ( $\mu$ M) @ 25 $\mu$ M ATP	yield (%)	Mass ([M+H])	observed Mass	Rt (min) (LC MS)	Rt (min) (prepHPLC)
	12			85				
	13			64	406.18	406.09	1.42	
	14			74	418.18	418.26	1.37	
	BRD5319	<b>0.14</b>	<b>0.065</b>	57	306.13	306.27	0.81	2.62
	BRD7953	<b>3.7</b>	<b>1.8</b>	7	336.1	336.19	0.59	0.99
	BRD9949	<b>0.032</b>	<b>0.02</b>	18	321.14	321.23	0.93	1.73
	BRD7071	<b>0.87</b>	<b>0.42</b>	76	321.14	321.31	0.86(acid)	1.67
	BRD2880	<b>0.53</b>	<b>0.24</b>	26	347.13	347.21	0.73(acid)	1.09
	BRD3192	<b>0.11</b>	<b>0.037</b>	55	347.13	347.3	0.79	1.9

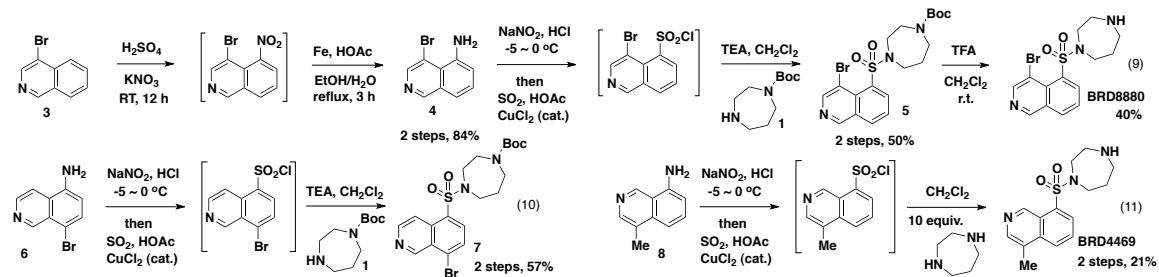
Structure	Compound	$IC_{50}$ ( $\mu M$ ) @ 100 $\mu M$ ATP	$IC_{50}$ ( $\mu M$ ) @ 25 $\mu M$ ATP	yield (%)	Mass ([M+H])	observed Mass	Rt (min) MS	Rt (min) (LC prepHPLC)
	BRD7569	<b>0.15</b>	<b>0.067</b>	23	337.14	337.34	0.22	1.83
	BRD8899	<b>0.025</b>	<b>0.011</b>	11	363.15	363.25	0.88	2.4
	BRD5749	<b>1.2</b>	<b>0.52</b>	51	363.15	363.28	0.9	2.95
	BRD4717	<b>0.14</b>	<b>0.073</b>	34	476.24	476.26	0.82	3.04
	BRD1469	<b>0.13</b>	<b>0.061</b>	48	476.24	476.44	0.77	3.23
	BRD0200	<b>0.21</b>	<b>0.084</b>	24	496.23	496.29	0.68	3.88
	BRD8254	<b>1.0</b>	<b>0.26</b>	37	496.23	496.39	1	3.03

Structure	Compound	IC <sub>50</sub> ( $\mu$ M) @ 100 $\mu$ M ATP	IC <sub>50</sub> ( $\mu$ M) @ 25 $\mu$ M ATP	yield (%)	Mass ([M+H] <sup>+</sup> )	observed Mass	Rt (min) (LC MS)	Rt (min) (prepHPLC)
	23			82	447.18	447.39	1.41	
	18			69	447.18	447.39	1.42	
	19			46	421.19	421.46	1.15	2.37
	BRD2816	>186	>186	51	463.2	463.33	1.2	3.62
	33			43	463.2	463.58	1.25	
	BRD2916	<b>31</b>	<b>15</b>	68	308.11	308.2	0.96	2.88
	BRD6284	<b>81</b>		12	502.06	502.18	1.73	4.32

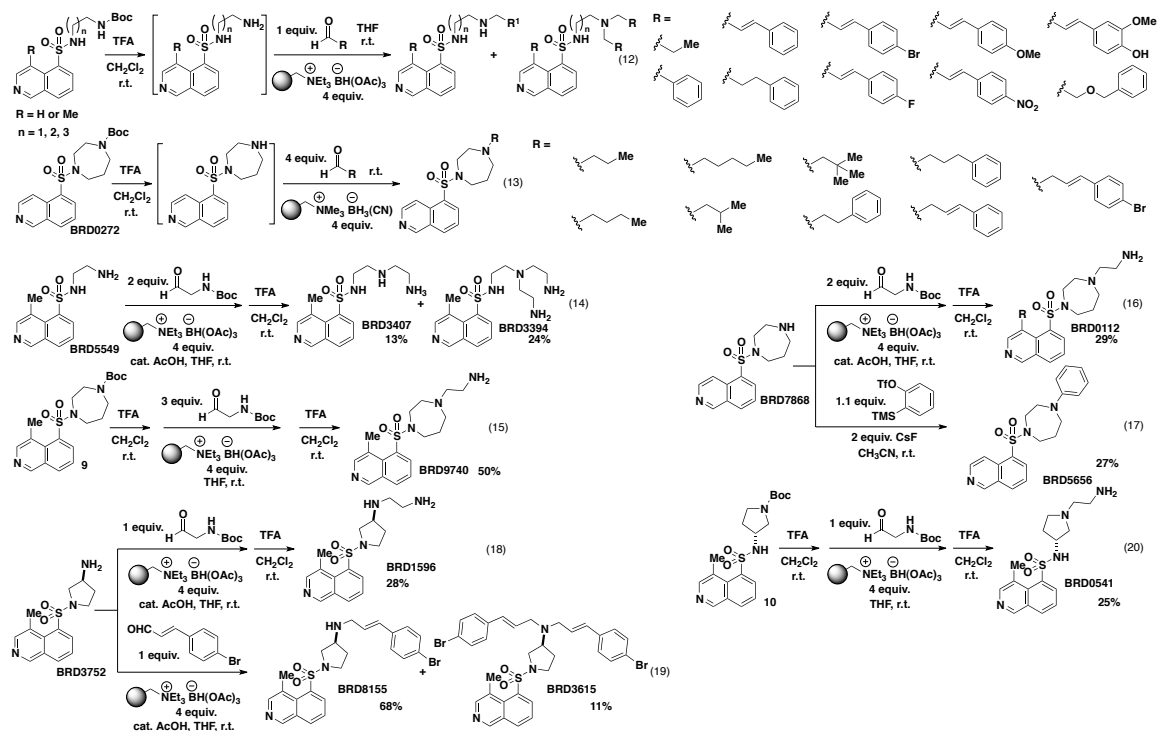
**Scheme S1.**



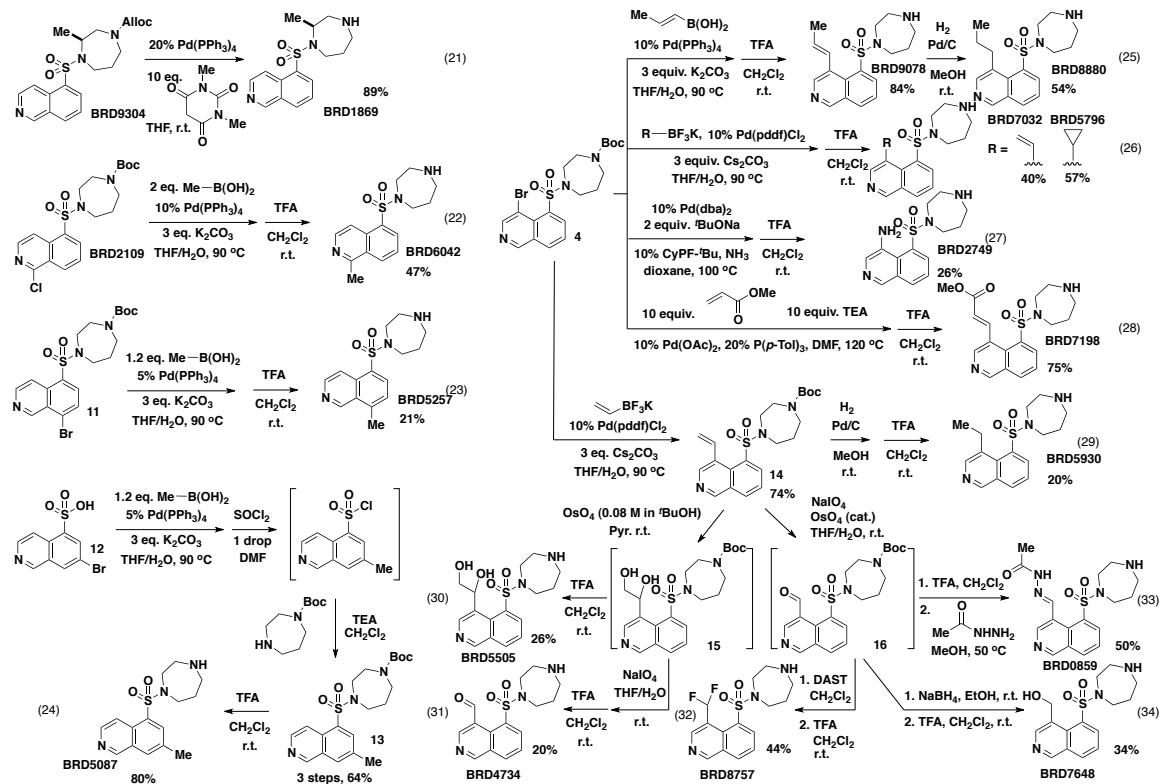
**Scheme S2.**



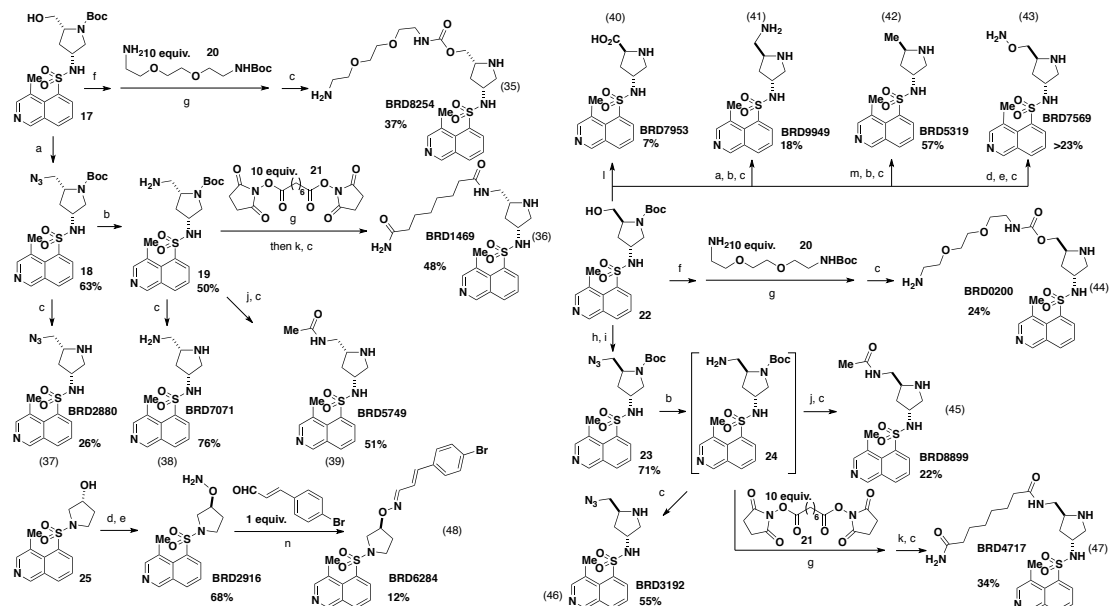
**Scheme S3.**



**Scheme S4.**



**Scheme S5.**



Reagents and conditions: a) 2 equiv. Bis(2,4-dichlorophenyl) phosphorochloridate, DMF, 60 °C; b) Pd/C, H<sub>2</sub>, MeOH, rt, 3 h; c) TFA/CH<sub>2</sub>Cl<sub>2</sub> = 1:1, rt, 1 h; d) N-Hydroxypthalimide, 1.5 equiv, DIAD, 1.5 equiv, PPh<sub>3</sub>, CH<sub>2</sub>Cl<sub>2</sub>, 0 °C ~ rt; e) N<sub>3</sub>H<sub>4</sub>, MeOH, rt; f) 10 equiv. CDI, CH<sub>2</sub>Cl<sub>2</sub>, rt, then CH<sub>2</sub>CN/H<sub>2</sub>O; g) 1.5 equiv. MsCl, TEA, CH<sub>2</sub>Cl<sub>2</sub>, 0 °C ~ rt; h) 10 equiv. NaN<sub>3</sub>, DMF, 90 °C, overnight; j) AcOH, 1.5 equiv. EDCl, CH<sub>2</sub>Cl<sub>2</sub>; k) excess NH<sub>3</sub>; l) 20% TEMPO, 2.5 eq. Ph(OAc)<sub>2</sub>, CH<sub>3</sub>CN/H<sub>2</sub>O; m) I<sub>2</sub>, PPh<sub>3</sub>, imidazole, THF, 0 °C ~ rt; n) cat. AcOH, DMSO, 60 °C.

## Materials and Methods.

Human full length STK33 containing an amino terminal histidine tag purified from SF21 cells was purchased from Millipore Corporation (catalog # 14-671-K). Myelin basic protein (bovine) was purchased from Millipore Corporation (catalog # 13-104). ATP, ADP, MOPS, MgCl<sub>2</sub>, Brij-35, glycerol, 2-mercaptoethanol, and BSA were purchased from Sigma-Aldrich. The 384-well general plates were purchased from VWR (Corning 3570); 384-well low volume plates were purchased from Greiner Bio-One (384W SV, HiBase, PS, LUMITRAC 200, Medium Binding, 30uL/well, catalog # 784075). CyBi®-Well vario was purchased from CyBio AG. CyBi tips were purchased from CyBio AG (CyBi-Tip Trays 384 standard; catalog # OL 3800-25-513-N). HTRF Transcreener ADP assay was purchased from Cis-bio US (catalog # 62ADPPC); ADP-Glo assays were purchased from Promega Corporation (catalog # V9103). The Envision 2012 multilabel reader was purchased from PerkinElmer, Inc. Multidrop Combi reagent dispenser and cassettes were purchased from Thermo Fisher Scientific, Inc.

Dry solvents were dispensed from a solvent purification system that passes solvents through packed columns (THF and CH<sub>2</sub>Cl<sub>2</sub>: dry neutral alumina; toluene: dry neutral alumina and Q5 reactant). Unless otherwise stated, all reagents were obtained from commercial sources and used without further purification. MP-triacetoxyborohydride (Macroporous triethylammonium methylpolystyrene triacetoxyborohydride) was purchased from Biotage (catalog# 800413, 1.8~2.4 mmol/g). <sup>1</sup>H NMR spectra were recorded on Varian Unity/Inova 500 (500MHz), or Bruker Ultrashield 300(300MHz) spectrometers. <sup>1</sup>H data are reported as follows: chemical shift in parts per million relative to CHCl<sub>3</sub> (7.27 ppm) or CH<sub>3</sub>OH (4.30 and 3.67 ppm) multiplicity (s, singlet; d, doublet; t, triplet; q, quartet; m, multiplet; br, broadened), coupling constant (Hz), and integration. <sup>13</sup>C magnetic resonance spectra were recorded on Varian Unity/Inova 500(125MHz) or Bruker Ultrashield 300(75MHz) spectrometers. <sup>13</sup>C chemical shifts are reported in parts per million relative to solvent. All <sup>13</sup>C spectra were determined with broadband decoupling.

Flash chromatography was performed either on EM Science silica gel 60 (230–400 mesh) or using a CombiFlash companion system (Teledyne ISCO, Inc.) with pre-packed FLASH silica gel columns (Biotage, Inc.). Compound purity and identity were determined by LC-MS (Alliance 2795, Waters, Milford, MA). Purity was measured by UV absorbance at 210 nm. Identity was determined on a SQ mass spectrometer by positive electrospray ionization. Mobile phase A consisted of either 0.01% ammonium hydroxide or 0.01% formic acid in water, while mobile phase B consisted of the same additives in acetonitrile. The gradient ran from 5% to 95% mobile phase B over 1.6 minutes at 3 mL/min. An XBridge C18, 3.5 um, 4.6x30 mm column was used with column temperature maintained at 40°C. 5 μL of sample solution were injected. Compounds were purified by mass-directed purification on a Waters Autopurification system (Milford, MA) (reverse-phase prep-HPLC). Collection was triggered on the (M+H)<sup>+</sup> and (M+Na)<sup>+</sup> ions on a ZQ mass spectrometer using positive electrospray ionization. Mobile phase A consisted of either 0.2% ammonium hydroxide in water, while mobile phase B consisted of the same additive in acetonitrile. The gradient ran from 5% to 95% mobile phase B over 5.0 minutes at 44 mL/min. An XBridge OBD Prep

C18, 5 um, 19x50 mm column was used at room temperature. The solvent gradient is determined by the retention time (RT) measured in LC-MS.

Retention Time (RT) LC-MS (min)	Purification Inlet Method
0.46~0.60	prep5min_5iso
0.61~0.75	prep5min_10iso
0.76~0.84	prep5min_10_15
0.85~1.06	prep5min_15_30
1.07~1.32	prep5min_20_35
1.33~1.52	prep5min_30_45
1.53~1.73	prep5min_45_60
1.74~1.81	prep5min_55_75

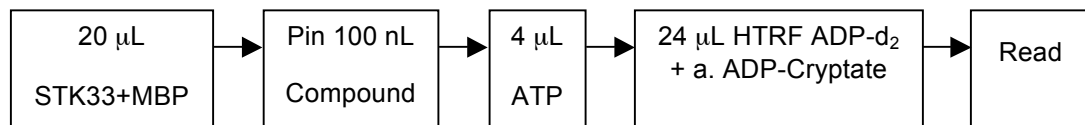
### Kinase assay:

Kinase reactions were performed under 10 mM MOPS-NaOH (pH 7.0), 10 mM MgCl<sub>2</sub>, 0.3 mM EDTA, 0.001% Brij-35, 0.5% glycerol, 0.01% 2-mercaptoethanol, and 0.1 mg/mL BSA. Reactions were initiated by the addition of ATP and incubated at 30 °C or room temperature for the indicated time. The enzyme concentration (STK33) and substrate concentration (MBP and ATP) were variable depending on the experiment. For inhibitors with IC<sub>50</sub> < 200 nM, the STK33 concentration was reduced to 9.6 nM and the kinase reaction time was extended to 120 minutes. Negative control (DMSO) was scaled to 100% kinase activity, whereas positive control (0.16 μM staurosporine, 100% inhibition) was scaled to 0% kinase activity.

For the HTRF assay, ADP-d2 and a. ADP-Cryptate solution was mixed at a 1:1 ratio to make the detection mixture. The detection mixture was added with an equal volume of the kinase reaction. The plate was incubated at room temperature for 60 minutes, after which fluorescence was read on an Envision instrument.

For the ADP-Glo assay, the kinase reaction solution and ADP-Glo reagent were mixed at a 1:1 ratio (totally 20 μL), which were incubated at room temperature for 50 minutes. Kinase detection reagent (20 μL) was added. The mixture was further incubated for 25 ~ 40 minutes before the plate was read on Envision for luminescence intensity.

### STK33 HTRF (Homogeneous Time Resolved Fluorescence) assay protocol for screening inhibitors



1. Add 20 mL total volume of STK33+MBP mixture (38.4 nM STK33, 24.5  $\mu$ M MBP, 10 mM MOPS-NaOH, pH 7.0, 10 mM MgCl<sub>2</sub>, 0.36 mM EDTA, 0.0012% Brij-35, 0.6% glycerol, 0.012% 2-mercaptoethanol, 0.12 mg/mL BSA) to 384-well general plates using Combi with Standard Cassette, high speed; fast spin down.
2. Pin transfer Compounds (100 nL)
3. After 15 minutes under room temperature, add 4  $\mu$ L ATP (10 mM MOPS-NaOH, pH 7.0, 10 mM MgCl<sub>2</sub>) with Combi, small cassette, high speed; note time of adding ATP to first plate, keep plates in order; spin down.
4. Incubate at room temperature for 70 minutes, starting from time of first plate from step 4.
5. Add 24  $\mu$ L total volume of HTRF reagent mixture (1:1 mixture of ADP-d<sub>2</sub> and a. ADP-Cryptate) to the 384-well general plates using Combi with small Cassette, high speed; fast spin down.
6. Incubate at room temperature for 60 minutes; read fluorescence on Envision 1 (Protocol: Cisbio HTRF Protocol; Label:LANCE-Cisbio HTRF Protocol)

#### Standard Curve:

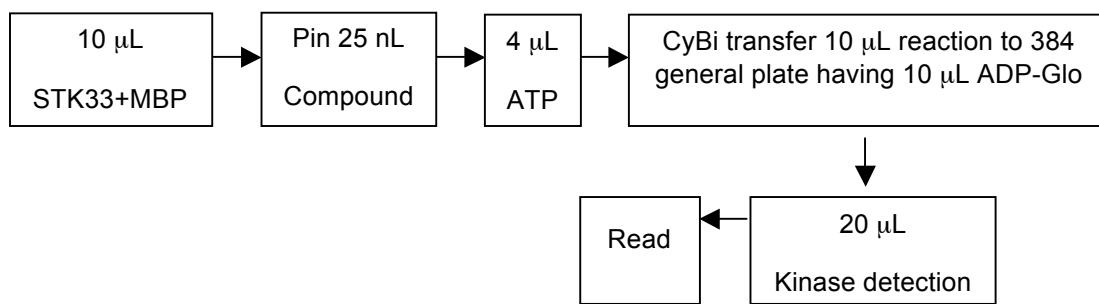
In order to calibrate the backgrounds under different ATP concentrations, standard curves are made based on the standard solutions with different ATP/ADP ratios. The ratio of emission intensity at 620 nm and 665 nm are calculated. Sigmoidal (variable slope) regression of ratio-[ADP] plot gives the equation:

$$\text{Ratio} = \text{Bottom} + (\text{Top-Bottom}) / [1 + (\text{EC50}/[\text{ADP}])^{\text{HillSlope}}]$$

#### Preparation of ATP to ADP conversion curves ([ATP]+[ADP]=100 mM)

% Conversion	100	33.33	11.11	3.70	1.23	0.41	0.14	0
[ADP] (mM)	100	33.33	11.11	3.70	1.23	0.41	0.14	0
[ATP] (mM)	0	66.67	88.99	96.30	98.77	99.59	99.86	100

#### STK33 ADP-Glo assay protocol for screening inhibitors



1. Add 10 mL total volume of STK33+MBP mixture (38.4 nM STK33, 24.5  $\mu$ M MBP, 10 mM MOPS-NaOH, pH 7.0, 10 mM MgCl<sub>2</sub>, 0.42 mM EDTA, 0.0014% Brij-35, 0.7% glycerol, 0.014% 2-mercaptoethanol, 0.14 mg/mL BSA) to 384-well low volume plates using Combi with Standard Cassette, high speed; fast spin down.
2. Pin transfer Compounds (25 nL)
3. After 15 minutes under room temperature, add 4  $\mu$ L ATP (10 mM MOPS-NaOH, pH 7.0, 10 mM MgCl<sub>2</sub>) with Combi, small cassette, high speed; note time of adding ATP to first plate, keep plates in order; spin down.
4. Incubate at room temperature for 70 minutes, starting from time of first plate from step 4.
5. Add 10  $\mu$ L total volume of ADP-Glo reagent mixture to 384-well general plates using Combi with Standard Cassette, high speed.
6. Transfer 10 mL reaction mixture using CyBi (program file: STK33\_v5) to 384-well general plates having the ADP-Glo reagent; note time of transfer.
7. Incubate at room temperature for 50 minutes.
8. Add 20 mL ADP-Glo kinase detection reagent using Combi with Standard Cassette, high speed; note time of transfer.
9. Incubate at room temperature for 35 minutes; read luminescence on Envision 1 (Protocol: Kinase-Glo 384 lum; Label: USLum-JoshK-US LUM 384 (cps))

#### Standard Curve:

In order to calibrate the backgrounds under different ATP concentrations, standard curves are made based on the standard solutions with different ATP/ADP ratios. Given the low conversion of ATP in the screening (<5%), the range of [ADP] is between 0 and 5 mM. Linear regression of Luminescence-[ADP] plot gives the equation:

$$\text{Luminescence} = \text{HillSlope} * [\text{ADP}] + \text{Y-intercept}$$

#### Preparation of ATP to ADP conversion curves ([ATP]+[ADP]=100 mM)

% Conversion	5	4	3	2	1.5	1	0.5	0
[ADP] (mM)	5	4	3	2	1.5	1	0.5	0
[ATP] (mM)	95	96	97	98	98.5	99	99.5	100

### **General procedure for synthesizing sulfonamides from sulfonyl chloride and amine:**

The amine (1.5 ~ 5 equiv.) and TEA (5 equiv.) were dissolved in anhydrous dichloromethane in a 4 mL capped vial. The solution was cooled in an ice bath and sulfonyl chloride (1 equiv.) was added. The ice bath was then removed; the solution was allowed to warm to room temperature and stirred overnight. The volatiles were removed by purging air. For Boc-protected diamines, removal of the protection was affected by treating the residue with 1:1 TFA/CH<sub>2</sub>Cl<sub>2</sub> for 1 h at room temperature. The volatiles were removed under reduced pressure. The residue was purified by prep-HPLC or flash chromatography over SiO<sub>2</sub>.

### **General procedure for coupling carboxylic acid and amine:**

To a solution of carboxylic acid (1~2 equiv.), amine (1 equiv.) and *N,N*-dimethylaminopyridine (DMAP, 0.1 equiv.) in dry CH<sub>2</sub>Cl<sub>2</sub> was added *N*-(3-Dimethylaminopropyl)-*N'*-ethylcarbodiimide hydrochloride (EDCI, 1.2 equiv.) at 0 °C with stirring. The reaction mixture was stirred at room temperature overnight. The mixture was quenched with water and extracted with EtOAc. The organic layers were then washed with saturated brine, dried over sodium sulfate, filtered, and evaporated under reduced pressure. The residue was purified by prep-HPLC.

### **General procedure for nitration and reduction to make aromatic amine:**

In a 20 mL capped vial was 4-bromoisoquinoline **3** (3g, 14 mmol) in sulfuric acid (5 mL, 92 mmol) to give light yellow solution. Under ice-cooling, a solution of potassium nitrate (1.6 g, 16 mmol) in 3 mL sulfuric acid was added dropwise. After 20h of stirring under room temperature the reaction mixture was poured in iced water (80 mL) containing aqueous ammonia (20 mL) and extracted with EA (100 mL × 3). The extract was dried over anhydrous sodium sulfate, and the solvent was distilled off under reduced pressure. In a 500 mL round-bottom flask was the residue in adding EtOH/H<sub>2</sub>O (80 mL) to give a yellow suspension. Acetic acid (6 g, 101 mmol) and iron (2.4 g, 43 mmol) were added. The solution was refluxed for 3 h. The acetic acid and alcohol were removed under vacuo. Saturated NaHCO<sub>3</sub> solution was added to basify the solution. Filtration was performed and the residue was extensively washed with EA. The filtrate was extracted with EA (100 mL × 4). The organic phase was combined and dried over anhydrous sodium sulfate. The solvent was removed *in vacuo* and the residue was purified via flash chromatography on silica (80g column, eluted by 0~5% MeOH in CH<sub>2</sub>Cl<sub>2</sub>) to give 4-bromoisoquinolin-5-amine **4** (2.7 g, 12 mmol, 84% yield) as a yellow solid.

### **General procedure for synthesizing sulfonyl chloride from aromatic amine:**

In a 20 mL capped vial, 4-bromoisoquinolin-5-amine **4** (106 mg, 0.475 mmol) was placed in concentrated hydrochloride acid (37% HCl, 2 mL) to give a yellow solution. Under ice-cooling, sodium nitrite (42.6 mg, 0.618 mmol) dissolved in water was added slowly. The stirring was continued for 15 minutes in an ice bath before the reaction mixture was pouring into the solution made by bubbling (15 min) sulfur dioxide into acetic acid (4 mL) in the presence of cupric chloride hydrate (50 mg, 0.293 mmol).

The mixture was stirred under room temperature for 1 h. Excess acetic acid was removed under reduced pressure. The solution was neutralized by adding a saturated  $\text{NaHCO}_3$  solution, after which extraction with  $\text{CH}_2\text{Cl}_2$  (20 mL  $\times$  3) was performed. The organic phase was combined and dried over anhydrous sodium sulfate. The solvent was removed *in vacuo*, and the residue was dissolved in dry  $\text{CH}_2\text{Cl}_2$  (3 mL). *Tert*-butyl 1,4-diazepane-1-carboxylate **1** (0.3 mL, 1.4 mmol) and TEA (0.1 mL, 0.72 mmol) were added. The mixture was stirred overnight under room temperature, concentrated, and purified by flash chromatography on silica (4g column, eluted by 0~100% EA in hexane) to give *tert*-butyl 4-(4-bromoisoquinolin-5-ylsulfonyl)-1,4-diazepane-1-carboxylate **5** (112 mg, 0.239 mmol, 50% yield) as a white solid.

#### **General procedure for reductive amination:**

MP-triacetoxyborohydride (4 equiv.) was added to the solution of amine (1 equiv.) and aldehyde (1~4 equiv.) in dry THF. The mixture was stirred overnight, after which filtration was performed, and the resin was washed with methanol. The combined solution was concentrated, and the product was purified by prep-HPLC.

#### **General procedure for Suzuki coupling:**

In a microwave tube, substrate (1 equiv.),  $\text{Pd}(\text{PPh}_3)_4$  (0.1 equiv.),  $\text{K}_2\text{CO}_3$ (3 equiv), and boronic acid (1~3 equiv.) were added. The tube was sealed and THF/water was added through a syringe. After degassing, the resulting mixture was heated to 90 °C for 4-12 h before cooling to room temperature and filtering through Celite. Upon removal of the solvents, the residue was purified through flash chromatography or subjected to TFA/ $\text{CH}_2\text{Cl}_2$  (1:1) solution for deprotection. The de-Boc product was purified by prep-HPLC. When Molander reagent was used instead of boronic acid, the  $\text{Pd}(\text{dppf})\text{Cl}_2$  was used as the palladium catalyst and  $\text{Cs}_2\text{CO}_3$  was used as the base.

#### **General procedure for hydrogenation:**

In a round-bottom flask, substrate, palladium on activated charcoal (10% Pd basis, 20~100% weight of substrate), and methanol were added. After degassing with hydrogen, the mixture was stirred under hydrogen at room temperature for 3 h before filtering through a syringe filter. Upon removal of the solvents, the residue was purified by prep-HPLC.

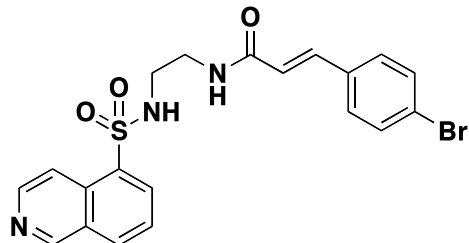
#### **General procedure for Mitsunobu reaction:**

To a stirred solution of alcohol substrate (1 equiv.), triphenylphosphine (1.5~2 equiv.), and N-hydroxyphthalimide (2 equiv.) in dry  $\text{CH}_2\text{Cl}_2$ , DIAD (2 equiv.) was added at 0 °C. After 2~8 h at room temperature, the reaction mixture was concentrated. Hydrazine hydrate was added at room temperature to the crude product in methanol. The stirring was continued at the same temperature for 1 h. The solvent was removed under reduced pressure. The residue solid was purified by prep-HPLC or subjected to deprotection of Boc (1:1 TFA/ $\text{CH}_2\text{Cl}_2$ , 1 h, room temperature).

### General procedure for converting hydroxyl group to azide:

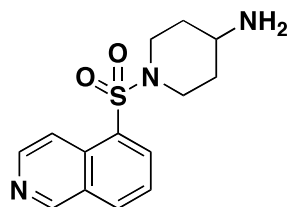
Method 1: To a stirred solution of alcohol (1 equiv.) in dry DMF was added bis (2,4-dichlorophenyl) phosphorochloridate (1.5 ~ 3 equiv.) at room temperature. The reaction mixture was stirred at 60 °C for 24 h and then quenched by the addition of water. The layers were separated and the aqueous layer was backextracted with EA. The combined organic layer was washed with brine and dried over anhydrous sodium sulfate.

Method 2: To a stirred solution of alcohol (1 equiv.) in dry CH<sub>2</sub>Cl<sub>2</sub> was added TEA (2 equiv.) and methanesulfonyl chloride (2 equiv.) at 0 °C. The reaction mixture was stirred at 0 °C for 2 h and then quenched by the addition of saturated NaHCO<sub>3</sub> (aq.). The layers were separated and the aqueous layer was extracted with CH<sub>2</sub>Cl<sub>2</sub>. The combined organic layer was washed with brine and dried over anhydrous sodium sulfate. The solvent was removed *in vacuo*, and the residue was dissolved in dry DMF, after which NaN<sub>3</sub> (10 equiv.) was added. The reaction mixture was stirred at 90 °C for 8 h, after which DMF was removed under reduced pressure. The residue was partitioned between brine and EA. The aqueous phase was extracted by EA. The combined organic layer was dried over anhydrous sodium sulfate. The solvent was removed *in vacuo* and the residue was purified by flash chromatography on silica (4g column, eluted by 0~100% EA in hexane) to give the azide.

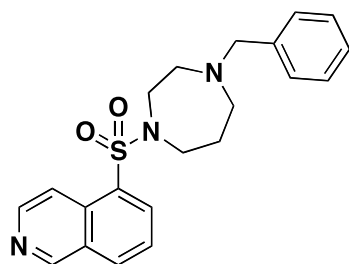


**(E)-3-(4-bromophenyl)-N-(2-(isoquinoline-5-sulfonamido)ethyl)acrylamide**

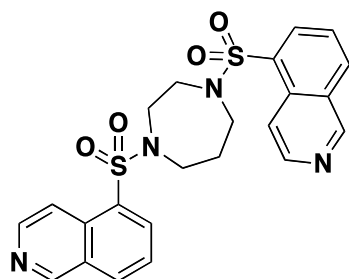
**(BRD6818).** <sup>1</sup>H NMR (300 MHz, CHLOROFORM-d) δ = 3.17 (2 H, td, J=3.7, 1.6 Hz), 3.49 (2 H, t, J=5.7 Hz), 6.22 (2 H, m), 7.31 (2 H, s), 7.43 (1 H, s), 7.49 (2 H, d, J=7.2 Hz), 7.71 (1 H, t, J=7.8 Hz), 8.19 (1 H, d, J=8.3 Hz), 8.45 (2 H, dd, J=7.3, 1.1 Hz), 8.69 (1 H, d, J=6.2 Hz), 9.32 (1 H, s) ppm.



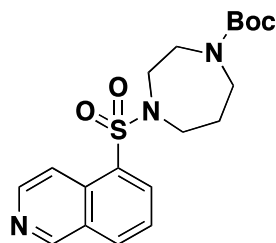
**1-(isoquinolin-5-ylsulfonyl)piperidin-4-amine (BRD3518).**  $^1\text{H}$  NMR (500 MHz, CHLOROFORM-d)  $\delta$  = 1.32 - 1.45 (2 H, m), 1.52 (4 H, br. s.), 1.86 (2 H, d,  $J$ =13.2 Hz), 2.63 - 2.76 (3 H, m), 3.78 (2 H, d,  $J$ =12.7 Hz), 7.73 (1 H, t,  $J$ =7.6 Hz), 8.23 (1 H, d,  $J$ =7.8 Hz), 8.40 (1 H, d,  $J$ =6.3 Hz), 8.52 (1 H, d,  $J$ =6.3 Hz), 8.70 (1 H, d,  $J$ =5.9 Hz), 9.37 (1 H, s) ppm.



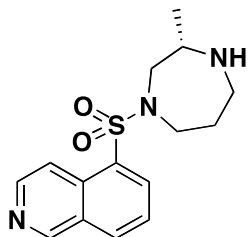
**5-(4-benzyl-1,4-diazepan-1-ylsulfonyl)isoquinoline (BRD5076).**  $^1\text{H}$  NMR (300 MHz, CHLOROFORM-d)  $\delta$  = 1.18 (1 H, s), 1.69 - 1.88 (2 H, m), 2.53 - 2.73 (4 H, m), 3.34 - 3.48 (4 H, m), 3.56 (2 H, s), 7.07 - 7.30 (7 H, m), 7.61 (1 H, t,  $J$ =7.8 Hz), 8.12 (1 H, d,  $J$ =8.1 Hz), 8.28 (1 H, dd,  $J$ =7.3, 1.1 Hz), 8.39 (1 H, d,  $J$ =6.2 Hz), 8.61 (1 H, d,  $J$ =6.2 Hz), 9.28 (1 H, s) ppm;  $^{13}\text{C}$  NMR (75 MHz, CHLOROFORM-d)  $\delta$  = 28.2, 46.8, 48.1, 54.4, 55.9, 62.1, 117.7, 125.8, 127.2, 128.3, 128.8, 129.2, 131.7, 133.0, 133.3, 134.6, 145.0, 153.2 ppm.



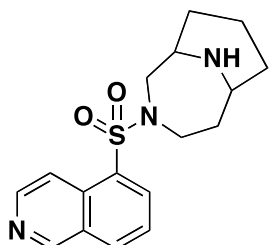
**1,4-bis(isoquinolin-5-ylsulfonyl)-1,4-diazepane (BRD2660).**  $^1\text{H}$  NMR (300 MHz, CHLOROFORM-d)  $\delta$  = 2.13 (2 H, s), 3.55 - 3.64 (8 H, m), 7.73 (2 H, t,  $J$ =7.8 Hz), 8.20 - 8.43 (4 H, m), 8.72 (2 H, d,  $J$ =6.0 Hz), 9.39 (2 H, d,  $J$ =0.9 Hz) ppm.



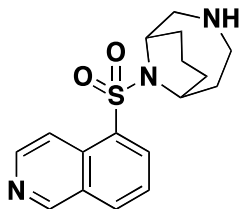
**tert-butyl 4-(isoquinolin-5-ylsulfonyl)-1,4-diazepane-1-carboxylate (BRD0272).**  $^1\text{H}$  NMR (300 MHz, CHLOROFORM-d)  $\delta$  = 1.43 (9 H, s), 1.94 - 1.99 (2 H, m), 3.34 - 3.48 (4 H, m), 3.48 - 3.58 (4 H, m), 7.71 (1 H, t,  $J=7.8$  Hz), 8.31 (1 H, d,  $J=8.1$  Hz), 8.28 (1 H, dd,  $J=7.3$ , 1.1 Hz), 8.41 (1 H, d,  $J=6.2$  Hz), 8.70 (1 H, d,  $J=6.2$  Hz), 9.35 (1 H, s) ppm.



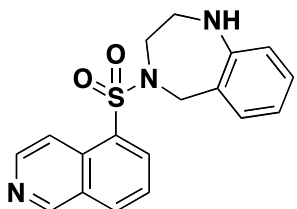
**(S)-5-(3-methyl-1,4-diazepan-1-ylsulfonyl)isoquinoline (BRD4719).**  $^1\text{H}$  NMR (500 MHz, CHLOROFORM-d)  $\delta$  = 1.07 (3 H, d,  $J=6.3$  Hz), 1.66 (2 H, d,  $J=2.4$  Hz), 1.72 - 1.84 (1 H, m), 1.88 - 2.00 (1 H, m), 2.74 (1 H, dd,  $J=13.9$ , 10.0 Hz), 2.85 (1 H, ddd,  $J=14.0$ , 10.1, 4.1 Hz), 3.01 (1 H, ddd,  $J=9.6$ , 6.5, 2.9 Hz), 3.13 (1 H, dt,  $J=13.7$ , 4.6 Hz), 3.28 (1 H, ddd,  $J=14.0$ , 8.4, 5.4 Hz), 3.67 - 3.81 (2 H, m), 7.70 (1 H, t,  $J=7.8$  Hz), 8.20 (1 H, d,  $J=7.8$  Hz), 8.33 (1 H, d,  $J=7.3$  Hz), 8.46 (1 H, d,  $J=6.3$  Hz), 8.71 (1 H, d,  $J=5.9$  Hz), 9.36 (1 H, s) ppm;  $^{13}\text{C}$  NMR (75 MHz, CHLOROFORM-d)  $\delta$  = 20.0, 31.2, 46.3, 47.9, 56.6, 57.8, 117.9, 126.1, 129.5, 131.9, 132.8, 133.5, 135.1, 145.3, 153.5 ppm.



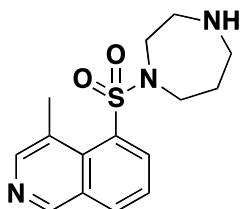
**3-(isoquinolin-5-ylsulfonyl)-3,10-diazabicyclo[4.3.1]decane (BRD3954).**  $^1\text{H}$  NMR (300 MHz, CHLOROFORM-d)  $\delta$  = 1.05 - 1.22 (4 H, m), 1.31 - 1.58 (3 H, m), 1.58 - 1.79 (2 H, m), 1.79 - 1.98 (2 H, m), 1.98 - 2.21 (2 H, m), 3.01 - 3.17 (1 H, m), 3.17 - 3.34 (3 H, m), 3.41 - 3.59 (2 H, m), 7.62 (1 H, t,  $J=7.7$  Hz), 8.12 (1 H, d,  $J=8.1$  Hz), 8.23 (1 H, dd,  $J=7.3$ , 1.1 Hz), 8.43 (1 H, d,  $J=6.0$  Hz), 8.62 (1 H, d,  $J=6.2$  Hz), 9.27 (1 H, s) ppm;  $^{13}\text{C}$  NMR (75 MHz, CHLOROFORM-d)  $\delta$  = 15.4, 28.2, 31.0, 33.2, 47.0, 47.9, 49.9, 53.6, 117.6, 125.9, 129.2, 131.7, 132.5, 133.2, 134.7, 145.1, 153.2 ppm.



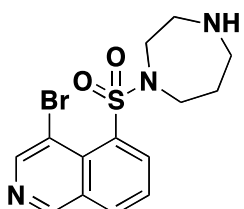
**10-(isoquinolin-5-ylsulfonyl)-3,10-diazabicyclo[4.3.1]decane (BRD2533).**  $^1\text{H}$  NMR (300 MHz, CHLOROFORM-d)  $\delta$  = 1.14 - 1.78 (6 H, m), 2.23 (2 H, m), 2.88 - 3.21 (4 H, m), 4.12 - 4.23 (1 H, m), 4.30 - 4.41 (1 H, m), 7.72 (1 H, t,  $J=7.7$  Hz), 8.18 - 8.27 (1 H, m), 8.39 (1 H, d,  $J=5.8$  Hz), 8.46 - 8.55 (1 H, m), 8.72 (1 H, d,  $J=6.0$  Hz), 9.38 (1 H, s) ppm.



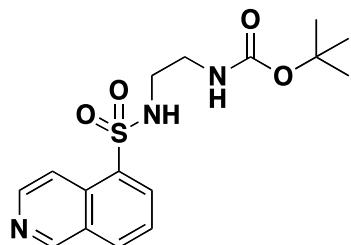
**4-(isoquinolin-5-ylsulfonyl)-2,3,4,5-tetrahydro-1H-benzo[e][1,4]diazepine (BRD0114).**  $^1\text{H}$  NMR (300 MHz, CHLOROFORM-d)  $\delta$  = 3.09 - 3.20 (2 H, m), 3.56 - 3.66 (2 H, m), 4.51 (2 H, s), 6.63 (1 H, d,  $J=7.5$  Hz), 6.86 (1 H, d,  $J=7.5$  Hz), 7.08 (1 H, d,  $J=1.5$  Hz), 7.12 - 7.20 (1 H, m), 7.65 (1 H, t,  $J=7.7$  Hz), 8.11 - 8.20 (1 H, m), 8.33 - 8.45 (2 H, m), 8.59 (1 H, d,  $J=6.0$  Hz), 9.30 (1 H, d,  $J=0.8$  Hz) ppm.



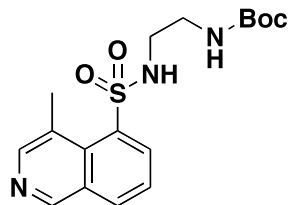
**5-(1,4-diazepan-1-ylsulfonyl)-4-methylisoquinoline (BRD3773).**  $^1\text{H}$  NMR (300 MHz, CHLOROFORM-d)  $\delta$  = 1.76 (1 H, br. s.), 1.89 (2 H, dq,  $J=6.3, 6.1$  Hz), 2.94 - 3.06 (7 H, m), 3.45 - 3.55 (2 H, m), 3.58 (2 H, t,  $J=6.2$  Hz), 7.52 (1 H, t,  $J=7.7$  Hz), 7.77 (1 H, d,  $J=7.3$  Hz), 8.07 (1 H, d,  $J=8.1$  Hz), 8.48 (1 H, s), 9.07 (1 H, s) ppm.



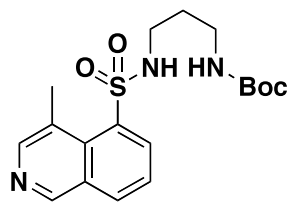
**5-(1,4-diazepan-1-ylsulfonyl)-4-bromoisoquinoline (BRD8880).**  $^1\text{H}$  NMR (300 MHz, CHLOROFORM-d)  $\delta$  = 1.24 - 1.40 (10 H, m), 1.40 - 1.46 (3 H, m), 1.86 - 2.01 (2 H, m), 3.26 - 3.56 (9 H, m), 7.47 - 7.59 (1 H, m), 7.68 - 7.83 (1 H, m), 8.03 (1 H, d,  $J=8.1$  Hz), 8.86 (1 H, s), 9.05 - 9.10 (1 H, m) ppm.



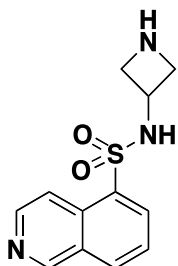
**tert-butyl 2-(isoquinoline-5-sulfonamido)ethylcarbamate (BRD4153).**  $^1\text{H}$  NMR (300 MHz, CHLOROFORM-d)  $\delta$  = 1.33 - 1.43 (9 H, m), 2.97 - 3.11 (2 H, m), 3.13 - 3.26 (2 H, m), 4.70 - 4.84 (1 H, m), 5.66 - 5.80 (1 H, m), 7.67 - 7.76 (1 H, m), 8.22 (1 H, d,  $J=8.1$  Hz), 8.36 - 8.47 (2 H, m), 8.71 (1 H, d,  $J=6.2$  Hz), 9.37 (1 H, s) ppm.



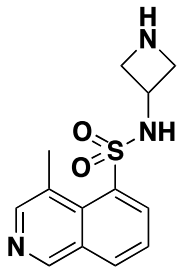
**tert-butyl 2-(4-methylisoquinoline-5-sulfonamido)ethylcarbamate (BRD9391).**  $^1\text{H}$  NMR (300 MHz, CHLOROFORM-d)  $\delta$  = 1.29 - 1.43 (9 H, m), 1.71 - 1.93 (1 H, m), 3.00 (3 H, s), 3.17 - 3.39 (4 H, m), 4.97 - 5.10 (1 H, m), 5.98 - 6.21 (1 H, m), 7.50 (1 H, t,  $J=7.8$  Hz), 8.05 (1 H, d,  $J=8.1$  Hz), 8.30 (1 H, d,  $J=7.2$  Hz), 8.46 (1 H, s), 9.06 (1 H, s) ppm.



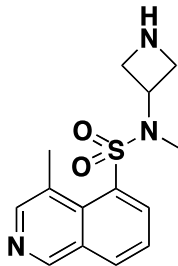
**tert-butyl 3-(4-methylisoquinoline-5-sulfonamido)propylcarbamate (BRD7177).**  $^1\text{H}$  NMR (500 MHz, CHLOROFORM-d)  $\delta$  = 1.46 (9 H, s), 1.69 - 1.80 (2 H, m), 3.10 (3 H, s), 3.23 (2 H, q,  $J=5.9$  Hz), 3.34 (2 H, d,  $J=5.4$  Hz), 4.91 (1 H, t,  $J=5.9$  Hz), 6.55 (1 H, br. s.), 7.56 (1 H, t,  $J=7.8$  Hz), 8.12 (1 H, d,  $J=7.8$  Hz), 8.32 (1 H, d,  $J=7.3$  Hz), 8.54 (1 H, s), 9.13 (1 H, s) ppm.



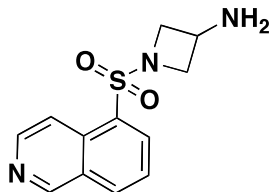
**N-(azetidin-3-yl)isoquinoline-5-sulfonamide (BRD4958).**  $^1\text{H}$  NMR (500 MHz, CHLOROFORM-d)  $\delta$  = 2.36 (4 H, br. s.), 2.43 (7 H, br. s.), 2.49 (2 H, br. s.), 3.29 - 3.35 (2 H, m), 3.56 - 3.66 (2 H, m), 4.20 (1 H, t,  $J=7.1$  Hz), 7.71 - 7.76 (1 H, m), 8.25 (1 H, d,  $J=8.3$  Hz), 8.44 (2 H, dd,  $J=13.7$ , 6.8 Hz), 8.74 (1 H, d,  $J=6.3$  Hz), 9.40 (1 H, s) ppm.



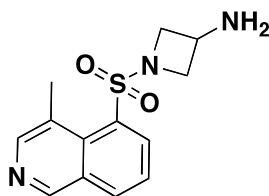
**N-(azetidin-3-yl)-4-methylisoquinoline-5-sulfonamide (BRD3966).**  $^1\text{H}$  NMR (300 MHz, CHLOROFORM-d)  $\delta$  = 2.05 (7 H, s), 3.09 (3 H, s), 3.72 (2 H, dd,  $J=8.7$ , 7.0 Hz), 3.86 - 4.01 (2 H, m), 4.33 (1 H, d,  $J=7.5$  Hz), 7.62 (1 H, t,  $J=7.7$  Hz), 8.17 (1 H, d,  $J=1.3$  Hz), 8.41 (1 H, dd,  $J=7.3$ , 1.3 Hz), 8.57 (1 H, s), 9.17 (1 H, s) ppm.



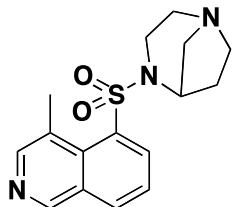
**N-(azetidin-3-yl)-N,4-dimethylisoquinoline-5-sulfonamide (BRD9325).**  $^1\text{H}$  NMR (300 MHz, CHLOROFORM-d)  $\delta$  = 1.64 - 1.85 (2 H, m), 3.06 (3 H, s), 3.19 (3 H, s), 3.80 (2 H, t,  $J=8.6$  Hz), 3.99 (2 H, t,  $J=8.4$  Hz), 4.97 (1 H, t,  $J=7.8$  Hz), 7.60 (1 H, t,  $J=7.7$  Hz), 7.86 - 7.95 (1 H, m), 8.18 (1 H, d,  $J=8.1$  Hz), 8.56 (1 H, s), 9.16 (1 H, s) ppm;  $^{13}\text{C}$  NMR (75 MHz, CHLOROFORM-d)  $\delta$  = 21.5, 31.1, 52.0, 52.2, 124.7, 127.6, 130.4, 130.7, 132.4, 134.7, 136.1, 148.7, 152.0 ppm.



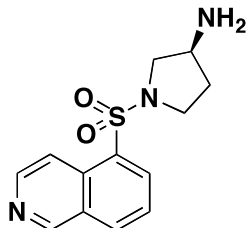
**1-(isoquinolin-5-ylsulfonyl)azetidin-3-amine (BRD5991).**  $^1\text{H}$  NMR (300 MHz, CHLOROFORM-d)  $\delta$  = 1.09 (1 H, t, J=7.3 Hz), 1.26 - 1.66 (2 H, m), 3.57 - 3.70 (2 H, m), 3.70 - 3.83 (1 H, m), 3.96 - 4.10 (2 H, m), 7.74 (1 H, t, J=7.8 Hz), 8.26 (1 H, d, J=8.3 Hz), 8.38 - 8.51 (2 H, m), 8.72 (1 H, d, J=6.0 Hz), 9.37 (1 H, s) ppm.



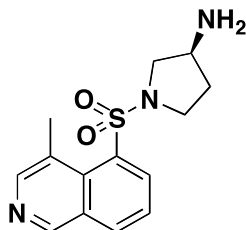
**1-(4-methylisoquinolin-5-ylsulfonyl)azetidin-3-amine (BRD5337).**  $^1\text{H}$  NMR (500 MHz, CHLOROFORM-d)  $\delta$  = 1.62 (3 H, br. s.), 3.10 (3 H, s), 3.82 (2 H, t, J=7.1 Hz), 3.86 - 3.93 (1 H, m), 4.08 (2 H, t, J=7.3 Hz), 7.65 (1 H, t, J=7.8 Hz), 8.21 (1 H, d, J=8.3 Hz), 8.56 (1 H, s), 8.71 (1 H, d, J=7.3 Hz), 9.16 (1 H, s) ppm.



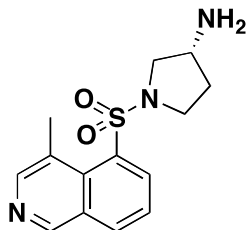
**5-(1,4-diazabicyclo[3.2.1]octan-4-ylsulfonyl)-4-methylisoquinoline (BRD1742).**  $^1\text{H}$  NMR (300 MHz, CHLOROFORM-d)  $\delta$  = 1.13 - 1.31 (1 H, m), 1.95 - 2.12 (2 H, m), 2.17 - 2.36 (1 H, m), 2.54 - 2.66 (1 H, m), 2.74 - 2.83 (1 H, m), 2.94 - 3.19 (7 H, m), 3.19 - 3.41 (2 H, m), 4.26 - 4.38 (1 H, m), 7.66 (1 H, t, J=7.9 Hz), 8.21 (1 H, d, J=8.1 Hz), 8.46 - 8.60 (2 H, m), 9.17 (1 H, s) ppm;  $^{13}\text{C}$  NMR (75 MHz, CHLOROFORM-d)  $\delta$  = 21.4, 31.0, 39.5, 50.6, 52.6, 54.9, 59.9, 124.8, 127.5, 130.3, 132.5, 134.8, 134.9, 135.4, 148.8, 152.1 ppm.



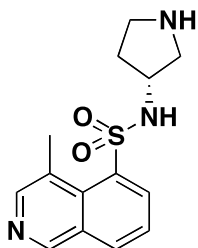
**(S)-1-(isoquinolin-5-ylsulfonyl)pyrrolidin-3-amine (BRD3590).**  $^1\text{H}$  NMR (300 MHz, CHLOROFORM-d)  $\delta$  = 1.39 - 1.77 (2 H, m), 2.00 - 2.16 (1 H, m), 2.99 - 3.14 (1 H, m), 3.43 (1 H, ddd,  $J=9.6, 8.1, 5.7$  Hz), 3.48 - 3.64 (3 H, m), 7.67 - 7.77 (1 H, m), 8.23 (1 H, d,  $J=8.3$  Hz), 8.46 (1 H, dd,  $J=7.3, 1.3$  Hz), 8.60 (1 H, d,  $J=6.2$  Hz), 8.71 (1 H, d,  $J=6.2$  Hz), 9.37 (1 H, d,  $J=0.9$  Hz) ppm.



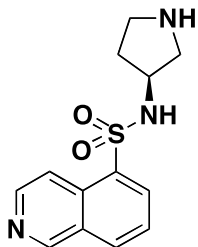
**(S)-1-(4-methylisoquinolin-5-ylsulfonyl)pyrrolidin-3-amine (BRD3752).**  $^1\text{H}$  NMR (300 MHz, CHLOROFORM-d)  $\delta$  = 1.42 (2 H, br. s.), 1.84 - 1.96 (1 H, m), 2.19 - 2.34 (1 H, m), 3.05 - 3.13 (3 H, m), 3.23 - 3.35 (1 H, m), 3.62 - 3.79 (3 H, m), 3.84 - 3.94 (1 H, m), 7.62 (1 H, t,  $J=7.8$  Hz), 8.16 (1 H, dd,  $J=8.2, 1.2$  Hz), 8.49 (1 H, dd,  $J=7.5, 1.3$  Hz), 8.56 (1 H, d,  $J=0.8$  Hz), 9.15 (1 H, s) ppm;  $^{13}\text{C}$  NMR (150 MHz, CHLOROFORM-d)  $\delta$  = 21.6, 34.8, 46.8, 51.6, 56.5, 125.0, 127.7, 130.4, 131.2, 132.3, 134.3, 136.3, 148.5, 151.9 ppm.



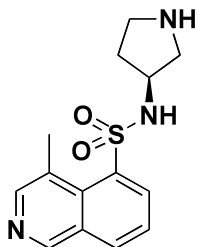
**(R)-1-(4-methylisoquinolin-5-ylsulfonyl)pyrrolidin-3-amine (BRD0828).**  $^1\text{H}$  NMR (500 MHz, CHLOROFORM-d)  $\delta$  = 1.89 (1 H, ddd,  $J=12.6, 3.8, 3.7$  Hz), 2.23 - 2.32 (1 H, m), 3.10 (3 H, s), 3.29 (1 H, dd,  $J=10.3, 3.4$  Hz), 3.66 - 3.77 (3 H, m), 3.87 - 3.93 (1 H, m), 7.62 (1 H, t,  $J=7.8$  Hz), 8.16 (1 H, d,  $J=8.3$  Hz), 8.48 (1 H, d,  $J=7.3$  Hz), 8.55 (1 H, s), 9.15 (1 H, s).



**(R)-4-methyl-N-(pyrrolidin-3-yl)isoquinoline-5-sulfonamide (BRD3695).**  $^1\text{H}$  NMR (500 MHz, CHLOROFORM-d)  $\delta$  = 1.89 - 2.00 (1 H, m), 2.12 - 2.25 (1 H, m), 2.96 (1 H, dd,  $J$ =15.9, 9.5 Hz), 3.07 (3 H, s), 3.09 - 3.25 (2 H, m), 3.87 - 4.01 (1 H, m), 5.49 (1 H, br. s.), 7.60 (1 H, t,  $J$ =7.8 Hz), 8.06 - 8.19 (1 H, m), 8.44 - 8.52 (1 H, m), 8.54 (1 H, s), 9.06 - 9.18 (1 H, m) ppm;  $^{13}\text{C}$  NMR (150 MHz, CHLOROFORM-d)  $\delta$  = 22.0, 30.0, 33.4, 45.0, 53.7, 54.7, 125.1, 127.6, 130.4, 132.5, 132.5, 134.8, 137.1, 148.7, 152.2 ppm.



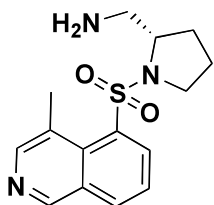
**(S)-N-(pyrrolidin-3-yl)isoquinoline-5-sulfonamide (BRD8943).**  $^1\text{H}$  NMR (300 MHz, CHLOROFORM-d)  $\delta$  = 1.44 - 1.58 (1 H, m), 1.79 - 1.97 (1 H, m), 2.63 - 2.74 (1 H, m), 2.76 - 3.03 (3 H, m), 3.61 - 3.95 (2 H, m), 7.67 - 7.78 (1 H, m), 8.24 (1 H, d,  $J$ =8.3 Hz), 8.43 (1 H, d,  $J$ =6.2 Hz), 8.49 (1 H, dd,  $J$ =7.3, 1.1 Hz), 8.69 (1 H, d,  $J$ =6.0 Hz), 9.39 (1 H, s) ppm.



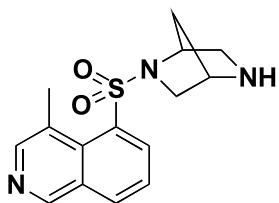
**(S)-4-methyl-N-(pyrrolidin-3-yl)isoquinoline-5-sulfonamide (BRD9573).**  $^1\text{H}$  NMR (500 MHz, CHLOROFORM-d)  $\delta$  = 1.85 - 1.96 (1 H, m), 2.19 (1 H, td,  $J$ =14.0, 7.6 Hz), 2.92 - 3.02 (1 H, m), 3.02 - 3.22 (6 H, m), 3.93 - 4.02 (1 H, m), 7.64 (1 H, t,  $J$ =7.8 Hz), 8.18 (1 H, d,  $J$ =7.8 Hz), 8.50 - 8.60 (2 H, m), 9.17 (1 H, s) ppm.



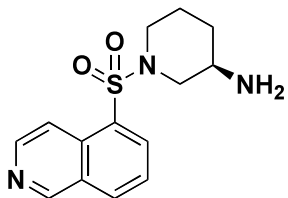
**(S)-(1-(isoquinolin-5-ylsulfonyl)pyrrolidin-2-yl)methanamine (BRD2246).**  $^1\text{H}$  NMR (300 MHz, CHLOROFORM-d)  $\delta$  = 1.58 - 1.86 (4 H, m), 2.75 - 2.88 (2 H, m), 3.40 (2 H, t,  $J=6.6$  Hz), 3.79 - 3.93 (1 H, m,  $J=7.3, 2.4, 1.3, 1.3$  Hz), 7.74 (1 H, t,  $J=7.8$  Hz), 8.24 (1 H, d,  $J=8.3$  Hz), 8.46 (1 H, dd,  $J=7.4, 1.2$  Hz), 8.63 - 8.75 (2 H, m), 9.37 (1 H, s) ppm;  $^{13}\text{C}$  NMR (75 MHz, CHLOROFORM-d)  $\delta$  = 24.4, 29.2, 46.1, 49.1, 62.3, 117.7, 126.0, 129.1, 132.2, 133.6, 133.7, 133.7, 145.2, 153.3 ppm.



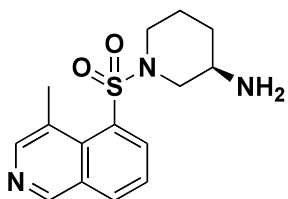
**(S)-(1-(4-methylisoquinolin-5-ylsulfonyl)pyrrolidin-2-yl)methanamine (BRD7471).**  $^1\text{H}$  NMR (500 MHz, CHLOROFORM-d)  $\delta$  = 1.26 (2 H, d,  $J=2.9$  Hz), 1.95 - 2.18 (4 H, m), 2.20 - 2.33 (1 H, m), 2.79 (1 H, dd,  $J=12.9, 7.6$  Hz), 2.96 (1 H, dd,  $J=13.2, 4.4$  Hz), 3.10 (3 H, s), 3.47 - 3.55 (1 H, m), 3.60 - 3.67 (1 H, m), 4.03 - 4.10 (1 H, m,  $J=7.4, 7.4, 3.9, 3.8$  Hz), 7.62 (1 H, t,  $J=7.8$  Hz), 8.17 (1 H, d,  $J=8.3$  Hz), 8.22 (1 H, d,  $J=7.3$  Hz), 8.56 (1 H, s), 9.15 (1 H, s) ppm;  $^{13}\text{C}$  NMR (150 MHz, CHLOROFORM-d)  $\delta$  = 21.7, 24.4, 29.3, 45.97, 49.6, 63.1, 124.7, 127.7, 130.3, 130.7, 132.3, 134.5, 136.3, 148.6, 151.9 ppm.



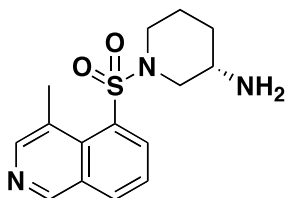
**5-((1S,4S)-2,5-diazabicyclo[2.2.1]heptan-2-ylsulfonyl)-4-methylisoquinoline (BRD4942).**  $^1\text{H}$  NMR (300 MHz, CHLOROFORM-d)  $\delta$  = 1.89 (3 H, d,  $J=10.9$  Hz), 2.00 - 2.10 (1 H, m), 2.98 - 3.14 (4 H, m), 3.29 - 3.45 (2 H, m), 3.51 (1 H, dd,  $J=9.1, 2.0$  Hz), 3.89 (1 H, s), 4.45 (1 H, s), 7.64 (1 H, t,  $J=7.8$  Hz), 8.13 - 8.23 (1 H, m), 8.46 - 8.60 (2 H, m), 9.16 (1 H, s) ppm.



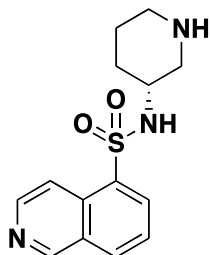
**(R)-1-(isoquinolin-5-ylsulfonyl)piperidin-3-amine (BRD0841).**  $^1\text{H}$  NMR (300 MHz, CHLOROFORM-d)  $\delta$  = 1.01 - 1.18 (1 H, m), 1.18 - 1.44 (2 H, m), 1.60 (1 H, dd,  $J$ =10.2, 3.6 Hz), 1.71 - 1.88 (2 H, m), 2.42 (1 H, dd,  $J$ =11.6, 8.9 Hz), 2.61 - 2.74 (1 H, m), 2.84 - 2.97 (1 H, m), 3.49 - 3.72 (2 H, m), 7.72 (1 H, t,  $J$ =7.8 Hz), 8.22 (1 H, d,  $J$ =8.1 Hz), 8.38 (1 H, dd,  $J$ =7.3, 1.3 Hz), 8.51 (1 H, d,  $J$ =6.2 Hz), 8.68 (1 H, d,  $J$ =6.2 Hz), 9.35 (1 H, s) ppm.



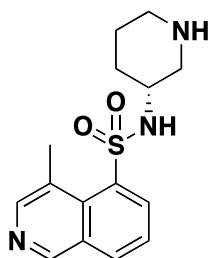
**(R)-1-(4-methylisoquinolin-5-ylsulfonyl)piperidin-3-amine (BRD3376).**  $^1\text{H}$  NMR (300 MHz, CHLOROFORM-d)  $\delta$  = 1.27 - 1.48 (3 H, m), 1.65 - 1.83 (1 H, m), 1.83 - 1.96 (1 H, m), 1.98 - 2.11 (1 H, m), 2.84 (1 H, dd,  $J$ =12.2, 8.9 Hz), 2.99 - 3.17 (5 H, m), 3.68 - 3.86 (2 H, m), 7.62 (1 H, t,  $J$ =7.7 Hz), 8.09 (1 H, dd,  $J$ =7.5, 1.1 Hz), 8.17 (1 H, dd,  $J$ =8.1, 1.3 Hz), 8.56 (1 H, s), 9.15 (1 H, s) ppm;  $^{13}\text{C}$  NMR (CHLOROFORM-d)  $\delta$  = 21.4, 24.0, 33.4, 46.5, 47.7, 54.2, 124.8, 127.6, 130.3, 131.4, 132.4, 134.7, 136.5, 148.7, 152.0 ppm.



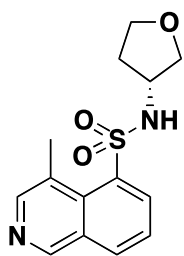
**(S)-1-(4-methylisoquinolin-5-ylsulfonyl)piperidin-3-amine (BRD3436).**  $^1\text{H}$  NMR (300 MHz, CHLOROFORM-d)  $\delta$  = 1.05 - 1.19 (2 H, m), 1.21 - 1.31 (1 H, m), 1.39 - 1.66 (7 H, m), 1.71 - 1.91 (2 H, m), 2.37 - 2.48 (1 H, m), 2.62 - 2.74 (1 H, m), 2.86 - 2.97 (1 H, m), 3.49 - 3.73 (3 H, m), 7.66 - 7.78 (1 H, m), 8.23 (1 H, d,  $J$ =8.3 Hz), 8.36 - 8.43 (1 H, m), 8.51 (1 H, d,  $J$ =6.2 Hz), 8.69 (1 H, d,  $J$ =6.2 Hz), 9.36 (1 H, s) ppm.



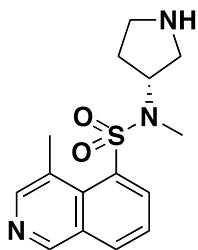
**(R)-N-(piperidin-3-yl)isoquinoline-5-sulfonamide (BRD0561).**  $^1\text{H}$  NMR (300 MHz, CHLOROFORM-d)  $\delta$  = 1.31 - 1.67 (5 H, m), 1.98 - 2.07 (1 H, m), 2.45 (1 H, dd,  $J$ =11.6, 5.7 Hz), 2.59 - 2.79 (3 H, m), 3.31 - 3.42 (1 H, m), 7.72 (1 H, t,  $J$ =7.8 Hz), 8.23 (1 H, d,  $J$ =7.9 Hz), 8.47 (2 H, dd,  $J$ =15.2, 6.7 Hz), 8.74 (1 H, d,  $J$ =6.0 Hz), 9.39 (1 H, s) ppm.



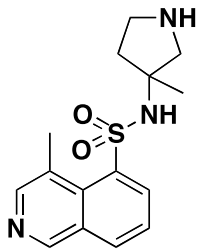
**(R)-4-methyl-N-(piperidin-3-yl)isoquinoline-5-sulfonamide (BRD4209).**  $^1\text{H}$  NMR (300 MHz, CHLOROFORM-d)  $\delta$  = 1.51 (2 H, br. s.), 1.75 (4 H, br. s.), 2.69 - 2.87 (4 H, m), 2.92 - 3.02 (1 H, m), 3.05 - 3.16 (3 H, m), 3.50 (1 H, br. s.), 7.62 (1 H, t,  $J$ =7.8 Hz), 8.16 (1 H, dd,  $J$ =8.1, 1.3 Hz), 8.56 (1 H, d,  $J$ =0.8 Hz), 8.62 (1 H, dd,  $J$ =7.5, 1.3 Hz), 9.16 (1 H, s) ppm.



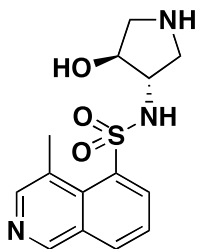
**(R)-4-methyl-N-(tetrahydrofuran-3-yl)isoquinoline-5-sulfonamide (BRD4357).**  $^1\text{H}$  NMR (300 MHz, CHLOROFORM-d)  $\delta$  = 1.95 - 2.10 (1 H, m), 2.21 - 2.38 (1 H, m), 3.8 (3 H, s), 3.73 - 3.88 (3 H, m), 3.93 - 4.16 (2 H, m), 7.63 (1 H, t,  $J$ =7.8 Hz), 8.12 - 8.24 (1 H, m), 8.47 - 8.60 (2 H, m), 9.16 (1 H, s) ppm.



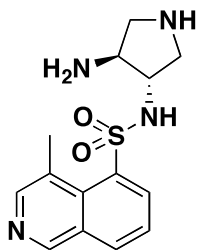
**(R)-N,4-dimethyl-N-(pyrrolidin-3-yl)isoquinoline-5-sulfonamide (BRD4618).**  $^1\text{H}$  NMR (300 MHz, CHLOROFORM-d)  $\delta$  = 1.59 - 1.73 (7 H, m), 1.95 - 2.21 (2 H, m), 2.89 - 2.99 (2 H, m), 3.01 (3 H, s), 3.02 - 3.16 (5 H, m), 3.24 (1 H, dd,  $J$ =11.4, 8.2 Hz), 4.46 - 4.60 (1 H, m), 7.62 (1 H, t,  $J$ =7.9 Hz), 8.10 - 8.21 (2 H, m), 8.56 (1 H, s), 9.16 (1 H, s) ppm.



**4-methyl-N-(3-methylpyrrolidin-3-yl)isoquinoline-5-sulfonamide (BRD4889).**  $^1\text{H}$  NMR (300 MHz, CHLOROFORM-d)  $\delta$  = 1.26 (1 H, t,  $J$ =7.1 Hz), 1.43 (3 H, s), 1.75 - 1.19 (1 H, m), 2.34 (2 H, s), 2.83 - 2.90 (1 H, m), 3.09 (3 H, s), 3.36 - 3.39 (1 H, m), 7.65 (1 H, d,  $J$ =8.3 Hz), 8.17 (1 H, dd,  $J$ =8.1, 1.5 Hz), 8.56 (1 H, s), 8.67 - 8.72 (1 H, m), 9.16 (1 H, s) ppm.

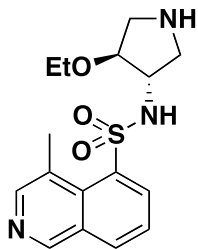


**N-((3S,4S)-4-hydroxypyrrolidin-3-yl)-4-methylisoquinoline-5-sulfonamide (BRD0227).**  $^1\text{H}$  NMR (300 MHz, MeOD)  $\delta$  = 2.74 - 2.85 (1 H, m), 2.88 - 2.98 (1 H, m), 3.05 (3 H, s), 3.11 - 3.19 (1 H, m), 3.31 - 3.39 (1 H, m), 3.60 (1 H, td,  $J$ =2.7, 0.9 Hz), 4.26 - 4.37 (1 H, m), 7.75 (1 H, t,  $J$ =7.7 Hz), 8.29 - 8.36 (1 H, m), 8.43 (1 H, s), 8.53 - 8.63 (1 H, m), 9.15 (1 H, s) ppm.



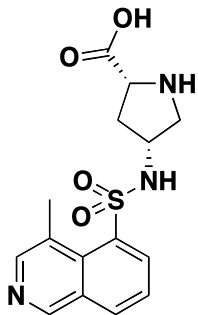
***N-((3S,4S)-4-aminopyrrolidin-3-yl)-4-methylisoquinoline-5-sulfonamide (BRD6696).***

$^1\text{H}$  NMR (300 MHz, MeOD)  $\delta$  = 1.76 - 1.91 (1 H, m), 2.55 - 2.67 (1 H, m), 2.84 - 2.95 (1 H, m), 3.00 - 3.08 (3 H, m), 3.14 - 3.24 (1 H, m), 3.24 - 3.32 (6 H, m), 7.77 (1 H, t,  $J$ =7.8 Hz), 8.33 (1 H, d,  $J$ =8.5 Hz), 8.45 (1 H, s), 8.55 (1 H, d,  $J$ =7.7 Hz), 9.16 (1 H, s) ppm.



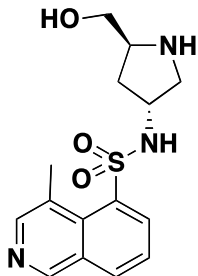
***N-((3S,4S)-4-ethoxypyrrrolidin-3-yl)-4-methylisoquinoline-5-sulfonamide***

**(BRD1230).**  $^1\text{H}$  NMR (300 MHz, MeOD)  $\delta$  = 1.07 (3 H, t,  $J$ =7.0 Hz), 2.81 - 2.91 (2 H, m), 2.98 - 3.16 (4 H, m), 3.42 (2 H, q,  $J$ =7.2 Hz), 3.64 - 3.73 (1 H, m), 4.01 (1 H, ddd,  $J$ =2.5, 1.2, 1.0 Hz), 7.74 (1 H, t,  $J$ =7.7 Hz), 8.33 (1 H, d,  $J$ =8.1 Hz), 8.44 (1 H, s), 8.58 (1 H, d,  $J$ =7.5 Hz), 9.16 (1 H, s) ppm.

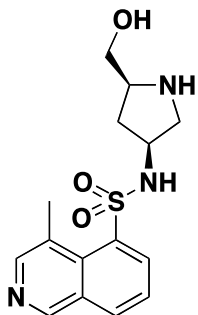


***(2R,4R)-4-(4-methylisoquinoline-5-sulfonamido)pyrrolidine-2-carboxylic acid***

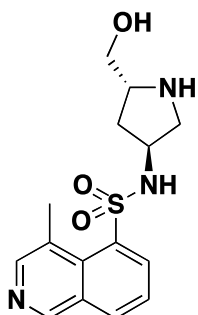
**(BRD0035).**  $^1\text{H}$  NMR (500 MHz, METHANOL-d4)  $\delta$  = 1.24 - 1.34 (4 H, m), 1.70 (2 H, dd,  $J$ =6.3, 3.4 Hz), 1.89 - 1.96 (2 H, m), 2.07 (2 H, d,  $J$ =14.2 Hz), 3.08 (3 H, s), 3.17 - 3.21 (1 H, m), 3.35 - 3.39 (2 H, m), 3.47 (1 H, d,  $J$ =2.0 Hz), 3.80 (1 H, s), 4.01 (1 H, s), 7.82 (1 H, t,  $J$ =7.8 Hz), 8.38 (1 H, d,  $J$ =8.3 Hz), 8.49 (1 H, s), 8.55 (1 H, d,  $J$ =7.3 Hz), 9.21 (1 H, s) ppm.



***N-((3R,5S)-5-(hydroxymethyl)pyrrolidin-3-yl)-4-methyisoquinoline-5-sulfonamide (BRD4980).*** <sup>1</sup>H NMR (500 MHz, CHLOROFORM-d) δ = 1.94 (2 H, t, J=6.1 Hz), 2.05 (1 H, s), 3.04 (1 H, dd, J=11.2, 3.9 Hz), 3.10 (3 H, s), 3.16 - 3.24 (1 H, m), 3.36 (1 H, d, J=4.9 Hz), 3.52 - 3.59 (2 H, m), 3.97 (1 H, s), 7.66 (1 H, t, J=7.6 Hz), 8.21 (1 H, d, J=7.8 Hz), 8.53 (1 H, d, J=8.3 Hz), 8.58 (1 H, s), 9.19 (1 H, s) ppm.

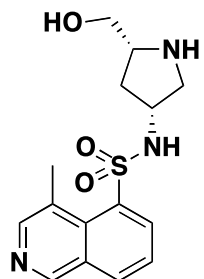


***N-((3S,5S)-5-(hydroxymethyl)pyrrolidin-3-yl)-4-methyisoquinoline-5-sulfonamide (BRD6875).*** <sup>1</sup>H NMR (300 MHz, MeOD) δ = 1.61 (1 H, s), 2.29 (1 H, s), 2.88 - 2.96 (1 H, m), 3.05 (3 H, s), 3.06 - 3.14 (1 H, m), 3.15 - 3.24 (3 H, m), 3.57 (2 H, d, J=4.7 Hz), 3.83 (1 H, s), 7.76 (1 H, t, J=7.8 Hz), 8.33 (1 H, d, J=8.1 Hz), 8.44 (1 H, s), 8.51 (1 H, d, J=7.5 Hz), 9.16 (1 H, s) ppm.

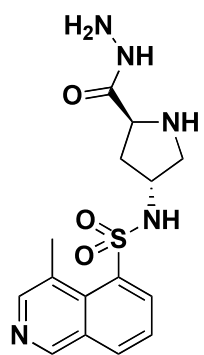


***N-((3S,5R)-5-(hydroxymethyl)pyrrolidin-3-yl)-4-methyisoquinoline-5-sulfonamide (BRD8313).*** <sup>1</sup>H NMR (500 MHz, CHLOROFORM-d) δ = 1.13 - 1.19 (2 H, m), 1.24 - 1.36 (2 H, m), 1.90 - 1.97 (2 H, m), 3.00 - 3.06 (1 H, m), 3.08 - 3.13 (2 H, m), 3.21 (1 H, dd, J=10.3, 4.9 Hz), 3.32 - 3.41 (1 H, m), 3.53 - 3.60 (2 H, m), 3.98 (1 H, dd, J=6.6, 4.6

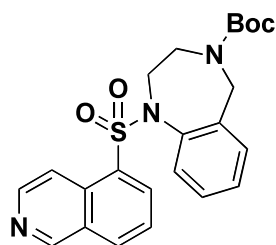
Hz), 7.62 - 7.69 (1 H, m), 8.21 (1 H, d, J=7.3 Hz), 8.53 (1 H, d, J=8.3 Hz), 8.56 - 8.60 (1 H, m), 9.15 - 9.21 (1 H, m) ppm.



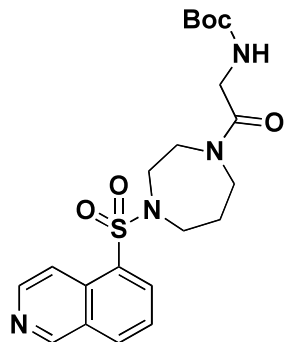
**N-((3R,5R)-5-(hydroxymethyl)pyrrolidin-3-yl)-4-methylisoquinoline-5-sulfonamide (BRD1045).** <sup>1</sup>H NMR (500 MHz, CHLOROFORM-d) δ = 1.81 (2 H, br. s.), 2.32 (1 H, ddd, J=13.8, 9.6, 7.3 Hz), 3.06 (1 H, dd, J=11.2, 4.9 Hz), 3.09 (3 H, s), 3.17 (1 H, d, J=10.7 Hz), 3.43 - 3.49 (1 H, m), 3.61 (1 H, dd, J=10.7, 3.9 Hz), 3.77 (1 H, dd, J=11.0, 2.7 Hz), 3.90 - 3.97 (1 H, m), 7.63 (1 H, t, J=7.8 Hz), 8.16 (1 H, d, J=8.3 Hz), 8.53 - 8.57 (2 H, m), 9.15 (1 H, s) ppm.



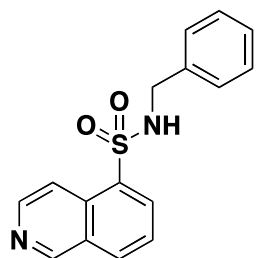
**N-((3R,5S)-5-(hydrazinecarbonyl)pyrrolidin-3-yl)-4-methylisoquinoline-5-sulfonamide (BRD7777).** <sup>1</sup>H NMR (500 MHz, CHLOROFORM-d) δ = 1.14 (2 H, t, J=7.3 Hz), 1.20 (2 H, t, J=6.8 Hz), 2.10 (2 H, s), 2.24 - 2.33 (2 H, m), 3.06 - 3.13 (4 H, m), 3.32 (2 H, d, J=6.8 Hz), 3.40 (1 H, d, J=6.8 Hz), 3.78 - 3.83 (1 H, m), 3.93 (1 H, d, J=5.4 Hz), 4.00 (1 H, d, J=6.3 Hz), 7.67 (1 H, t, J=7.6 Hz), 8.22 (1 H, d, J=7.3 Hz), 8.46 - 8.50 (1 H, m), 8.58 (1 H, s), 9.19 (1 H, s) ppm.



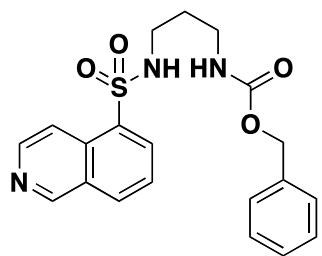
**tert-butyl 1-(isoquinolin-5-ylsulfonyl)-2,3-dihydro-1*H*-benzo[*e*][1,4]diazepine-4(5*H*)-carboxylate (BRD0119).**  $^1\text{H}$  NMR (300 MHz, CHLOROFORM-d)  $\delta$  = 1.31 - 1.37 (9 H, m), 3.48 - 3.77 (3 H, m), 3.85 - 4.13 (3 H, m), 6.92 - 7.02 (1 H, m), 7.08 - 7.25 (3 H, m), 7.61 - 7.74 (1 H, m), 8.08 - 8.17 (1 H, m), 8.20 - 8.28 (1 H, m), 8.31 - 8.41 (1 H, m), 8.56 (1 H, ddd,  $J$ =4.8, 2.1, 1.0 Hz), 9.32 - 9.42 (1 H, br.s.) ppm.



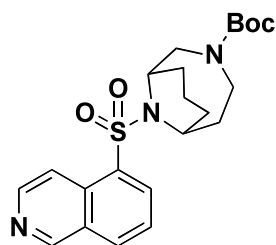
**tert-butyl 2-(4-(isoquinolin-5-ylsulfonyl)-1,4-diazepan-1-yl)-2-oxoethylcarbamate (BRD9370).**  $^1\text{H}$  NMR (300 MHz, CHLOROFORM-d)  $\delta$  = 1.23 (1 H, t,  $J$ =7.2 Hz), 1.31 - 1.44 (9 H, s), 1.92 - 2.00 (2 H, m), 2.02 (1 H, s), 3.31 - 3.60 (6 H, m), 3.61 - 3.77 (2 H, m), 3.88 (2 H, dd,  $J$ =9.3, 4.4 Hz), 5.45 (1 H, d,  $J$ =15.3 Hz), 7.60 - 7.72 (1 H, m), 8.19 (1 H, d,  $J$ =8.1 Hz), 8.26 - 8.37 (2 H, m), 8.61 - 8.71 (1 H, m), 9.33 (1 H, s) ppm.



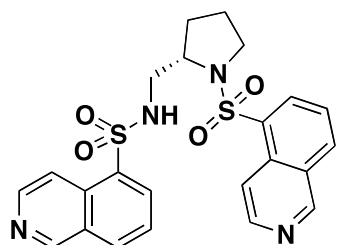
**N-benzylisoquinoline-5-sulfonamide (BRD2850).**  $^1\text{H}$  NMR (300 MHz, CHLOROFORM-d)  $\delta$  = 4.05 - 4.20 (2 H, m), 5.40 - 5.62 (1 H, m), 6.94 - 7.08 (2 H, m), 7.08 - 7.20 (3 H, m), 7.67 (1 H, t,  $J$ =7.8 Hz), 8.18 (1 H, d,  $J$ =8.3 Hz), 8.35 - 8.48 (2 H, m), 8.57 - 8.71 (1 H, m), 9.25 - 9.38 (1 H, br.s.) ppm.



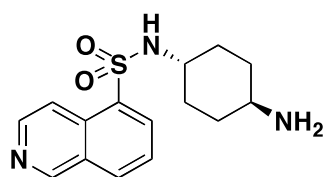
**benzyl 3-(isoquinoline-5-sulfonamido)propylcarbamate (BRD0886).**  $^1\text{H}$  NMR (300 MHz, MeOD)  $\delta$  = 2.86 (2 H, t,  $J=7.0$  Hz), 3.01 (2 H, t,  $J=6.7$  Hz), 4.94 - 4.98 (2 H, m), 7.21 - 7.32 (5 H, m), 7.72 - 7.81 (1 H, m), 8.31 - 8.46 (2 H, m), 8.53 (1 H, d,  $J=6.6$  Hz), 8.57 - 8.63 (1 H, m), 9.35 (1 H, s) ppm.



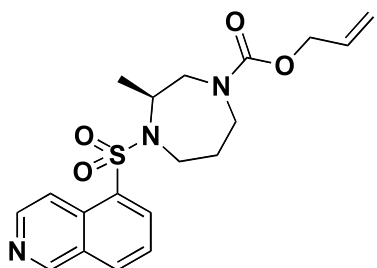
**tert-butyl 10-(isoquinolin-5-ylsulfonyl)-3,10-diazabicyclo[4.3.1]decane-3-carboxylate (BRD4468).**  $^1\text{H}$  NMR (300 MHz, CHLOROFORM-d)  $\delta$  = 1.22 - 1.38 (2 H, m), 1.38 - 1.52 (9 H, m), 1.64 - 1.84 (3 H, m), 2.13 - 2.28 (1 H, m), 3.09 - 3.28 (2 H, m), 3.87 - 4.12 (2 H, m), 4.17 - 4.41 (2 H, m), 7.71 (1 H, t,  $J=7.7$  Hz), 8.22 (1 H, d,  $J=8.3$  Hz), 8.35 (3 H, d,  $J=6.4$  Hz), 8.48 (1 H, d,  $J=7.3$  Hz), 8.72 (1 H, dd,  $J=6.2, 2.3$  Hz), 9.38 (1 H, s) ppm;  $^{13}\text{C}$  NMR (75 MHz, CHLOROFORM-d)  $\delta$  = 14.8, 15.1, 28.3, 28.5, 28.5, 31.1, 31.3, 32.3, 33.3, 46.1, 46.3, 49.2, 49.3, 52.5, 52.6, 53.0, 54.6, 79.8, 117.4, 125.9, 129.2, 131.2, 133.3, 133.6, 135.2, 145.2, 153.5, 154.4, 155.1 ppm.



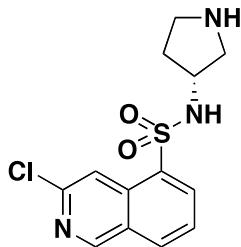
**(S)-N-((1-(isoquinolin-5-ylsulfonyl)pyrrolidin-2-yl)methyl)isoquinoline-5-sulfonamide (BRD3078).**  $^1\text{H}$  NMR (300 MHz, CHLOROFORM-d)  $\delta$  = 1.45 - 1.75 (4 H, m), 2.98 - 3.09 (2 H, m), 3.14 - 3.33 (2 H, m), 3.64 - 3.78 (1 H, m), 5.52 (1 H, s), 7.04 - 7.15 (2 H, m), 7.65 (2 H, ddd,  $J=10.5, 7.9, 7.6$  Hz), 8.11 - 8.21 (2 H, m), 8.26 (1 H, dd,  $J=7.3, 1.1$  Hz), 8.32 - 8.40 (2 H, m), 8.50 (1 H, d,  $J=6.2$  Hz), 8.56 - 8.61 (1 H, m), 8.68 (1 H, d,  $J=6.2$  Hz), 9.28 (1 H, s), 9.33 (1 H, s) ppm.



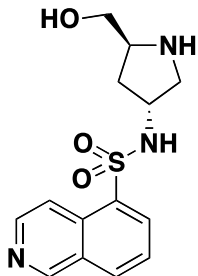
**N-((1*r*,4*r*)-4-aminocyclohexyl)isoquinoline-5-sulfonamide (BRD6645).**  $^1\text{H}$  NMR (300 MHz, CHLOROFORM-d)  $\delta$  = 0.96 - 1.26 (5 H, m), 1.66 - 1.81 (4 H, m), 2.50 - 2.62 (1 H, m), 3.12 (1 H, dddd,  $J$ =8.0, 5.4, 2.2, 1.5 Hz), 4.57 - 4.71 (1 H, m), 7.74 (1 H, t,  $J$ =7.8 Hz), 8.24 (1 H, d,  $J$ =8.1 Hz), 8.39 (1 H, d,  $J$ =6.2 Hz), 8.50 (1 H, d,  $J$ =7.3 Hz), 8.73 (1 H, d,  $J$ =6.2 Hz), 9.40 (1 H, s) ppm.



**(*S*)-allyl 4-(isoquinolin-5-ylsulfonyl)-3-methyl-1,4-diazepane-1-carboxylate (BRD9304).**  $^1\text{H}$  NMR (300 MHz, CHLOROFORM-d)  $\delta$  = 0.71 - 0.87 (3 H, m), 1.07 - 1.23 (1 H, m), 1.45 - 1.75 (2 H, m), 2.91 - 3.16 (3 H, m), 3.55 - 3.81 (2 H, m), 3.81 - 3.96 (1 H, m), 4.17 - 4.38 (2 H, m), 4.38 - 4.60 (1 H, m), 5.03 - 5.29 (2 H, m), 5.68 - 5.96 (1 H, m), 7.62 (1 H, t,  $J$ =7.8 Hz), 8.13 (1 H, d,  $J$ =8.5 Hz), 8.20 - 8.28 (1 H, m), 8.37 (1 H, dd,  $J$ =13.6, 7.3 Hz), 8.61 (1 H, t,  $J$ =5.3 Hz), 9.27 (1 H, s) ppm;  $^{13}\text{C}$  NMR (75 MHz, CHLOROFORM-d)  $\delta$  = 16.5, 16.6, 28.7, 29.2, 41.1, 47.7, 48.0, 51.6, 51.9, 53.3, 53.5, 53.6, 66.1, 66.2, 117.3, 117.5, 117.6, 125.9, 129.0, 129.1, 131.4, 131.5, 132.9, 133.0, 133.6, 133.6, 133.7, 134.0, 135.16, 145.2, 153.2, 153.3, 155.1, 155.3 ppm.

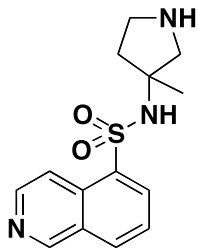


**(*R*)-3-chloro-N-(pyrrolidin-3-yl)isoquinoline-5-sulfonamide (BRD9082).**  $^1\text{H}$  NMR (300 MHz, CHLOROFORM-d)  $\delta$  = 1.45 - 1.63 (1 H, m), 1.84 - 2.04 (1 H, m), 2.74 (1 H, dd,  $J$ =11.2, 3.3 Hz), 2.79 - 3.08 (3 H, m), 3.78 - 3.88 (1 H, m), 3.88 - 4.12 (2 H, m), 7.72 (1 H, dd,  $J$ =8.1, 7.3 Hz), 8.24 (1 H, d,  $J$ =8.1 Hz), 8.43 - 8.55 (2 H, m), 9.20 (1 H, s) ppm.

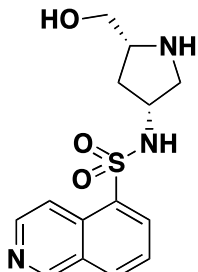


***N*-((3*R*,5*S*)-5-(hydroxymethyl)pyrrolidin-3-yl)isoquinoline-5-sulfonamide**

**(BRD1303).** <sup>1</sup>H NMR (300 MHz, CHLOROFORM-d) δ = 1.38 - 1.51 (1 H, m), 1.58 - 1.70 (1 H, m), 1.95 - 2.14 (1 H, m), 2.72 - 2.87 (2 H, m), 2.90 - 3.04 (1 H, m), 3.22 - 3.36 (1 H, m), 3.36 - 3.63 (3 H, m), 3.74 - 3.87 (1 H, m), 7.68 - 7.81 (1 H, m), 8.18 - 8.31 (1 H, m), 8.39 - 8.46 (1 H, m), 8.46 - 8.54 (1 H, m), 8.70 - 8.77 (1 H, m), 9.38 - 9.42 (1 H, m) ppm.

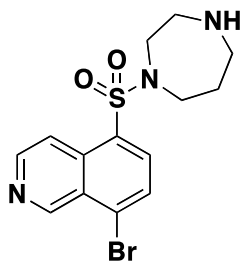


***N*-(3-methylpyrrolidin-3-yl)isoquinoline-5-sulfonamide (BRD5165).** <sup>1</sup>H NMR (300 MHz, CHLOROFORM-d) δ = 1.19 (3 H, s), 1.52 - 1.65 (1 H, m), 1.86 - 2.04 (2 H, m), 2.49 - 2.62 (1 H, m), 2.75 - 2.88 (2 H, m), 2.90 - 3.05 (1 H, m), 7.64 (1 H, t, J=7.6 Hz), 8.09 - 8.19 (1 H, m), 8.29 (1 H, d, J=6.2 Hz), 8.43 (1 H, dd, J=7.5, 1.3 Hz), 8.64 (1 H, d, J=5.8 Hz), 9.30 (1 H, s) ppm.

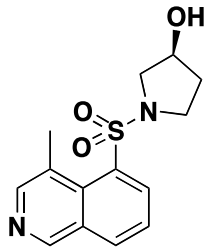


***N*-((3*R*,5*R*)-5-(hydroxymethyl)pyrrolidin-3-yl)isoquinoline-5-sulfonamide**

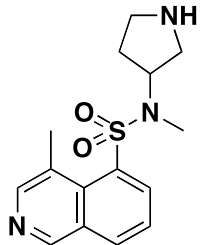
**(BRD7787).** <sup>1</sup>H NMR (500 MHz, CHLOROFORM-d) δ = 1.34 (1 H, d, J=14.2 Hz), 1.49 (1 H, t, J=7.1 Hz), 2.03 (2 H, ddd, J=13.9, 9.5, 7.3 Hz), 2.74 - 2.89 (2 H, m), 3.30 (1 H, dd, J=9.0, 4.1 Hz), 3.41 (1 H, dd, J=10.7, 3.4 Hz), 3.54 - 3.66 (2 H, m), 3.76 - 3.86 (1 H, m), 7.73 (1 H, t, J=7.8 Hz), 8.23 (1 H, d, J=8.3 Hz), 8.41 (1 H, d, J=6.3 Hz), 8.49 (1 H, d, J=7.3 Hz), 8.71 (1 H, d, J=6.3 Hz), 9.34 - 9.42 (1 H, m) ppm.



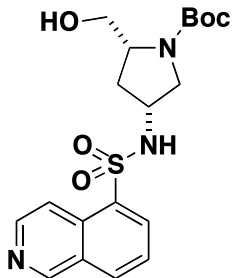
**5-(1,4-diazepan-1-ylsulfonyl)-8-bromoisoquinoline (BRD9509).**  $^1\text{H}$  NMR (300 MHz, CHLOROFORM-d)  $\delta$  = 2.03 - 2.22 (2 H, m), 2.81 - 3.15 (9 H, m), 3.22 - 3.34 (4 H, m), 3.50 - 3.58 (2 H, m), 3.89 - 3.99 (2 H, m), 7.67 (1 H, dd,  $J$ =8.3, 4.7 Hz), 7.95 (1 H, d,  $J$ =8.3 Hz), 8.31 - 8.39 (1 H, m), 8.67 (1 H, dd,  $J$ =8.5, 1.1 Hz), 9.08 (1 H, dd,  $J$ =2.7, 1.0 Hz) ppm.



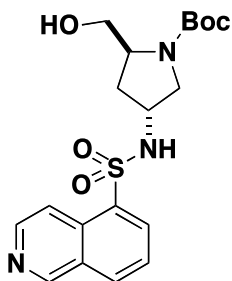
**(S)-1-(4-methylisoquinolin-5-ylsulfonyl)pyrrolidin-3-ol (BRD2334).**  $^1\text{H}$  NMR (300 MHz, CHLOROFORM-d)  $\delta$  = 2.07 - 2.33 (2 H, m), 2.40 (1 H, m), 3.10 (3 H, s), 3.59 (1 H, d,  $J$ =11.3 Hz), 3.64 - 3.87 (3 H, m), 4.66 - 4.77 (1 H, m), 7.61 (1 H, t,  $J$ =7.5 Hz), 8.15 (1 H, d,  $J$ =8.5 Hz), 8.39 (1 H, d,  $J$ =7.3 Hz), 8.55 (1 H, s), 9.14 (1 H, s) ppm.



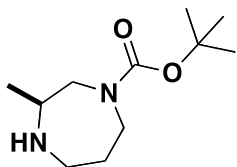
**N,4-dimethyl-N-(pyrrolidin-3-yl)isoquinoline-5-sulfonamide (BRD4275).**  $^1\text{H}$  NMR (300 MHz, CHLOROFORM-d)  $\delta$  = 1.96 - 2.20 (2 H, m), 2.89 - 3.04 (5 H, m), 3.04 - 3.15 (4 H, m), 3.18 - 3.31 (1 H, m), 4.43 - 4.60 (1 H, m), 7.62 (1 H, t,  $J$ =7.7 Hz), 8.07 - 8.23 (2 H, m), 8.56 (1 H, s), 9.16 (1 H, s) ppm.



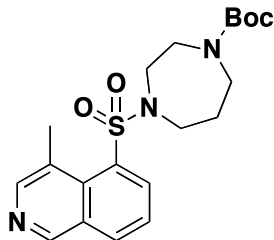
**(2*R*,4*R*)-tert-butyl 2-(hydroxymethyl)-4-(isoquinoline-5-sulfonamido)pyrrolidine-1-carboxylate (26).** <sup>1</sup>H NMR (500 MHz, CHLOROFORM-d) δ = 1.34 (4 H, br. s.), 1.38 (6 H, br. s.), 1.43 - 1.50 (1 H, m), 1.51 (1 H, d, J=6.3 Hz), 1.58 (6 H, s), 1.66 - 1.75 (1 H, m), 2.13 - 2.27 (1 H, m), 2.30 - 2.43 (1 H, m), 2.95 (1 H, br. s.), 3.02 - 3.13 (1 H, m), 3.13 - 3.27 (1 H, m), 3.33 - 3.45 (2 H, m), 3.45 - 3.54 (1 H, m), 3.86 (2 H, d, J=4.9 Hz), 3.96 - 4.20 (2 H, m), 6.91 (1 H, dd, J=6.8, 3.4 Hz), 7.73 (1 H, t, J=7.8 Hz), 8.11 - 8.20 (1 H, m), 8.24 (1 H, d, J=8.3 Hz), 8.39 (1 H, d, J=5.9 Hz), 8.49 (1 H, d, J=7.3 Hz), 8.60 (1 H, dd, J=6.6, 2.7 Hz), 8.71 (1 H, d, J=2.4 Hz), 9.38 (1 H, br. s.) ppm.



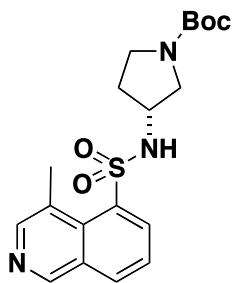
**(2*S*,4*R*)-tert-butyl 2-(hydroxymethyl)-4-(isoquinoline-5-sulfonamido)pyrrolidine-1-carboxylate (27).** <sup>1</sup>H NMR (300 MHz, CHLOROFORM-d) δ = 1.28 - 1.42 (9 H, s), 1.55 - 1.79 (2 H, m), 1.79 - 1.96 (1 H, m), 3.13 - 3.25 (1 H, m), 3.29 - 3.43 (1 H, m), 3.43 - 3.54 (1 H, m), 3.54 - 3.67 (1 H, m), 3.82 - 4.03 (2 H, m), 5.26 - 5.42 (1 H, m), 7.76 (1 H, t, J=7.8 Hz), 8.27 (1 H, d, J=8.1 Hz), 8.40 (1 H, d, J=6.0 Hz), 8.50 (1 H, dd, J=7.4, 1.2 Hz), 8.72 (1 H, d, J=6.0 Hz), 9.41 (1 H, s) ppm.



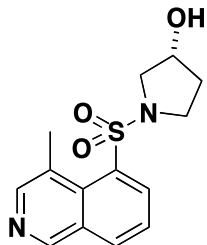
**(S)-tert-butyl 3-methyl-1,4-diazepane-1-carboxylate (28).** <sup>1</sup>H NMR (300 MHz, CHLOROFORM-d) δ = 0.97 - 1.12 (3 H, m), 1.32 - 1.51 (9 H, m), 1.58 - 1.79 (2 H, m), 1.79 - 2.03 (1 H, m), 2.53 - 2.78 (2 H, m), 2.82 - 2.97 (1 H, m), 3.02 - 3.29 (2 H, m), 3.61 - 3.83 (1 H, m) ppm.



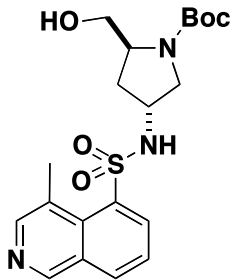
**tert-butyl 4-(4-methylisoquinolin-5-ylsulfonyl)-1,4-diazepane-1-carboxylate (9).** <sup>1</sup>H NMR (300 MHz, CHLOROFORM-d) δ = 1.40 - 1.57 (10 H, m), 2.06 (2 H, d, J=5.8 Hz), 2.99 - 3.13 (3 H, m), 3.45 - 3.73 (8 H, m), 5.31 (2 H, s), 7.59 (1 H, t, J=7.6 Hz), 7.74 (1 H, s), 8.07 - 8.22 (1 H, m), 8.56 (1 H, s), 9.15 (1 H, s) ppm.



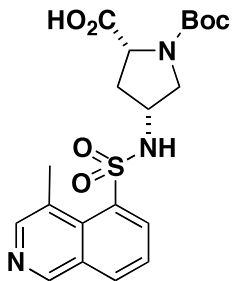
**(R)-tert-butyl 3-(4-methylisoquinoline-5-sulfonamido)pyrrolidine-1-carboxylate (10).** <sup>1</sup>H NMR (300 MHz, CHLOROFORM-d) δ = 1.35 (9 H, br. s.), 1.97 (2 H, br. s.), 2.11 (1 H, br. s.), 2.97 (3 H, s), 3.28 (4 H, br. s.), 3.92 (1 H, br. s.), 6.19 (1 H, br. s.), 7.49 (1 H, s), 8.04 (1 H, br. s.), 8.44 (1 H, br. s.), 9.05 (1 H, s) ppm.



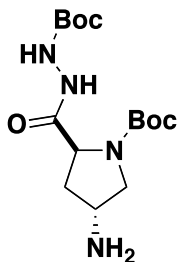
**(R)-1-(4-methylisoquinolin-5-ylsulfonyl)pyrrolidin-3-ol (25).** <sup>1</sup>H NMR (300 MHz, CHLOROFORM-d) δ = 2.07 (2 H, br. s.), 3.01 (3 H, s), 3.52 (1 H, s), 3.64 (3 H, d, J=3.6 Hz), 4.63 (1 H, br. s.), 7.43 - 7.60 (1 H, m), 8.04 (1 H, s), 8.30 (1 H, s), 8.45 (1 H, s), 9.04 (1 H, s) ppm.



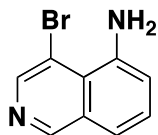
**(2*S*,4*R*)-*tert*-butyl 2-(hydroxymethyl)-4-(4-methylisoquinoline-5-sulfonamido)pyrrolidine-1-carboxylate (22).** <sup>1</sup>H NMR (500 MHz, CHLOROFORM-d) δ = 1.46 (9 H, br. s.), 1.68 (2 H, br. s.), 2.01 (1 H, d, J=3.4 Hz), 2.08 - 2.21 (1 H, m), 3.07 (3 H, s), 3.52 (1 H, br. s.), 3.55 - 3.67 (2 H, m), 3.70 (1 H, br. s.), 4.07 (1 H, br. s.), 4.15 (2 H, br. s.), 5.29 (1 H, br. s.), 7.64 (1 H, t, J=7.8 Hz), 8.20 (1 H, d, J=7.8 Hz), 8.49 (1 H, d, J=7.3 Hz), 8.57 (1 H, s), 9.18 (1 H, s) ppm.



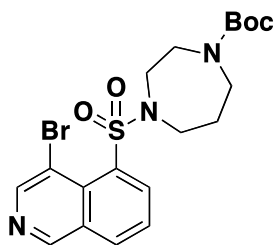
**(2*R*,4*R*)-1-(*tert*-butoxycarbonyl)-4-(4-methylisoquinoline-5-sulfonamido)pyrrolidine-2-carboxylic acid (30).** <sup>1</sup>H NMR (300 MHz, MeOD) δ = 1.11 - 1.18 (1 H, m), 1.21 - 1.27 (1 H, m), 1.34 - 1.41 (9 H, m), 1.98 - 2.10 (1 H, m), 2.64 (1 H, dd, J=6.7, 5.9 Hz), 3.02 (3 H, s), 3.32 - 3.41 (1 H, m), 3.53 - 3.62 (1 H, m), 3.74 (1 H, dd, J=10.7, 6.2 Hz), 3.86 - 3.97 (1 H, m), 4.10 - 4.21 (1 H, m), 7.74 (1 H, t, J=7.9 Hz), 8.13 (1 H, s), 8.31 (1 H, d, J=8.1 Hz), 8.42 (1 H, s), 8.53 (1 H, d, J=7.5 Hz), 9.14 (1 H, s) ppm.



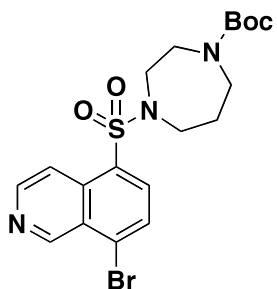
**(2*S*,4*R*)-*tert*-butyl 4-amino-2-(2-(*tert*-butoxycarbonyl)hydrazinecarbonyl)pyrrolidine-1-carboxylate (31).** <sup>1</sup>H NMR (500 MHz, METHANOL-d4) δ = 1.26 - 1.37 (1 H, m), 1.42 - 1.53 (19 H, m), 1.93 - 1.97 (1 H, m), 2.00 - 2.15 (1 H, m), 2.17 - 2.30 (1 H, m), 2.85 - 2.90 (1 H, m), 2.99 - 3.04 (1 H, m), 3.13 - 3.23 (1 H, m), 3.61 - 3.75 (2 H, m), 4.28 - 4.39 (1 H, m) ppm.



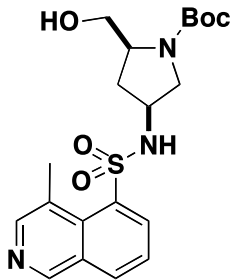
**4-bromoisoquinolin-5-amine (3).**  $^1\text{H}$  NMR (500 MHz, CHLOROFORM-d)  $\delta$  = 5.25 (2 H, br. s.), 6.94 (1 H, d,  $J$ =7.3 Hz), 7.35 - 7.39 (1 H, m), 7.42 (1 H, t,  $J$ =7.8 Hz), 8.53 (1 H, s), 9.00 (1 H, s) ppm.



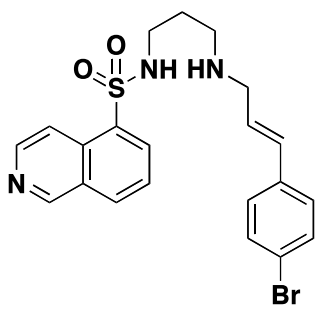
***tert*-butyl 4-(4-bromoisoquinolin-5-ylsulfonyl)-1,4-diazepane-1-carboxylate (4).**  $^1\text{H}$  NMR (300 MHz, CHLOROFORM-d)  $\delta$  = 1.32 - 1.47 (10 H, m), 1.57 (1 H, s), 2.00 (2 H, br. s.), 3.43 (4 H, s), 3.56 (5 H, br. s.), 7.60 (1 H, s), 7.79 (1 H, s), 8.09 (1 H, s), 8.93 (1 H, s), 9.14 (1 H, s) ppm.



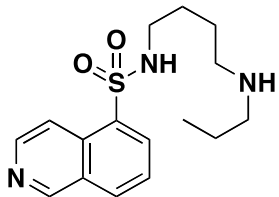
***tert*-butyl 4-(8-bromoisoquinolin-5-ylsulfonyl)-1,4-diazepane-1-carboxylate (6).**  $^1\text{H}$  NMR (300 MHz, CHLOROFORM-d)  $\delta$  = 1.37 - 1.46 (9 H, m), 1.98 (2 H, t,  $J$ =5.8 Hz), 3.43 (2 H, t,  $J$ =5.9 Hz), 3.50 - 3.65 (6 H, m), 7.63 (1 H, dd,  $J$ =8.4, 4.1 Hz), 7.91 (1 H, d,  $J$ =7.9 Hz), 8.34 (1 H, d,  $J$ =7.9 Hz), 8.62 (1 H, d,  $J$ =8.9 Hz), 9.06 (1 H, br. s.) ppm;  $^{13}\text{C}$  NMR (150 MHz, CHLOROFORM-d)  $\delta$  = 14.5, 21.3, 28.7, 28.8, 45.9, 46.5, 48.5, 50.3, 50.4, 51.3, 51.8, 53.7, 60.6, 79.9, 80.0, 123.0, 123.3, 128.2, 128.6, 129.5, 129.6, 133.1, 136.3, 136.4, 137.5, 137.7, 144.7, 151.8, 151.9, 155.2, 155.5 ppm.



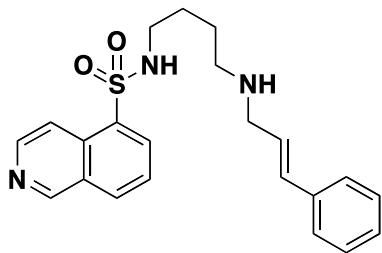
**(2*S*,4*S*)-*tert*-butyl 2-(hydroxymethyl)-4-(4-methyliisoquinoline-5-sulfonamido)pyrrolidine-1-carboxylate (32).** <sup>1</sup>H NMR (300 MHz, CHLOROFORM-d) δ = 1.20 - 1.28 (1 H, m), 1.37 - 1.45 (9 H, m), 1.89 - 2.15 (1 H, m), 2.49 (1 H, dddd, J=5.2, 3.8, 2.3, 1.1 Hz), 2.98 - 3.11 (3 H, m), 3.48 - 3.68 (3 H, m), 3.88 - 4.06 (2 H, m), 4.14 - 4.30 (1 H, m), 7.59 (1 H, t, J=7.6 Hz), 8.07 - 8.17 (1 H, m), 8.44 - 8.57 (2 H, m), 9.11 (1 H, br. s.) ppm.



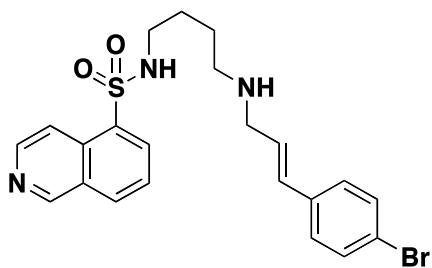
**(E)-*N*-(3-(3-(4-bromophenyl)allylamino)propyl)isoquinoline-5-sulfonamide (BRD5149).** <sup>1</sup>H NMR (300 MHz, CHLOROFORM-d) δ = 2.50 - 2.63 (2 H, m), 2.93 - 3.03 (2 H, m), 3.16 - 3.26 (2 H, m), 6.14 (1 H, dt, J=15.9, 6.1 Hz), 6.32 - 6.47 (1 H, m), 7.11 - 7.20 (2 H, m), 7.32 - 7.42 (2 H, m), 7.62 (1 H, t, J=7.7 Hz), 8.12 (1 H, d, J=8.1 Hz), 8.32 - 8.41 (2 H, m), 8.56 (1 H, d, J=6.2 Hz), 9.29 (1 H, s) ppm.



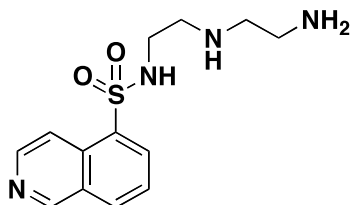
***N*-(4-(propylamino)butyl)isoquinoline-5-sulfonamide (BRD1524).** <sup>1</sup>H NMR (500 MHz, CHLOROFORM-d) δ = 0.99 (3 H, t, J=7.5 Hz), 1.55 - 1.62 (2 H, m), 1.62 - 1.75 (4 H, m), 2.69 - 2.76 (4 H, m), 2.90 - 2.97 (2 H, m), 7.70 (1 H, t, J=7.9 Hz), 8.20 (1 H, d, J=8.4 Hz), 8.43 (1 H, d, J=7.3 Hz), 8.53 (1 H, d, J=6.2 Hz), 8.68 (1 H, d, J=6.2 Hz), 9.36 (1 H, s) ppm.



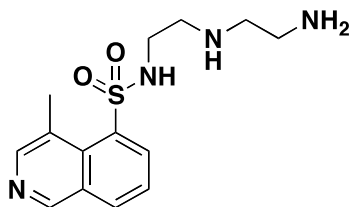
**(E)-N-(4-(cinnamylamino)butyl)isoquinoline-5-sulfonamide (BRD2874).**  $^1\text{H}$  NMR (300 MHz, CHLOROFORM-d)  $\delta$  = 1.39 - 1.65 (4 H, m), 2.56 - 2.70 (2 H, m), 2.91 (2 H, t,  $J$ =5.6 Hz), 3.47 (2 H, d,  $J$ =6.4 Hz), 6.34 - 6.49 (1 H, m), 6.53 - 6.66 (1 H, m), 7.20 - 7.37 (3 H, m), 7.37 - 7.47 (2 H, m), 7.60 - 7.71 (1 H, m), 8.17 (1 H, d,  $J$ =8.1 Hz), 8.44 (1 H, dd,  $J$ =7.3, 1.1 Hz), 8.53 (2 H, q,  $J$ =6.2 Hz), 9.34 (1 H, s) ppm.



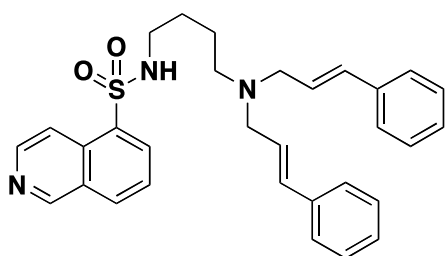
**(E)-N-(4-(3-(4-bromophenyl)allylamino)butyl)isoquinoline-5-sulfonamide (BRD6081).**  $^1\text{H}$  NMR (300 MHz, CHLOROFORM-d)  $\delta$  = 1.33 - 1.56 (4 H, m), 2.49 - 2.62 (2 H, m), 2.82 (2 H, t,  $J$ =5.7 Hz), 3.30 - 3.40 (2 H, m), 6.26 - 6.40 (1 H, m), 6.40 - 6.51 (1 H, m), 7.14 - 7.24 (2 H, m), 7.29 - 7.39 (2 H, m), 7.53 - 7.64 (1 H, m), 8.09 (1 H, d,  $J$ =8.3 Hz), 8.30 - 8.44 (2 H, m), 8.45 - 8.51 (2 H, m), 9.26 (1 H, s) ppm.



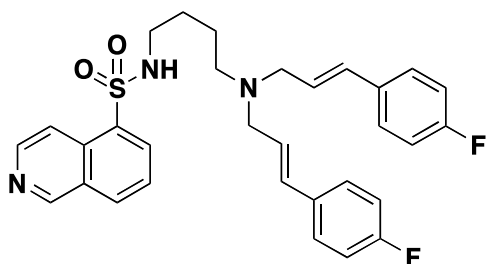
**N-(2-(2-aminoethylamino)ethyl)isoquinoline-5-sulfonamide (BRD4009).**  $^1\text{H}$  NMR (300 MHz, MeOD)  $\delta$  = 2.56 - 2.70 (4 H, m), 2.71 - 2.83 (4 H, m), 2.84 - 2.99 (4 H, m), 7.80 (1 H, t,  $J$ =7.9 Hz), 8.38 (1 H, d,  $J$ =8.3 Hz), 8.41 - 8.48 (1 H, m), 8.49 - 8.56 (1 H, m), 8.58 - 8.64 (1 H, m), 9.37 (1 H, s) ppm.



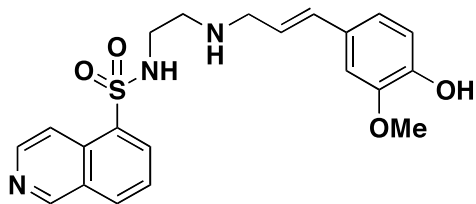
**N-(2-(2-aminoethylamino)ethyl)-4-methyliisoquinoline-5-sulfonamide (BRD3407).**  $^1\text{H}$  NMR (300 MHz, MeOD)  $\delta$  = 1.85 (1 H, s), 2.58 - 2.69 (2 H, m), 2.70 - 2.80 (3 H, m), 2.95 - 3.00 (3 H, m), 3.10 - 3.19 (4 H, m), 7.70 (1 H, d,  $J=7.9$  Hz), 8.21 - 8.30 (1 H, m), 8.33 - 8.41 (2 H, m), 9.09 (1 H, s) ppm.



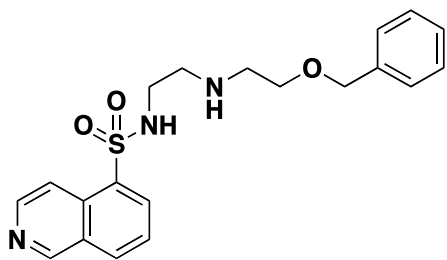
**N-(4-(dicinnamylamino)butyl)isoquinoline-5-sulfonamide (BRD2686).**  $^1\text{H}$  NMR (300 MHz, CHLOROFORM-d)  $\delta$  = 1.33 - 1.56 (4 H, m), 2.25 - 2.43 (2 H, m), 2.72 - 2.87 (2 H, m), 3.10 - 3.24 (4 H, m), 6.11 - 6.29 (2 H, m), 6.32 - 6.46 (2 H, m), 7.03 - 7.29 (10 H, m), 7.43 - 7.51 (1 H, m), 8.00 (1 H, d,  $J=8.1$  Hz), 8.28 (1 H, dd,  $J=7.3, 1.1$  Hz), 8.34 - 8.44 (2 H, m), 9.18 (1 H, s) ppm.



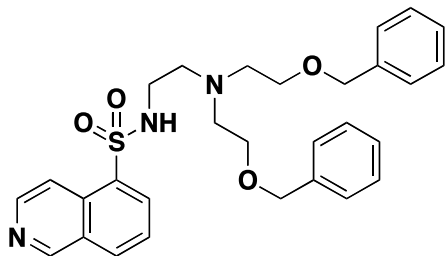
**N-(4-(bis((E)-3-(4-fluorophenyl)allyl)amino)butyl)isoquinoline-5-sulfonamide (BRD5822).**  $^1\text{H}$  NMR (300 MHz, CHLOROFORM-d)  $\delta$  = 2.42 - 2.60 (2 H, m), 2.96 (2 H, t,  $J=5.2$  Hz), 3.32 (4 H, d,  $J=6.8$  Hz), 6.30 (2 H, dt,  $J=15.8, 6.8$  Hz), 6.43 - 6.58 (2 H, m), 6.94 - 7.08 (4 H, m), 7.30 - 7.40 (4 H, m), 7.65 (1 H, t,  $J=7.8$  Hz), 8.18 (1 H, d,  $J=8.3$  Hz), 8.43 (1 H, dd,  $J=7.3, 1.1$  Hz), 8.56 (2 H, q,  $J=6.2$  Hz), 9.35 (1 H, s) ppm.



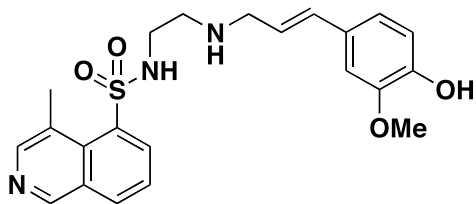
**(E)-N-(2-(3-(4-hydroxy-3-methoxyphenyl)allylamino)ethyl)isoquinoline-5-sulfonamide (BRD8902).**  $^1\text{H}$  NMR (300 MHz, MeOD)  $\delta$  = 1.86 - 1.95 (1 H, m), 2.01 (1 H, s), 2.53 - 2.65 (2 H, m), 2.95 - 3.04 (3 H, m), 3.13 - 3.22 (3 H, m), 3.79 - 3.87 (3 H, m), 5.80 - 5.98 (1 H, m), 6.31 (1 H, d,  $J$ =15.4 Hz), 6.67 - 6.81 (2 H, m), 6.92 (1 H, s), 7.76 (1 H, t,  $J$ =7.9 Hz), 8.32 (1 H, d,  $J$ =8.5 Hz), 8.44 (1 H, d,  $J$ =7.3 Hz), 8.49 - 8.56 (1 H, m), 8.57 - 8.64 (1 H, m), 9.32 (1 H, s) ppm.



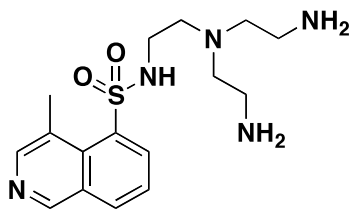
**N-(2-(2-(benzyloxy)ethylamino)ethyl)isoquinoline-5-sulfonamide (BRD1600).**  $^1\text{H}$  NMR (300 MHz, MeOD)  $\delta$  = 2.52 - 2.65 (4 H, m), 2.96 (2 H, t,  $J$ =6.1 Hz), 3.44 (2 H, t,  $J$ =5.3 Hz), 4.45 (2 H, s), 7.20 - 7.35 (5 H, m), 7.79 (1 H, t,  $J$ =7.8 Hz), 8.37 (1 H, d,  $J$ =8.1 Hz), 8.42 - 8.48 (1 H, m), 8.50 - 8.55 (1 H, m), 8.56 - 8.62 (1 H, m), 9.36 (1 H, s) ppm.



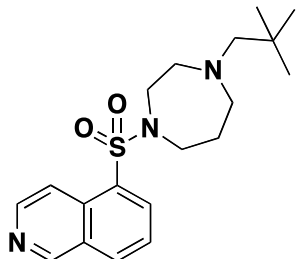
**N-(2-(bis(2-(benzyloxy)ethyl)amino)ethyl)isoquinoline-5-sulfonamide (BRD5967).**  $^1\text{H}$  NMR (300 MHz, MeOD)  $\delta$  = 2.44 - 2.59 (4 H, m), 2.92 (2 H, t,  $J$ =6.3 Hz), 3.27 - 3.34 (4 H, m), 4.32 - 4.41 (4 H, m), 7.10 - 7.34 (10 H, m), 7.69 - 7.79 (1 H, m), 8.28 - 8.36 (1 H, m), 8.37 - 8.44 (1 H, m), 8.44 - 8.57 (2 H, m), 9.27 - 9.35 (1 H, m) ppm.



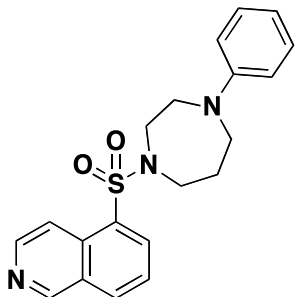
**(E)-N-(2-(3-(4-hydroxy-3-methoxyphenyl)allylamino)ethyl)-4-methylisoquinoline-5-sulfonamide (BRD9159).**  $^1\text{H}$  NMR (300 MHz, MeOD)  $\delta$  = 2.89 - 3.00 (2 H, m), 3.00 - 3.09 (3 H, m), 3.31 - 3.38 (1 H, m), 3.44 - 3.51 (1 H, m), 3.83 (3 H, s), 6.08 (1 H, d,  $J=15.4$  Hz), 6.45 - 6.60 (1 H, m), 6.71 (1 H, d,  $J=8.1$  Hz), 6.79 - 6.88 (1 H, m), 6.98 (1 H, s), 7.68 - 7.79 (1 H, m), 8.28 - 8.34 (1 H, m), 8.39 (1 H, dd,  $J=7.6, 1.4$  Hz), 8.44 (1 H, s), 8.52 (1 H, s), 9.15 (1 H, s) ppm.



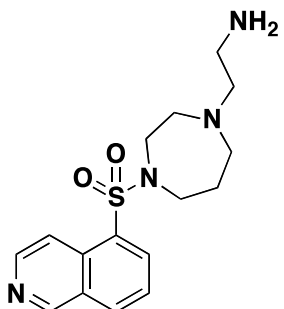
**N-(2-(bis(2-aminoethyl)amino)ethyl)-4-methylisoquinoline-5-sulfonamide (BRD3394).**  $^1\text{H}$  NMR (300 MHz, MeOD)  $\delta$  = 2.51 - 2.59 (3 H, m), 2.61 - 2.68 (2 H, m), 2.73 - 2.81 (3 H, m), 2.95 - 3.01 (3 H, m), 3.11 - 3.18 (3 H, m), 7.70 (1 H, d,  $J=7.7$  Hz), 8.26 (1 H, dd,  $J=8.2, 0.8$  Hz), 8.34 (1 H, s), 8.35 - 8.40 (1 H, m), 9.09 (1 H, s) ppm.



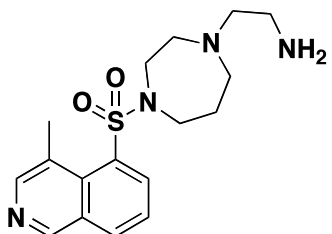
**5-(4-neopentyl-1,4-diazepan-1-ylsulfonyl)isoquinoline (BRD5665).**  $^1\text{H}$  NMR (300 MHz, MeOD)  $\delta$  = 0.81 - 0.93 (9 H, m), 1.87 - 2.02 (2 H, m), 2.35 - 2.46 (2 H, m), 2.89 - 3.09 (4 H, m), 3.42 - 3.61 (4 H, m), 7.71 (1 H, t,  $J=7.9$  Hz), 8.22 (1 H, d,  $J=8.5$  Hz), 8.31 - 8.39 (1 H, m), 8.47 (1 H, d,  $J=6.2$  Hz), 8.61 - 8.76 (1 H, br.s.), 9.37 (1 H, br.s.) ppm.



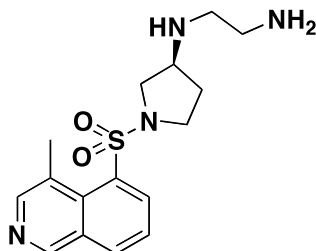
**5-(4-phenyl-1,4-diazepan-1-ylsulfonyl)isoquinoline (BRD5656).** Compound **BRD5656** was synthesized following the known procedure.<sup>1</sup> <sup>1</sup>H NMR (300 MHz, CHLOROFORM-d) δ = 1.91 - 2.07 (2 H, m), 3.22 (2 H, t, J=6.0 Hz), 3.43 - 3.52 (2 H, m), 3.52 - 3.67 (4 H, m), 6.53 (2 H, d, J=7.9 Hz), 6.59 (1 H, t, J=7.3 Hz), 7.05 - 7.12 (2 H, m), 7.56 (1 H, t, J=7.8 Hz), 8.08 (1 H, d, J=8.3 Hz), 8.21 (1 H, dd, J=7.4, 1.2 Hz), 8.31 (1 H, d, J=6.2 Hz), 8.55 (1 H, d, J=6.2 Hz), 9.24 (1 H, s) ppm.



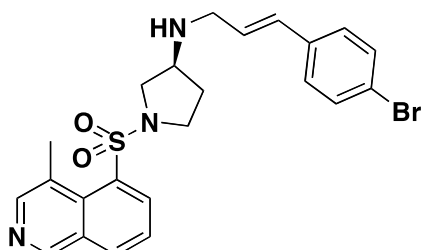
**2-(4-(isoquinolin-5-ylsulfonyl)-1,4-diazepan-1-yl)ethanamine (BRD0112).** <sup>1</sup>H NMR (500 MHz, METHANOL-d4) δ = 1.89 (2 H, t, J=5.9 Hz), 2.70 (2 H, t, J=5.9 Hz), 2.79 (4 H, td, J=11.1, 5.6 Hz), 2.87 (2 H, t, J=5.9 Hz), 3.49 - 3.57 (4 H, m), 7.85 (1 H, t, J=7.8 Hz), 8.43 (2 H, d, J=7.3 Hz), 8.54 (1 H, d, J=6.3 Hz), 8.65 (1 H, d, J=5.9 Hz), 9.41 (1 H, s) ppm.



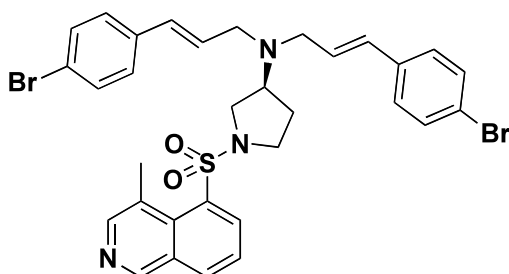
**2-(4-(4-methylisoquinolin-5-ylsulfonyl)-1,4-diazepan-1-yl)ethanamine (BRD9740).** <sup>1</sup>H NMR (500 MHz, CHLOROFORM-d) δ = 1.73 (5 H, br. s.), 1.96 - 2.08 (2 H, m), 2.70 (2 H, t, J=5.9 Hz), 2.82 (2 H, t, J=5.9 Hz), 2.87 - 2.95 (4 H, m), 3.10 (3 H, s), 3.59 - 3.71 (4 H, m), 7.61 (1 H, t, J=7.8 Hz), 7.87 (1 H, d, J=7.3 Hz), 8.16 (1 H, d, J=7.8 Hz), 8.57 (1 H, s), 9.16 (1 H, s) ppm.



**(S)-N<sup>1</sup>-(1-(4-methylisoquinolin-5-ylsulfonyl)pyrrolidin-3-yl)ethane-1,2-diamine (BRD1596).**  $^1\text{H}$  NMR (300 MHz, MeOD)  $\delta$  = 1.97 - 2.10 (1 H, m), 2.26 - 2.40 (1 H, m), 2.73 - 2.86 (2 H, m), 2.86 - 2.94 (2 H, m), 3.06 (3 H, s), 3.39 (1 H, dd,  $J=9.2, 4.7$  Hz), 3.55 - 3.66 (2 H, m), 3.66 - 3.79 (2 H, m), 7.78 (1 H, t,  $J=7.8$  Hz), 8.37 (1 H, dd,  $J=8.4, 1.2$  Hz), 8.43 (1 H, dd,  $J=7.5, 1.3$  Hz), 8.47 (1 H, s), 9.19 (1 H, s) ppm.

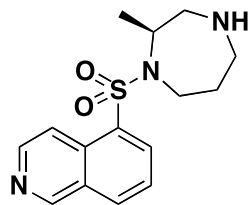


**(S,E)-N-(3-(4-bromophenyl)allyl)-1-(4-methylisoquinolin-5-ylsulfonyl)pyrrolidin-3-amine (BRD8155).**  $^1\text{H}$  NMR (300 MHz, CHLOROFORM-d)  $\delta$  = 1.94 - 2.07 (1 H, m), 2.23 - 2.40 (1 H, m), 3.10 (3 H, s), 3.41 - 3.52 (3 H, m), 3.61 - 3.78 (4 H, m), 6.24 - 6.40 (1 H, m), 6.49 - 6.61 (1 H, m), 7.21 - 7.30 (3 H, m), 7.42 - 7.52 (2 H, m), 7.57 (1 H, t,  $J=7.8$  Hz), 8.15 (1 H, dd,  $J=8.2, 1.2$  Hz), 8.49 (1 H, dd,  $J=7.5, 1.3$  Hz), 8.56 (1 H, s), 9.15 (1 H, s) ppm;  $^{13}\text{C}$  NMR (75 MHz, CHLOROFORM-d)  $\delta$  = 21.6, 32.6, 46.9, 49.8, 53.6, 57.4, 125.0, 127.8, 128.4, 130.6, 131.1, 131.8, 134.4, 148.5, 151.9 ppm.

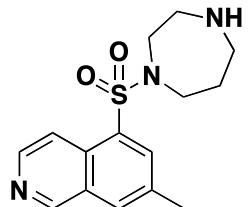


**(S)-N,N-bis((E)-3-(4-bromophenyl)allyl)-1-(4-methylisoquinolin-5-ylsulfonyl)pyrrolidin-3-amine (BRD3615).**  $^1\text{H}$  NMR (300 MHz, CHLOROFORM-d)  $\delta$  = 1.60 (3 H, td,  $J=3.5, 2.0$  Hz), 3.09 (3 H, s), 3.35 - 3.47 (5 H, m), 3.48 - 3.66 (3 H, m), 3.72 (2 H, s), 3.77 - 3.88 (1 H, m), 6.20 - 6.34 (2 H, m), 6.45 - 6.57 (2 H, m), 7.20 - 7.31 (6 H, m), 7.44

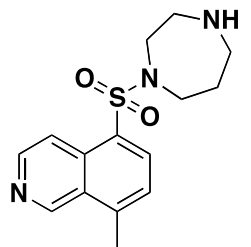
- 7.51 (4 H, m), 7.57 (1 H, t,  $J=7.8$  Hz), 8.11 - 8.22 (2 H, m), 8.57 (1 H, s), 9.16 (1 H, s) ppm.



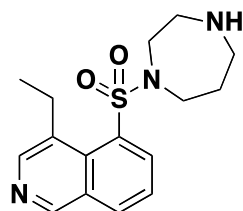
**(S)-5-(2-methyl-1,4-diazepan-1-ylsulfonyl)isoquinoline (BRD1869).** Sulfonamide **BRD9304** (20 mg, 0.051 mmol, 1 equiv.) and *N,N'*-dimethylbarbituric acid (80 mg, 0.51 mmol, 10 equiv.) were dissolved in dry THF (2.6 mL). After the addition of tetrakis(triphenylphosphine)palladium(0) (6 mg, 0.0051 mmol, 0.1 equiv.), the solution was degassed with nitrogen and stirred for 2 h under room temperature. The solution was filtered through a short column of Celite and the column was washed by EA. The solvent was removed under reduced pressure and the residue was purified by prep-HPLC.  $^1\text{H}$  NMR (300 MHz, CHLOROFORM-d)  $\delta$  = 0.75 - 0.85 (3 H, m), 1.46 - 1.61 (2 H, m), 1.61 - 1.84 (2 H, m), 2.51 (1 H, dd,  $J=14.5, 8.7$  Hz), 2.62 - 2.75 (1 H, m), 3.02 - 3.31 (3 H, m), 3.88 - 4.01 (1 H, m), 4.03 - 4.16 (1 H, m), 7.71 (1 H, t,  $J=7.8$  Hz), 8.21 (1 H, d,  $J=8.3$  Hz), 8.40 (1 H, d,  $J=6.2$  Hz), 8.56 - 8.61 (1 H, m), 8.72 (1 H, d,  $J=6.2$  Hz), 9.36 (1 H, s) ppm.



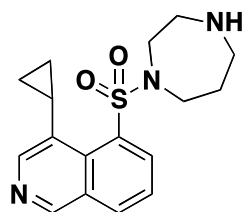
**5-(1,4-diazepan-1-ylsulfonyl)-7-methylisoquinoline (BRD5087).**  $^1\text{H}$  NMR (300 MHz, CHLOROFORM-d)  $\delta$  = 1.65 (3 H, s), 1.85 (2 H, t,  $J=5.9$  Hz), 2.64 (3 H, s), 2.90 - 3.04 (4 H, m), 3.40 - 3.56 (4 H, m), 7.97 (1 H, s), 8.24 (1 H, d,  $J=1.7$  Hz), 8.39 (1 H, d,  $J=6.2$  Hz), 8.64 (1 H, d,  $J=6.2$  Hz), 9.28 (1 H, s) ppm.



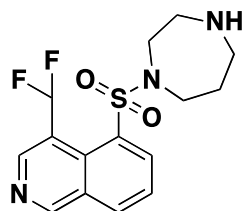
**5-(1,4-diazepan-1-ylsulfonyl)-8-methylisoquinoline (BRD5257).**  $^1\text{H}$  NMR (300 MHz, CHLOROFORM-d)  $\delta$  = 2.07 - 2.17 (2 H, m), 2.78 (3 H, s), 3.20 - 3.41 (4 H, m), 3.49 - 3.58 (2 H, m), 3.96 (2 H, ddd,  $J=5.0, 3.6, 1.1$  Hz), 7.44 - 7.50 (1 H, m), 7.58 (1 H, dd,  $J=8.5, 4.1$  Hz), 8.35 - 8.48 (3 H, m), 9.05 (1 H, dd,  $J=4.1, 1.5$  Hz) ppm.



**5-(1,4-diazepan-1-ylsulfonyl)-4-ethylisoquinoline (BRD5930).**  $^1\text{H}$  NMR (300 MHz, CHLOROFORM-d)  $\delta$  = 1.38 (3 H, t,  $J=7.4$  Hz), 1.93 - 2.05 (2 H, m), 3.05 - 3.16 (4 H, m), 3.55 - 3.71 (6 H, m), 7.62 (1 H, d,  $J=7.9$  Hz), 7.82 - 7.90 (1 H, m), 8.12 - 8.20 (1 H, m), 8.64 (1 H, s), 9.15 (1 H, s) ppm.

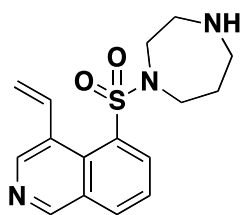


**5-(1,4-diazepan-1-ylsulfonyl)-4-(difluoromethyl)isoquinoline (BRD8757).**  $^1\text{H}$  NMR (300 MHz, CHLOROFORM-d)  $\delta$  = 0.80 - 0.92 (2 H, m), 1.18 - 1.28 (2 H, m), 1.90 - 2.02 (2 H, m), 3.02 - 3.15 (4 H, m), 3.16 - 3.30 (1 H, m), 3.51 - 3.68 (4 H, m), 7.56 - 7.66 (1 H, m), 7.87 (1 H, d,  $J=7.2$  Hz), 8.10 - 8.20 (1 H, m), 8.54 (1 H, s), 9.13 (1 H, s) ppm.

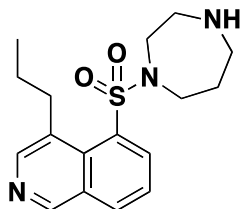


**5-(1,4-diazepan-1-ylsulfonyl)-4-(difluoromethyl)isoquinoline (BRD8757).** To a solution of **14** (8.5 mg, 0.02 mmol) in 2 mL THF/water (1:1) was added a solution of OsO<sub>4</sub> in *t*-BuOH (0.08 M, 5  $\mu$ L, 0.4  $\mu$ mol, 0.02 equiv.) and sodium periodate (8.7 mg, 0.04 mmol, 2 equiv.). The reaction mixture was stirred overnight under room temperature. 2 mL 1 M NaHSO<sub>3</sub> (aq.) was added. After a further 90 minutes the mixture was diluted with 2 mL water and extracted first with CHCl<sub>3</sub> (3 x 4 mL) and then with EA (3 x 4 mL). Drying over sodium sulfate and the evaporation of the solvent from the organic phase gave an oily residue (**16**). Under nitrogen, the mixture of the crude product

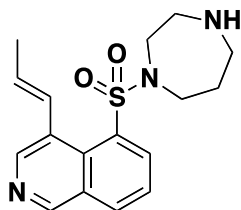
**16** and DAST (0.05 mL, 0.4 mmol, 20 equiv.) in dry CH<sub>2</sub>Cl<sub>2</sub> was refluxed for 16 h. The reaction was quenched with water and extracted with EA. The organic layers were then washed with saturated brine, dried over sodium sulfate, filtered, and evaporated under reduced pressure. The residue was treated with TFA/CH<sub>2</sub>Cl<sub>2</sub> (1:1) at room temperature. The volatiles were removed under reduced pressure and the residue was purified by prep-HPLC to afford **BRD8757** (1.5 mg, 22% yield over 3 steps). <sup>1</sup>H NMR (300 MHz, CHLOROFORM-d) δ = 1.19 - 1.30 (5 H, m), 1.67 - 1.87 (19 H, m), 2.01 - 2.12 (3 H, m), 3.14 - 3.23 (4 H, m), 3.62 - 3.71 (4 H, m), 7.70 - 7.78 (1 H, m), 8.04 - 8.09 (1 H, m), 8.25 - 8.31 (1 H, m), 8.36 (1 H, t, J=53 Hz), 9.26 (1 H, s), 9.44 (1 H, s) ppm.



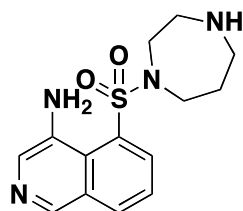
**5-(1,4-diazepan-1-ylsulfonyl)-4-vinylisoquinoline (BRD7032).** <sup>1</sup>H NMR (300 MHz, CHLOROFORM-d) δ = 1.90 - 2.22 (3 H, m), 3.03 - 3.16 (3 H, m), 3.48 - 3.67 (4 H, m), 5.53 (1 H, dd, J=10.7, 1.5 Hz), 5.68 (1 H, dd, J=17.0, 1.5 Hz), 7.66 (1 H, t, J=7.8 Hz), 7.91 - 8.07 (2 H, m), 8.19 (1 H, dd, J=8.0, 1.0 Hz), 8.74 (1 H, d, J=0.8 Hz), 9.24 (1 H, s) ppm; <sup>13</sup>C NMR (75 MHz, CHLOROFORM-d) δ = 31.2, 47.6, 48.9, 51.1, 52.6, 117.2, 125.3, 129.8, 129.9, 130.0, 130.3, 134.0, 136.2, 136.9, 146.4, 153.0 ppm.



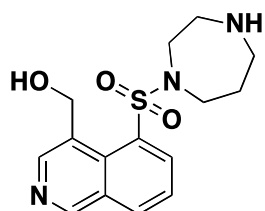
**5-(1,4-diazepan-1-ylsulfonyl)-4-propylisoquinoline (BRD7132).** <sup>1</sup>H NMR (300 MHz, CHLOROFORM-d) δ = 1.06 (3 H, t, J=7.3 Hz), 1.65 - 1.77 (3 H, m), 1.90 - 2.03 (2 H, m), 3.06 - 3.14 (3 H, m), 3.49 - 3.70 (6 H, m), 7.59 (1 H, t, J=7.7 Hz), 7.85 (1 H, dd, J=7.3, 1.4 Hz), 8.10 - 8.19 (1 H, m), 8.61 (1 H, s), 9.14 (1 H, s) ppm.



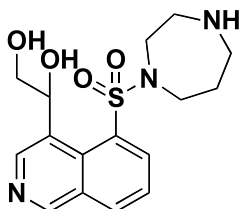
**(E)-5-(1,4-diazepan-1-ylsulfonyl)-4-(prop-1-enyl)isoquinoline (BRD9078).**  $^1\text{H}$  NMR (500 MHz, CHLOROFORM-d)  $\delta$  = 1.63 - 1.82 (2 H, m), 1.90 - 2.01 (2 H, m), 2.06 (3 H, d,  $J$ =6.3 Hz), 3.10 (4 H, d,  $J$ =5.9 Hz), 3.51 - 3.69 (4 H, m), 6.09 (1 H, dd,  $J$ =15.4, 6.6 Hz), 7.58 - 7.73 (2 H, m), 7.92 (1 H, d,  $J$ =7.3 Hz), 8.16 (1 H, d,  $J$ =7.8 Hz), 8.67 (1 H, s), 9.19 (1 H, s) ppm;  $^{13}\text{C}$  NMR (75 MHz, CHLOROFORM-d)  $\delta$  = 19.1, 31.9, 48.1, 49.3, 51.4, 53.3, 125.4, 125.4, 129.8, 129.8, 130.1, 130.3, 130.8, 130.9, 134.1, 136.8, 146.5, 152.5 ppm.



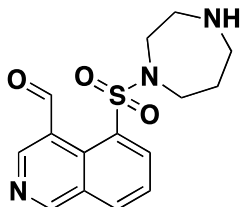
**5-(1,4-diazepan-1-ylsulfonyl)isoquinolin-4-amine (BRD2749).** Compound **BRD2749** was synthesized following the known procedure.<sup>2</sup>  $^1\text{H}$  NMR (500 MHz, CHLOROFORM-d)  $\delta$  = 1.85 - 1.92 (2 H, m), 3.02 - 3.08 (4 H, m), 3.54 - 3.58 (2 H, m), 3.60 (2 H, t,  $J$ =6.1 Hz), 7.56 (1 H, t,  $J$ =7.8 Hz), 8.03 (1 H, d,  $J$ =7.3 Hz), 8.08 (1 H, d,  $J$ =9.3 Hz), 8.16 (1 H, s), 8.69 (1 H, s) ppm.



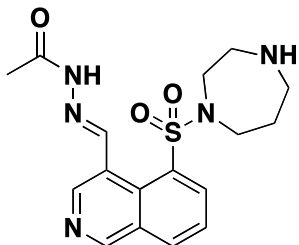
**(5-(1,4-diazepan-1-ylsulfonyl)isoquinolin-4-yl)methanol (BRD7648).** To a solution of **14** (8.5 mg, 0.02 mmol) in 2 mL THF/water (1:1) was added a solution of OsO<sub>4</sub> in *t*-BuOH (0.08 M, 5  $\mu$ L, 0.4  $\mu$ mol, 0.02 equiv.) and sodium periodate (8.7 mg, 0.04 mmol, 2 equiv.). The reaction mixture was stirred overnight under room temperature. 2 mL 1 M NaHSO<sub>3</sub> (aq.) were added. After a further 90 minutes the mixture was diluted with 2 mL water and extracted first with CHCl<sub>3</sub> (3 x 4 mL) and then with EA (3 x 4 mL). Drying over sodium sulfate and evaporation of the solvent from the organic phase gave an oily residue (**16**). To the crude **16** dissolved in 1.5 mL ethanol, NaBH<sub>4</sub> (6 mg, 0.15 mmol) was added at room temperature. The mixture was stirred for 1 h at the same temperature, quenched with water and extracted with EA. The organic layers were then washed with saturated brine, dried over sodium sulfate, filtered, and evaporated under reduced pressure. The residue was treated with TFA/CH<sub>2</sub>Cl<sub>2</sub> (1:1) at room temperature. The volatiles were removed under reduced pressure, and the residue was purified by prep-HPLC to afford **BRD7648** (2.2 mg, 34% yield over 3 steps).  $^1\text{H}$  NMR (500 MHz, CHLOROFORM-d)  $\delta$  = 1.98 (2 H, dt,  $J$ =12.2, 6.1 Hz), 3.09 - 3.17 (4 H, m), 3.60 - 3.65 (2 H, m), 3.69 (2 H, t,  $J$ =6.3 Hz), 5.41 - 5.47 (2 H, m), 7.67 (1 H, t,  $J$ =7.8 Hz), 7.95 (1 H, d,  $J$ =7.8 Hz), 8.23 (1 H, d,  $J$ =8.3 Hz), 8.81 (1 H, s), 9.28 (1 H, s) ppm.



**1-(5-(1,4-diazepan-1-ylsulfonyl)isoquinolin-4-yl)ethane-1,2-diol (BRD5505).** To a solution of **14** (6.1 mg, 0.014 mmol) in 1 mL dry pyridine was added a solution of OsO<sub>4</sub> in t-BuOH (0.08 M, 0.4 mL, 0.016 mmol). The reaction mixture was stirred overnight under room temperature. 2 mL 1 M NaHSO<sub>3</sub> (aq.) were added. After a further 90 minutes the mixture was diluted with 2 mL water and extracted first with CHCl<sub>3</sub> (3 x 4 mL) and then with EA (3 x 4 mL). Drying over sodium sulfate and the evaporation of the solvent from the organic phase gave an oily residue that was subjected to TFA/CH<sub>2</sub>Cl<sub>2</sub> (1:1) directly. The final product was purified by prep-HPLC to afford **BRD5505** (1.3 mg, 26% yield). <sup>1</sup>H NMR (500 MHz, CHLOROFORM-d) δ = 2.88 - 2.93 (2 H, m), 2.98 (1 H, s), 3.00 - 3.06 (2 H, m), 3.22 (1 H, s), 3.41 (2 H, d, J=5.9 Hz), 3.45 - 3.54 (3 H, m), 3.71 - 3.82 (3 H, m), 3.84 - 3.90 (2 H, m), 6.42 (1 H, dd, J=8.1, 4.1 Hz), 7.69 (1 H, t, J=7.6 Hz), 8.24 (1 H, d, J=8.3 Hz), 8.40 (1 H, d, J=7.3 Hz), 9.07 (1 H, s), 9.28 (1 H, s) ppm.

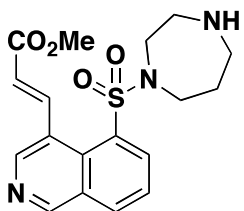


**5-(1,4-diazepan-1-ylsulfonyl)isoquinoline-4-carbaldehyde (BRD4734).** To a solution of the crude diol **15** in 2 mL THF/water (1:1) was added NaIO<sub>4</sub> (3.5 mg, 0.0162 mmol) at 0 °C. The solution was warmed to room temperature and stirred overnight, then diluted with ethyl acetate before it was quenched with an aqueous 20% Na<sub>2</sub>S<sub>2</sub>O<sub>3</sub> solution. The organic layer was separated, washed with an aqueous 20% Na<sub>2</sub>S<sub>2</sub>O<sub>3</sub> solution, water and brine, dried over sodium sulfate, filtered and concentrated. The residue was treated by 1:1 TFA/CH<sub>2</sub>Cl<sub>2</sub> for 1 h at room temperature. The volatiles were removed under reduced pressure, and the residue was purified by prep-HPLC to afford **BRD4734** 0.9 mg in 20% yield over three steps. <sup>1</sup>H NMR (500 MHz, CHLOROFORM-d) δ = 1.88 - 1.94 (2 H, m), 3.02 - 3.10 (4 H, m), 3.45 - 3.50 (2 H, m), 3.53 (2 H, t, J=6.1 Hz), 7.83 (1 H, d, J=7.8 Hz), 8.32 (2 H, dd, J=11.5, 7.6 Hz), 9.05 (1 H, s), 9.49 (1 H, s), 11.01 (1 H, s) ppm.

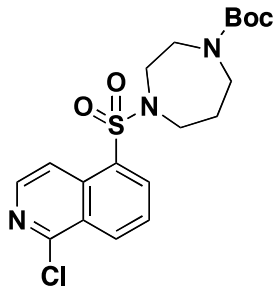


**(E)-N'-(5-(1,4-diazepan-1-ylsulfonyl)isoquinolin-4-yl)methylene)acetohydrazide (BRD0859).**

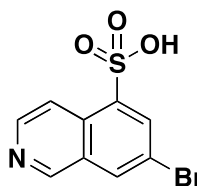
To the solution of **BRD4734** (1 equiv.) and acetohydrazide (1 equiv.) in dry methanol, was added a catalytic amount of acetic acid (0.1 equiv.). The mixture was stirred overnight under 50 °C, after which the solution was concentrated and the product **BRD0859** was purified by prep-HPLC. <sup>1</sup>H NMR (300 MHz, CHLOROFORM-d) δ = 1.91 - 1.98 (2 H, m), 2.05 (1 H, s), 2.43 (3 H, s), 2.91 (1 H, s), 2.98 (1 H, s), 3.04 - 3.15 (4 H, m), 3.54 - 3.66 (4 H, m), 7.73 (1 H, d, J=8.7 Hz), 7.99 (1 H, dd, J=7.3, 1.1 Hz), 8.25 (1 H, dd, J=8.6, 1.0 Hz), 9.05 (1 H, s), 9.10 (1 H, s), 9.35 (1 H, s) ppm.



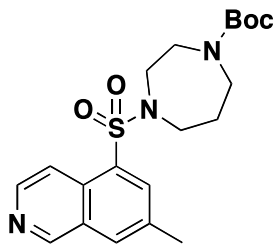
**(E)-methyl 3-(5-(1,4-diazepan-1-ylsulfonyl)isoquinolin-4-yl)acrylate (BRD7198).** In a 5 mL microwave tube was added **4** (9.9 mg, 0.021 mmol, 1 equiv.), tri-o-tolylphosphine (1.3 mg, .0004 mmol, 0.2 equiv.), diacetoxypalladium (0.5 mg, 0.002 mmol, 0.1 equiv.) in dry DMF. The solution was degassed with nitrogen, and TEA (0.03 mL, 0.21 mmol, 10 equiv.) and methyl acrylate (0.02 mL, 0.21 mmol, 10 equiv.) were added through a syringe. The mixture was stirred overnight under 120 °C, after which the solution was filtered through a short column of Celite and the column was washed by EA. The solvent was removed under reduced pressure, and the residue was treated with TFA/CH<sub>2</sub>Cl<sub>2</sub> (1:1). The final product was purified by prep-HPLC to give **BRD7198** (5.9 mg, 0.016 mmol, 75% yield) as a white solid. <sup>1</sup>H NMR (300 MHz, CHLOROFORM-d) δ = 1.88 - 1.99 (2 H, m), 3.03 - 3.12 (4 H, m), 3.50 - 3.66 (4 H, m), 3.88 (3 H, s), 6.37 (1 H, d, J=15.4 Hz), 7.67 - 7.78 (1 H, m), 8.08 (1 H, dd, J=7.3, 0.8 Hz), 8.18 - 8.29 (1 H, m), 8.76 (1 H, s), 9.01 (1 H, d, J=15.1 Hz), 9.32 (1 H, s) ppm.



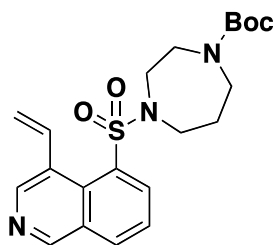
**tert-butyl 4-(1-chloroisoquinolin-5-ylsulfonyl)-1,4-diazepane-1-carboxylate (BRD2109).**  $^1\text{H}$  NMR (500 MHz, CHLOROFORM-d)  $\delta$  = 1.45 (9 H, s), 1.94 - 2.05 (2 H, m), 3.34 - 3.47 (4 H, m), 3.50 - 3.65 (4 H, m), 7.13 - 7.23 (1 H, m), 7.24 - 7.31 (1 H, m), 7.74 - 7.82 (1 H, m), 8.31 - 8.41 (1 H, m), 8.41 - 8.49 (1 H, m), 8.66 (1 H, d,  $J$ =8.3 Hz) ppm.



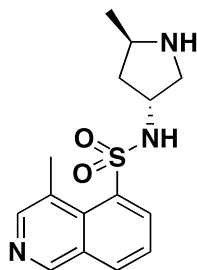
**7-bromoisoquinoline-5-sulfonic acid (12).**  $^3\text{H}$  NMR (300 MHz, DMSO-d6)  $\delta$  = 8.41 (1 H, d,  $J$ =2.3 Hz), 8.68 - 8.79 (2 H, m), 8.99 (1 H, d,  $J$ =6.6 Hz), 9.73 (1 H, s) ppm.



**tert-butyl 4-(7-methoxyisoquinolin-5-ylsulfonyl)-1,4-diazepane-1-carboxylate (13).**  $^1\text{H}$  NMR (300 MHz, CHLOROFORM-d)  $\delta$  = 1.23 - 1.41 (9 H, m), 1.83 - 1.94 (2 H, m), 2.55 (3 H, s), 3.22 - 3.37 (4 H, m), 3.37 - 3.52 (4 H, m), 7.89 (1 H, s), 8.12 (1 H, d,  $J$ =11.3 Hz), 8.26 (1 H, d,  $J$ =6.2 Hz), 8.55 (1 H, d,  $J$ =5.7 Hz), 9.19 (1 H, s) ppm.

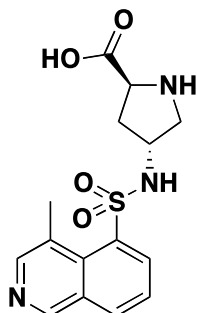


**tert-butyl 4-(4-vinylisoquinolin-5-ylsulfonyl)-1,4-diazepane-1-carboxylate (14).**  $^1\text{H}$  NMR (300 MHz, CHLOROFORM-d)  $\delta$  = 1.51 (9 H, s), 2.01 – 2.10 (2 H, m), 3.36 - 3.71 (8 H, m), 5.52 (1 H, dd,  $J$ =10.8, 1.2 Hz), 5.68 (1 H, dd,  $J$ =16.9, 1.4 Hz), 7.64 (1 H, t,  $J$ =7.7 Hz), 7.80 - 8.04 (2 H, m), 8.19 (1 H, d,  $J$ =8.1 Hz), 8.63 - 8.86 (1 H, m), 9.12 - 9.39 (1 H, m) ppm;  $^{13}\text{C}$  NMR (150 MHz, CHLOROFORM-d)  $\delta$  = 28.5, 28.6, 28.7, 28.9, 45.9, 46.4, 49.3, 50.5, 50.5, 51.9, 52.2, 80.2, 80.3, 117.6, 125.6, 125.6, 129.9, 130.2, 130.5, 134.4, 134.4, 136.3, 137.1, 146.7, 153.3, 155.5 ppm.



**4-methyl-N-((3*R*,5*R*)-5-methylpyrrolidin-3-yl)isoquinoline-5-sulfonamide**

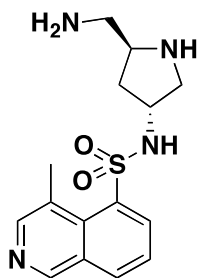
**(BRD5319).** To a solution of **22** (10 mg, 0.024 mmol, 1 equiv.) in dry THF (0.5 mL) was added triphenylphosphine (12.5 mg, 0.047 mmol, 2 equiv), imidazole (6.5 mg, 0.095 mmol, 4 equiv), and iodine (12 mg, 0.047 mmol, 2 equiv) at room temperature. The mixture was refluxed for 2 h. The solvent was evaporated and the residue was dissolved in EA (10 mL), washed with Na<sub>2</sub>S<sub>2</sub>O<sub>3</sub> (aq.), dried over sodium sulfate, and concentrated. The residue was further subjected to hydrogenation and deprotection as described in the general procedure to afford **BRD5319** (4.1 mg, 57% yield over 3 steps), which is purified by prep-HPLC.  $^1\text{H}$  NMR (500 MHz, CHLOROFORM-d)  $\delta$  = 1.19 (3 H, d,  $J$ =6.3 Hz), 1.26 (2 H, t,  $J$ =7.1 Hz), 1.69 (1 H, ddd,  $J$ =13.4, 8.3, 8.1 Hz), 2.94 (1 H, dd,  $J$ =11.2, 4.9 Hz), 3.09 (3 H, s), 3.37 - 3.48 (2 H, m), 3.74 (1 H, q,  $J$ =6.8 Hz), 3.94 - 4.04 (1 H, m), 7.64 (1 H, t,  $J$ =7.8 Hz), 8.18 (1 H, d,  $J$ =7.8 Hz), 8.51 (1 H, d,  $J$ =7.3 Hz), 8.57 (1 H, s), 9.17 (1 H, s) ppm.



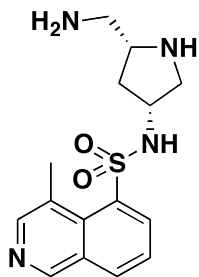
**(2*S*,4*R*)-4-(4-methylisoquinoline-5-sulfonamido)pyrrolidine-2-carboxylic acid**

**(BRD7953).** To a 4 mL capped vial were added alcohol **22** (14.8 mg, 0.035 mmol, 1 equiv.), TEMPO (1.1 mg, 0.007 mmol, 0.2 equiv.), and bis-acetoxy-iodobenzene (BAIB) (30 mg, 0.093 mmol, 2.7 equiv.) in 0.5 mL acetonitrile/water (1:1). The reaction mixture

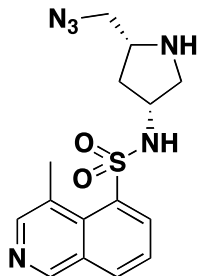
was stirred for 2 h and quenched with a saturated aqueous  $\text{Na}_2\text{SO}_3$  solution (3 mL). Acetonitrile was evaporated under reduced pressure, acidified with a 1 M HCl solution ( $\text{pH} \sim 3$ ). The acidic aqueous phase was extracted three times with EA. The combined organic extracts were dried over sodium sulfate, filtered, and evaporated *in vacuo* to yield an oily residue that was subjected to TFA/CH<sub>2</sub>Cl<sub>2</sub> (1:1) directly. Final product **BRD7953** (0.8 mg, 7% yield over two steps) was purified by prep-HPLC. <sup>1</sup>H NMR (300 MHz, MeOD)  $\delta$  = 1.27 (1 H, s), 1.91 (1 H, d,  $J=1.1$  Hz), 2.41 (2 H, dd,  $J=7.5, 6.6$  Hz), 3.01 - 3.06 (3 H, m), 3.95 (1 H, d,  $J=6.2$  Hz), 4.10 (1 H, s), 7.74 - 7.82 (1 H, m), 8.32 - 8.38 (1 H, m), 8.38 - 8.43 (1 H, m), 8.45 (1 H, s), 9.17 (1 H, s) ppm.



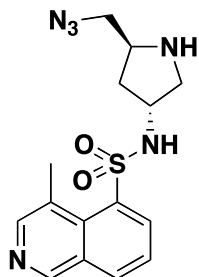
**N-((3R,5S)-5-(aminomethyl)pyrrolidin-3-yl)-4-methylisoquinoline-5-sulfonamide (BRD9949).** <sup>1</sup>H NMR (500 MHz, METHANOL-d4)  $\delta$  = 1.76 - 1.89 (1 H, m), 2.11 (1 H, s), 2.62 - 2.76 (2 H, m), 2.98 (1 H, dd,  $J=11.5, 5.1$  Hz), 3.09 (3 H, s), 3.19 (1 H, dd,  $J=11.5, 6.1$  Hz), 3.35 - 3.44 (1 H, m), 3.81 - 3.92 (1 H, m), 7.80 (1 H, t,  $J=7.8$  Hz), 8.37 (1 H, d,  $J=8.3$  Hz), 8.45 - 8.55 (2 H, m), 9.21 (1 H, s) ppm.



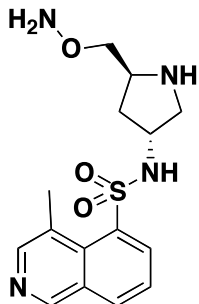
**N-((3R,5R)-5-(aminomethyl)pyrrolidin-3-yl)-4-methylisoquinoline-5-sulfonamide (BRD7071).** <sup>1</sup>H NMR (300 MHz, MeOD)  $\delta$  = 2.69 - 2.74 (1 H, m), 2.85 (1 H, d,  $J=7.3$  Hz), 3.01 - 3.07 (3 H, m), 3.10 - 3.19 (2 H, m), 3.78 (2 H, s), 7.71 - 7.80 (1 H, m), 8.33 (1 H, d,  $J=8.3$  Hz), 8.44 (1 H, s), 8.46 - 8.53 (1 H, m), 9.16 (1 H, s) ppm; <sup>13</sup>C NMR (150 MHz, MeOD)  $\delta$  = 20.9, 34.9, 36.2, 52.0, 52.3, 54.9, 55.0, 58.8, 63.8, 125.7, 125.8, 128.5, 130.6, 132.5, 132.6, 134.6, 134.6, 137.5, 137.6, 146.7, 151.7 ppm.



***N-((3R,5R)-5-(azidomethyl)pyrrolidin-3-yl)-4-methylisoquinoline-5-sulfonamide (BRD2880).***  $^1\text{H}$  NMR (500 MHz, CHLOROFORM-d)  $\delta$  = 2.31 - 2.39 (1 H, m), 3.02 - 3.10 (2 H, m), 3.12 (3 H, s), 3.37 - 3.45 (2 H, m), 3.49 - 3.56 (1 H, m), 3.96 (1 H, d,  $J$ =3.4 Hz), 5.38 (1 H, d,  $J$ =8.3 Hz), 7.65 (1 H, t,  $J$ =7.8 Hz), 8.20 (1 H, d,  $J$ =8.3 Hz), 8.56 - 8.63 (2 H, m), 9.18 (1 H, s) ppm.

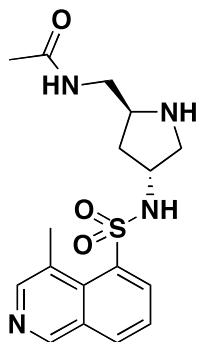


***N-((3R,5S)-5-(azidomethyl)pyrrolidin-3-yl)-4-methylisoquinoline-5-sulfonamide (BRD3192).***  $^1\text{H}$  NMR (300 MHz, CHLOROFORM-d)  $\delta$  = 1.96 - 2.08 (2 H, m), 3.00 (1 H, dd,  $J$ =11.2, 4.6 Hz), 3.09 (3 H, s), 3.26 (2 H, dt,  $J$ =11.7, 5.9 Hz), 3.31 - 3.40 (1 H, m), 3.50 - 3.60 (1 H, m), 3.94 - 4.03 (1 H, m), 7.64 (1 H, t,  $J$ =7.8 Hz), 8.20 (1 H, dd,  $J$ =8.2, 1.2 Hz), 8.51 (1 H, dd,  $J$ =7.5, 1.3 Hz), 8.57 (1 H, s), 9.18 (1 H, s) ppm;  $^{13}\text{C}$  NMR (75 MHz, CHLOROFORM-d)  $\delta$  = 21.7, 36.5, 53.0, 54.9, 55.6, 56.0, 124.9, 127.1, 130.2, 132.2, 132.8, 134.9, 148.7, 152.1 ppm.

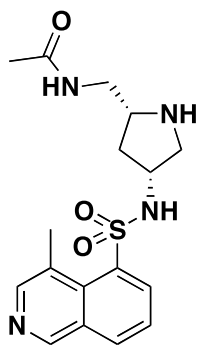


***N-((3R,5S)-5-(aminooxymethyl)pyrrolidin-3-yl)-4-methylisoquinoline-5-sulfonamide (BRD7569).***  $^1\text{H}$  NMR (500 MHz, METHANOL-d4)  $\delta$  = 1.87 - 1.96 (1 H, m), 2.00 - 2.08 (1 H, m), 2.92 (1 H, dd,  $J$ =11.2, 5.9 Hz), 3.08 (3 H, s), 3.25 (1 H, dd,  $J$ =11.5, 6.1 Hz),

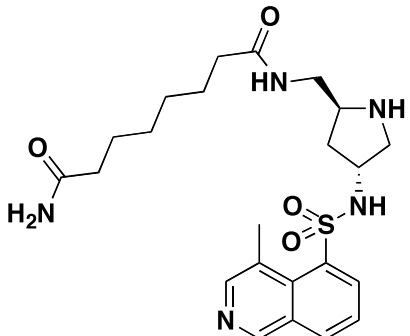
3.52 - 3.62 (2 H, m), 3.63 - 3.69 (1 H, m), 3.83 - 3.90 (1 H, m), 7.79 (1 H, t,  $J=7.8$  Hz), 8.36 (1 H, d,  $J=8.3$  Hz), 8.48 (1 H, s), 8.51 (1 H, d,  $J=7.3$  Hz), 9.19 (1 H, s) ppm.



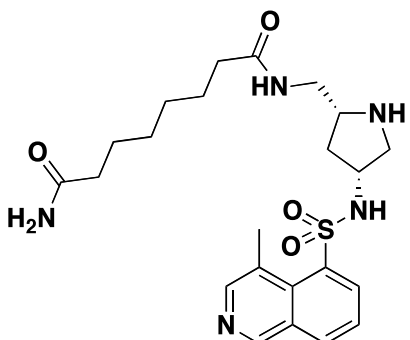
**N-((2S,4R)-4-(4-methylisoquinoline-5-sulfonamido)pyrrolidin-2-yl)methyl)acetamide (BRD8899).**  $^1\text{H}$  NMR (500 MHz, METHANOL-d4)  $\delta$  = 1.78 - 1.87 (1 H, m), 1.93 (3 H, s), 1.98 - 2.06 (1 H, m), 2.87 (1 H, dd,  $J=11.2, 5.9$  Hz), 3.05 - 3.08 (3 H, m), 3.17 - 3.28 (3 H, m), 3.38 - 3.46 (1 H, m), 3.81 - 3.88 (1 H, m), 7.78 (1 H, t,  $J=7.8$  Hz), 8.35 (1 H, d,  $J=8.3$  Hz), 8.46 (1 H, s), 8.49 (1 H, d,  $J=6.3$  Hz), 9.18 (1 H, s) ppm;  $^{13}\text{C}$  NMR (150 MHz, METHANOL-d4)  $\delta$  = 22.2, 22.7, 37.5, 44.6, 54.2, 55.9, 58.4, 127.0, 129.9, 132.0, 133.8, 133.8, 135.9, 138.8, 148.0, 153.0, 173.8 ppm.



**N-((2R,4R)-4-(4-methylisoquinoline-5-sulfonamido)pyrrolidin-2-yl)methyl)acetamide (BRD5749).**  $^1\text{H}$  NMR (500 MHz, METHANOL-d4)  $\delta$  = 1.52 (1 H, dd,  $J=8.1, 5.1$  Hz), 1.91 - 1.98 (3 H, m), 2.26 - 2.38 (1 H, m), 2.86 - 2.92 (1 H, m), 3.02 - 3.06 (3 H, m), 3.11 (1 H, dd,  $J=11.2, 6.8$  Hz), 3.19 (1 H, dd,  $J=14.9, 8.1$  Hz), 3.23 - 3.28 (2 H, m), 3.80 (1 H, t,  $J=7.3$  Hz), 7.75 (1 H, t,  $J=7.8$  Hz), 8.32 (1 H, d,  $J=7.8$  Hz), 8.44 (1 H, s), 8.47 (1 H, d,  $J=7.3$  Hz), 9.15 (1 H, s) ppm.

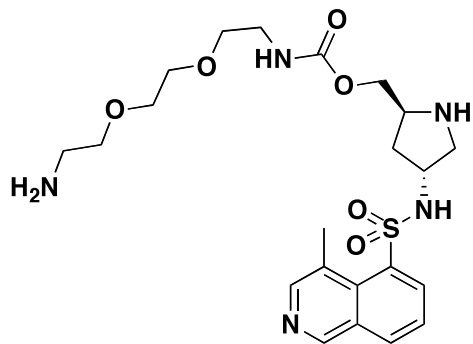


**$N^1-((2S,4R)-4-(4\text{-methoxyquinoline-5-sulfonamido})\text{pyrrolidin-2-yl})\text{methyl}\text{octane-diamide (BRD4717)}$** . To bis(2,5-dioxopyrrolidin-1-yl) octanedioate **21** (10 equiv.) dissolved in 1 mL DMF was added amine **24**, which was obtained by hydrogenation of azide **24** (11 mg, 0.024 mmol, 1 equiv.). The reaction mixture was stirred at room temperature overnight, after which ammonia (2 mL, 1 mmol, 0.5 M in THF) was added. The reaction mixture was stirred at room temperature for 2 h and volatiles were removed under reduced pressure to yield an oily residue. The residue was subjected to TFA/CH<sub>2</sub>Cl<sub>2</sub> (1:1) directly, and the final product **BRD4717** (4 mg, 34% yield over four steps) was purified by prep-HPLC. <sup>1</sup>H NMR (500 MHz, CHLOROFORM-d)  $\delta$  = 1.39 (3 H, td,  $J=12.0, 6.3$  Hz), 1.49 - 1.56 (5 H, m), 1.56 - 1.73 (36 H, m), 2.18 (2 H, dddd,  $J=8.3, 5.6, 5.4, 2.7$  Hz), 2.22 - 2.30 (3 H, m), 2.81 - 2.87 (1 H, m), 2.90 - 2.92 (3 H, m), 2.97 - 3.00 (3 H, m), 3.04 (1 H, dd,  $J=12.0, 4.6$  Hz), 3.08 - 3.11 (3 H, m), 3.15 (1 H, d,  $J=12.2$  Hz), 3.56 - 3.62 (2 H, m), 3.94 (1 H, ddd,  $J=4.5, 2.4, 2.3$  Hz), 5.50 - 5.55 (1 H, m), 6.02 - 6.08 (1 H, m), 6.19 (1 H, dd,  $J=6.3, 4.4$  Hz), 7.65 (1 H, t,  $J=7.8$  Hz), 8.04 (1 H, s), 8.19 (1 H, d,  $J=8.3$  Hz), 8.49 (1 H, d,  $J=6.3$  Hz), 8.56 (1 H, s), 9.17 (1 H, s) ppm.

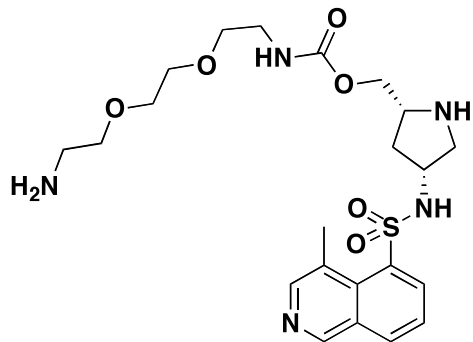


**$N^1-((2R,4R)-4-(4\text{-methoxyquinoline-5-sulfonamido})\text{pyrrolidin-2-yl})\text{methyl}\text{octane-diamide (BRD1469)}$** . To bis(2,5-dioxopyrrolidin-1-yl) octanedioate **21** (10 equiv.) dissolved in 1 mL DMF, was added amine **19**, which was obtained by hydrogenation of azide **18** (6.7 mg, 0.015 mmol, 1 equiv.). The reaction mixture was stirred at room temperature overnight, after which ammonia (2 mL, 1 mmol, 0.5 M in THF) was added. The reaction mixture was stirred at room temperature for 2 h and volatiles were removed under reduced pressure to yield an oily residue. The residue was subjected to TFA/CH<sub>2</sub>Cl<sub>2</sub> (1:1) directly, and the final product **BRD1469** (3.4 mg, 48% yield over four steps) was purified by prep-HPLC. <sup>1</sup>H NMR (500 MHz, CHLOROFORM-d)  $\delta$  = 1.34 -

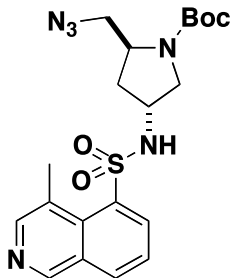
1.47 (4 H, m), 1.54 (2 H, d,  $J=9.3$  Hz), 1.64 (14 H, br. s.), 1.67 - 1.87 (7 H, m), 2.19 - 2.34 (5 H, m), 3.02 - 3.13 (4 H, m), 3.23 (1 H, dd,  $J=11.2, 6.3$  Hz), 3.30 - 3.43 (2 H, m), 3.47 - 3.56 (1 H, m), 3.84 - 3.93 (1 H, m), 5.53 (1 H, br. s.), 6.05 (1 H, br. s.), 6.32 (1 H, d,  $J=4.9$  Hz), 7.65 (1 H, t,  $J=7.8$  Hz), 8.17 (1 H, d,  $J=7.8$  Hz), 8.48 (1 H, d,  $J=7.3$  Hz), 8.56 (1 H, s), 9.16 (1 H, s) ppm.



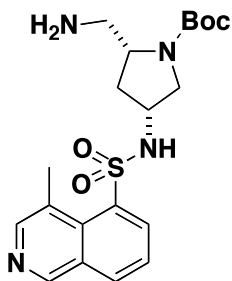
**((2*S*,4*R*)-4-(4-methoxyquinoline-5-sulfonamido)pyrrolidin-2-yl)methyl 2-(2-aminoethoxy)ethylcarbamate (BRD0200).** Compound **BRD0200** was synthesized following known procedure.<sup>4</sup>  $^1\text{H}$  NMR (500 MHz, CHLOROFORM-d)  $\delta$  = 1.83 (2 H, dd,  $J=14.4, 7.1$  Hz), 1.91 - 2.15 (13 H, m), 2.91 (2 H, t,  $J=5.1$  Hz), 2.99 - 3.08 (2 H, m), 3.10 (3 H, s), 3.23 (1 H, dd,  $J=11.2, 5.4$  Hz), 3.39 (2 H, q,  $J=5.0$  Hz), 3.51 - 3.61 (4 H, m), 3.61 - 3.69 (6 H, m), 3.92 - 4.00 (2 H, m), 4.06 (1 H, dd,  $J=11.2, 4.4$  Hz), 5.56 (1 H, br. s.), 7.65 (1 H, t,  $J=7.6$  Hz), 8.19 (1 H, d,  $J=6.8$  Hz), 8.51 (1 H, d,  $J=6.3$  Hz), 8.57 (1 H, s), 9.17 (1 H, s) ppm.



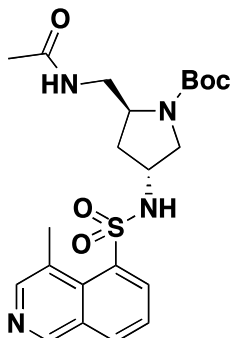
**((2*R*,4*R*)-4-(4-methoxyquinoline-5-sulfonamido)pyrrolidin-2-yl)methyl 2-(2-aminoethoxy)ethylcarbamate (BRD8254).** Compound **BRD8254** was synthesized following known procedure.**Error! Bookmark not defined.**  $^1\text{H}$  NMR (300 MHz, MeOD)  $\delta$  = 2.33 (1 H, s), 2.78 - 2.92 (3 H, m), 2.99 - 3.08 (3 H, m), 3.09 - 3.19 (1 H, m), 3.48 - 3.59 (4 H, m), 3.59 - 3.65 (4 H, m), 3.80 (1 H, d,  $J=7.5$  Hz), 3.96 - 4.11 (2 H, m), 7.72 - 7.82 (1 H, m), 8.31 - 8.38 (1 H, m), 8.42 - 8.54 (2 H, m), 9.17 (1 H, s) ppm.



**(2*S*,4*R*)-*tert*-butyl 2-(azidomethyl)-4-(4-methyisoquinoline-5-sulfonamido)pyrrolidine-1-carboxylate (23).**  $^1\text{H}$  NMR (300 MHz, CHLOROFORM-d)  $\delta$  = 1.45 (9 H, s), 2.01 - 2.07 (1 H, m), 2.07 - 2.29 (2 H, m), 2.97 - 3.08 (3 H, m), 3.23 - 3.35 (1 H, m), 3.35 - 3.60 (1 H, m), 3.60 - 3.70 (1 H, m), 3.96 - 4.20 (3 H, m), 5.87 - 6.08 (1 H, m), 7.60 (1 H, t,  $J$ =7.5 Hz), 8.16 (1 H, d,  $J$ =8.3 Hz), 8.44 (1 H, d,  $J$ =6.6 Hz), 8.48 - 8.64 (1 H, m), 9.00 - 9.32 (1 H, m) ppm;  $^{13}\text{C}$  NMR (75 MHz, CHLOROFORM-d)  $\delta$  = 13.7, 14.2, 21.1, 21.7, 28.4, 30.7, 55.2, 60.4, 64.4, 124.9, 132.2, 132.4, 134.9, 136.6, 148.5, 152.0 ppm.

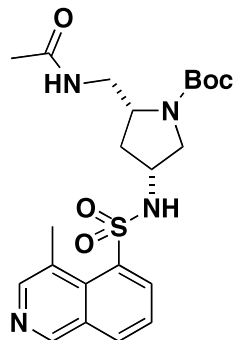


**(2*R*,4*R*)-*tert*-butyl 2-(aminomethyl)-4-(4-methyisoquinoline-5-sulfonamido)pyrrolidine-1-carboxylate (19).**  $^1\text{H}$  NMR (300 MHz, MeOD)  $\delta$  = 1.43 (9 H, s), 1.85 - 1.97 (1 H, m), 2.42 - 2.53 (1 H, m), 3.06 (3 H, s), 3.71 - 3.87 (3 H, m), 7.72 - 7.80 (1 H, m), 8.33 (1 H, d,  $J$ =8.1 Hz), 8.44 (1 H, s), 8.51 (1 H, d,  $J$ =7.7 Hz), 9.16 (1 H, s) ppm.

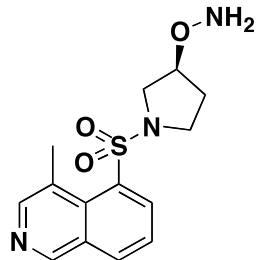


**(2*S*,4*R*)-*tert*-butyl 2-(acetamidomethyl)-4-(4-methyisoquinoline-5-sulfonamido)pyrrolidine-1-carboxylate (BRD2816).**  $^1\text{H}$  NMR (500 MHz, CHLOROFORM-d)  $\delta$  = 1.19 - 1.32 (1 H, m), 1.46 (9 H, br. s.), 1.94 (3 H, s), 2.01 - 2.09 (1 H, m), 2.16 - 2.27 (1 H, m), 3.07 (3 H, s), 3.15 - 3.26 (1 H, m), 3.33 - 3.45 (1 H, m), 3.45 - 3.55 (1 H, m), 3.55 - 3.71

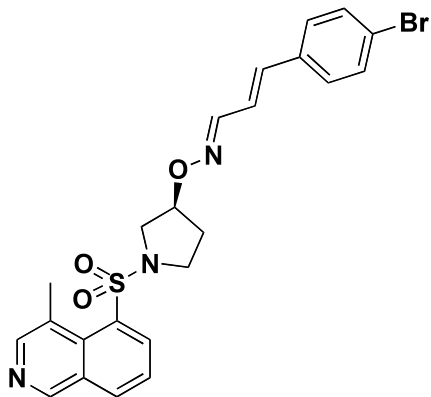
(1 H, m), 3.94 - 4.17 (2 H, m), 6.00 - 6.16 (1 H, m), 7.13 (1 H, d,  $J=3.9$  Hz), 7.66 (1 H, t,  $J=7.6$  Hz), 8.20 (1 H, d,  $J=7.8$  Hz), 8.47 (1 H, d,  $J=7.3$  Hz), 8.50 - 8.66 (1 H, m), 9.06 - 9.29 (1 H, m) ppm.



**(2*R*,4*R*)-*tert*-butyl 2-(acetamidomethyl)-4-(4-methylisoquinoline-5-sulfonamido) pyrrolidine-1-carboxylate (33).**  $^1\text{H}$  NMR (500 MHz, CHLOROFORM-d)  $\delta$  = 1.37 - 1.54 (9 H, m), 2.01 - 2.12 (4 H, m), 2.25 - 2.38 (1 H, m), 3.03 - 3.15 (3 H, m), 3.50 - 3.73 (4 H, m), 3.93 (1 H, br. s.), 4.03 (1 H, d,  $J=6.3$  Hz), 6.73 (1 H, br. s.), 7.62 (1 H, t,  $J=7.6$  Hz), 7.96 (1 H, br. s.), 8.15 (1 H, d,  $J=8.3$  Hz), 8.38 (1 H, d,  $J=6.3$  Hz), 8.56 (1 H, s), 9.15 (1 H, s) ppm;  $^{13}\text{C}$  NMR (150 MHz, CHLOROFORM-d)  $\delta$  = 22.0, 23.5, 28.7, 28.8, 34.1, 44.0, 53.3, 54.3, 56.5, 80.8, 125.1, 127.9, 130.4, 131.5, 132.6, 134.6, 137.1, 148.6, 148.7, 152.1, 172.3 ppm.



**(*S*)-*O*-(1-(4-methylisoquinolin-5-ylsulfonyl)pyrrolidin-3-yl)hydroxylamine (BRD2916).**  $^1\text{H}$  NMR (300 MHz, CHLOROFORM-d)  $\delta$  = 2.05 - 2.25 (2 H, m), 2.25 - 2.37 (1 H, m), 2.94 - 3.13 (4 H, m), 3.48 - 3.68 (3 H, m), 3.68 - 3.86 (2 H, m), 4.40 - 4.52 (1 H, m), 5.43 - 5.60 (2 H, m), 7.56 - 7.69 (1 H, m), 8.12 - 8.30 (2 H, m), 8.56 (1 H, s), 9.16 (1 H, s) ppm.



**(1E,2E)-3-(4-bromophenyl)acrylaldehyde *O*-(S)-1-(4-methylisoquinolin-5-ylsulfonyl)pyrrolidin-3-yl oxime (BRD6284).** To the solution of oxyamine **BRD2916** (1 equiv.) and trans-4-Bromocinnamaldehyde (1 equiv.) in dry methanol, was added a catalytic amount of acetic acid (0.1 equiv.). The mixture was stirred overnight under 50 °C, after which the solution was concentrated and the product was purified by prep-HPLC. <sup>1</sup>H NMR (500 MHz, METHANOL-d4) δ = 2.42 (2 H, br. s.), 3.07 (3 H, s), 3.65 (2 H, d, J=7.8 Hz), 3.77 (2 H, d, J=3.9 Hz), 3.83 (2 H, s), 6.95 (1 H, d, J=9.8 Hz), 7.01 - 7.07 (1 H, m), 7.48 (2 H, m), 7.55 (2 H, m), 7.76 (1 H, s), 8.17 (1 H, d, J=9.8 Hz), 8.32 - 8.38 (2 H, m), 8.48 (1 H, s), 9.19 (1 H, s) ppm.

#### References:

1. Liu Z, Larock RC (2006) Facile N-arylation of amines and sulfonamides and o-arylation of phenols and arenecarboxylic acids. *J Org Chem* 71:3198-3209.
2. Vo GD, Hartwig JF (2009) Palladium-catalyzed coupling of ammonia with aryl chlorides, bromides, iodides, and sulfonates: a general method for the preparation of primary arylamines. *J Am Chem Soc* 131:11049-11061.
3. Joseph S, Li R, Myers MR, Aburub A, Dai JP, Schmid CR (2007) *PCT Int Appl WO* 2007149730 A2 20071227.
4. Wang X, Imber BS, Schreiber SL (2008) Small-molecule reagents for cellular pull-down experiments. *Bioconjugate Chem* 19:585-587.